

ASTROCHEMISTRY AND COMPOSITIONS OF PLANETARY SYSTEMS

KARIN I. ÖBERG

Harvard-Smithsonian Center for Astrophysics, 60 Garden St., Cambridge, MA 02138

EDWIN A. BERGIN

Department of Astronomy, University of Michigan, 1085 S. University Avenue, Ann Arbor, MI 48109, USA and

Authors' version of review to appear in Physics Reports (October 8, 2020)

ABSTRACT

Planets form and obtain their compositions in disks of gas and dust around young stars. The chemical compositions of these planet-forming disks regulate all aspects of planetary compositions from bulk elemental inventories to access to water and reactive organics, i.e. a planet's hospitality to life and its chemical origins. Disk chemical structures are in their turn governed by a combination of *in situ* chemical processes, and inheritance of molecules from the preceding evolutionary stages of the star formation process. In this review we present our current understanding of the chemical processes active in pre- and protostellar environments that set the initial conditions for disks, and the disk chemical processes that evolve the chemical conditions during the first million years of planet formation. We review recent observational, laboratory and theoretical discoveries that have led to the present view of the chemical environment within which planets form, and their effects on the compositions of nascent planetary systems. We also discuss the many unknowns that remain and outline some possible pathways to addressing them.

1. INTRODUCTION

The goal of this review is to present the astrochemistry most relevant to predicting and interpreting the volatile compositions of planetary systems. The past decades have witnessed a revolution in planetary science, increasing the number of known planets from eight around the Sun to many thousands of exoplanets around other stars. Many of these exoplanets are strange compared to expectations from the solar system (Winn and Fabrycky 2015; Dawson and Johnson 2018), and planetary compositions are emerging as a major tool to constrain the origins of specific planets, as well as families of planets (Öberg et al. 2011c; Madhusudhan 2019). Doing this well requires a detailed understanding of the elemental composition of the gas and solids from which planets form. Furthermore, a subset of the known exoplanets are Earth-like in the sense that they are rocky and temperate, i.e. at the right temperature to sustain liquid water. For this set of potentially habitable exoplanets, we have a second set of compositional questions which relates to their hospitality for life and origins of life chemistry: do they form with water and ready access to reactive organic molecules, sulfur and phosphorus? These questions too depend on the composition of the planet-forming material, but this time on the detailed molecular composition.

Planets form in disks of gas and dust around young stars (e.g. Lissauer 1993; Andrews et al. 2018). The complete composition of dust and gas is relevant to predicting planet compositions, but in this review we will mostly limit ourselves to the volatile components, i.e. the gas and icy grain mantles. Based on theory as well as on direct observations of disks, and data from our own solar system, disk compositions are in their turn a product of both *in situ* disk chemical processes, and inheritance of molecular material from the preceding evolutionary stages (Mumma and Charnley 2011; Cleeves et al. 2014; Ceccarelli et al. 2014; Drozdovskaya et al. 2014; Huang et al. 2017). A complete model of the astrochemical origins of compositions of planetary systems must then include the chemical evolution from the onset of cloud formation, via star formation within molecular clouds, to the final stages of planet formation in disks.

In the remainder of this section we briefly review the formation of Solar-type stars and their accompanying planetary systems, astrochemical reactions, and astrochemical methods. This is followed by a section on the chemical foundations, i.e. the division of elements between volatile carriers, and the formation of water and of the first organics, that develop in molecular clouds and cloud cores. In the subsequent section we review how the chemistry evolves in the protostellar stage, and existing constraints on the chemical composition of the protostellar precursors to the mature, planet-forming disks. The final section treats observations and theory of chemistry in planet-forming disks and how they relate to observed volatile compositions within the solar system.

1.1. Formation of stars and planetary systems

Stars span a large range of masses, and the star formation process depends on the mass of the final star. For the purpose of predicting planetary compositions, low-mass stars (less than two solar masses) are the most relevant. They constitute the vast majority of stars and therefore planet hosts in the Galaxy, and their long life times are likely a

pre-requisite for the origins of life. There are several excellent reviews of low-mass star formation going back to Shu et al. (1987), whose illustration of low-mass star formation we have updated in Figure 1. More recently star formation has been reviewed by McKee and Ostriker (2007) and Luhman (2012). Here we present a brief summary of the current understanding of low-mass star formation, which will be the context for the remainder of the review.

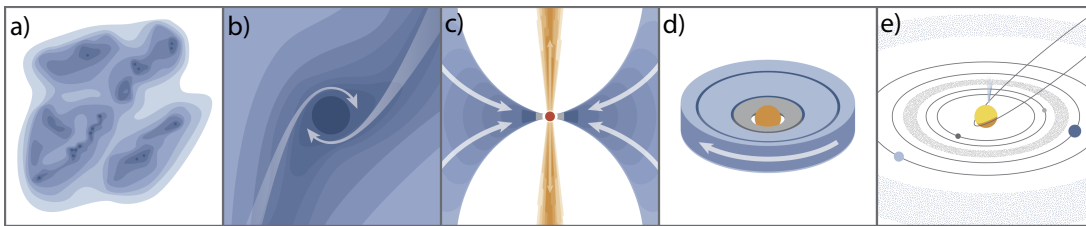


FIG. 1.— Cartoon of the different stages characterizing low-mass (Solar-like) star and planet formation. **a:** Stars form in dense cores in interstellar molecular clouds. **b:** Star formation begins when such a dense core begins to collapse due to self-gravity. **c:** As the collapse proceeds the center heats up forming a protostar. Accretion of remnant cloud material continues, funneled through a disk, which is formed as a consequence of cloud angular momentum. This stage is also characterized by outflows of material. **d:** Following dispersal of the cloud remnant the now pre-main sequence star is left with a circumstellar disk, which is the formation sites of planets. The disk gas is dispersed through disk winds within $\sim 2\text{--}5$ Myrs, putting a halt to Gas Giant formation. **e:** Rocky and icy planets can continue to grow for another 100 Myrs at which time a mature planetary system exists. Image credit: K. Peek.

Stars form in over-dense regions in the interstellar medium, referred to as clouds (Fig. 1a). Clouds mostly consist of gas, but approximately one percent of the mass of the cloud is in the form of sub-micron dust particles, initially composed of silicates and carbonaceous material (Draine 2003; Henning et al. 2010; Chiar et al. 2013; Jones et al. 2013). These dust grains can become coated with icy mantles of more volatile species, which have a profound impact on the chemical evolution during star formation (Herbst and van Dishoeck 2009). Star formation is mainly associated with dense molecular clouds (Heyer and Dame 2015), where densities are $> 10^2 n_{\text{H}} \text{ cm}^{-3}$ (hydrogen nuclei per cubic centimeter), which result in cloud interiors that are therefore well shielded from external radiation, resulting in low temperature and most elements being bound up in molecules. UV radiation chemistry is still key to understand cloud chemical structures, however, since competition between molecular formation and photodissociation during cloud assembly determines the initial chemical compositions of dense clouds (Bergin et al. 2004a; Glover and Mac Low 2007; Clark et al. 2012; Seifried et al. 2017).

Figure 1a also illustrates that within dense clouds there are even denser sub-structures referred to as dense cores. Compared to the large scale dense cloud, these are characterized by orders of magnitude higher densities, $\sim 10^6$ vs. $\sim 10^2 - 10^4$, and lower temperatures, on the order of 10 K (Benson and Myers 1989; Bergin and Tafalla 2007). Typical core sizes are on the order of a tenth of a parsec. Some dense cores are dense enough that they can begin to collapse, overcoming turbulence, thermal and magnetic pressure. Cores that are fated to collapse are referred to as pre-stellar. This collapse is initially isothermal and somewhat asymmetrical due to preservation of cloud angular momentum (Fig. 1b). As the collapse proceeds, the center of the collapsing core becomes optically thick and heats up: a protostar has formed (Fig. 1c).

During the protostellar stage the central protostar continues to accrete mass from the surrounding cloud core, or protostellar envelope. Within the envelope the temperature and density increases towards the center due to stellar heating. To preserve angular momentum some of the accreting material spreads out into a disk, which simultaneously serves to funnel matter onto the star. Angular momentum is also removed from the system through the launch of protostellar outflows and jets (Fig. 1c).

As the protostellar system evolves, more and more mass is found in the star and disk compared to the remnant envelope. The envelope is finally dispersed on time scales of ~ 1 Myr, leaving the a pre-main sequence star and a Keplerian disk (Fig. 1d). The change of name from protostar to pre-main sequence star signifies that the central star has become hot enough for fusion. The circumstellar disk is often referred to as a proto-planetary or planet-forming disk to signify that these disks are where planets assemble (Williams and Cieza 2011). Recent observations suggest, however, that planet formation may begin much earlier, already at the protostellar stage (ALMA Partnership et al. 2015; Harsono et al. 2018).

The protoplanetary disk stage lasts for $\sim 1\text{--}10$ Myrs based on disk occurrence rates in stellar clusters with known median ages (Mamajek 2009). During this time the disk material is accreted onto the star, onto planets, and dispersed through interactions with stellar photo-evaporative winds (Ercolano and Koepferl 2014). What is left behind is a nascent planetary system that can continue to evolve for 100s of Myrs due to collisions between remaining planets and planetesimals. No more gas can be added to planets at this point, and the formation time scale for Gas Giants is therefore set by this protoplanetary disk gas dispersion time scale. For a discussion of astrophysical and solar system constraints on gas dispersion timescale the reader is referred to Pascucci and Tachibana (2010).

Each of the above evolutionary stages are characterized by a unique set of density, temperature and radiation structures, and a unique chemical starting point. It is therefore not surprising that while molecular lines are associated with all stages of star and planet formation, the kind of molecule that is observable changes during the star and planet formation process. Figure 2 shows the emission pattern of six characteristic molecules commonly used to explore cloud structure (HCN), PDRs (C_2H), prestellar cores (N_2H^+), protostellar outflows (H_2O), protostellar cores (complex

organics), and protoplanetary disks (H_2CO).

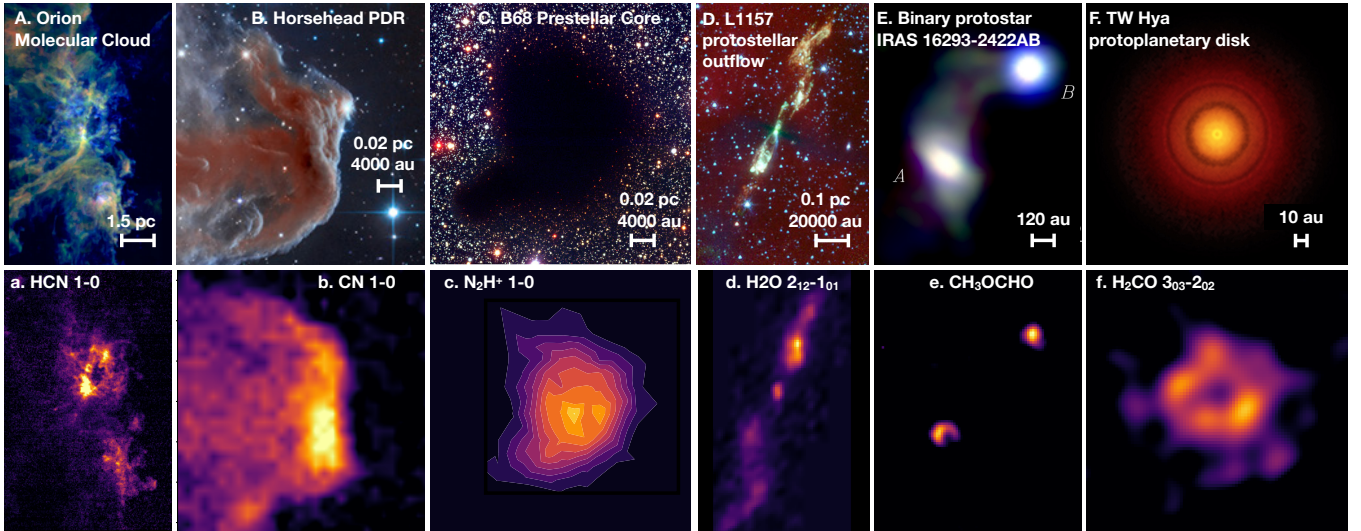


FIG. 2.— Illustrations of characteristic chemical structures associated with the different stages and scales of star and planet formation. A. The Orion Molecular Cloud (OMC) as seen in CO emission (Image credit & copyright J. Pety, the ORION-B Collaboration & IRAM). a. The OMC in HCN 1-0 emission (data from Pety et al. (2017)). B. The Horsehead photodominated region (PDR) (Image credit: Robert Gendler; ESO, VISTA, HLA, Hubble Heritage Team (STScI/AURA)). B. CN 1 – 0 towards the Horsehead PDR (data from Guzmán et al. (2015b)). C. The B68 prestellar core (Credit: ESO). c. B68 in N_2H^+ 1 – 0 emission (data from Bergin et al. (2001)). D. The outflow L1157 in infrared emission (Image credit: NASA/JPL/Spitzer). d. The same outflow in H_2O 179 μm line emission (Nisini et al. 2010). E. The binary protostar IRAS 16293-2422 in dust emission at 1 mm, and in e. in emission from a strong CH_3OCHO line from Jørgensen et al. (2016). F. Protoplanetary disk TW Hya from Andrews et al. (2016). The same disk in H_2CO line emission from Öberg et al. (2017).

1.2. Chemical reactions in interstellar and circumstellar environments

Before considering the chemistry of specific regions associated with the formation of planetary systems it is useful to consider the chemistry most of them have in common. Even the densest phases of star and planet formation are rarified compared to planetary atmospheres. With a few exceptions they are too rarified to allow for three-body reactions of the kind $A + B + C \rightarrow ABC^* \rightarrow AB + C$, where three species collide on timescales shorter than the dissociation timescales of an excited molecular complex, and the $A - B$ bond formation energy is carried away by C . The lack of three-body reactions in space limits what kind of bond formation can occur (Herbst and Klemperer 1973). A second important limitation is that most of the environments we consider in this review are cold, and atoms and molecules therefore lack sufficient kinetic energy to overcome substantial reaction barriers, though tunneling can mitigate this for some types of reactions (e.g. Hasegawa and Herbst 1993; Cazaux et al. 2011; Hama et al. 2015).

With these limitations in mind the top panels of Fig. 3 illustrate the most common bond formation, destruction, and rearrangement reactions in astrochemical gas-phase chemistry networks. In the absence of three-body reactions, bonds form through radiative association and associative detachments, where the bond formation energy is carried away by photons and electrons, respectively. Under most interstellar conditions, radiative association is the most important gas-phase bond formation pathway. Even so, for many reactions of the form $A + B \rightarrow AB + h\nu$ a prohibitory number of collisions is required for a bond formation event to take place, because collision and dissociation are fast ($\tau_{\text{diss}} \sim 10^{-13}$ s) compared to vibrational transitions ($\tau_{\text{rad}} \sim 10^{-3}$ s), corresponding to a very low effective reaction rate. The rate is higher for reactions with accessible electronic transitions, which reduces τ_{rad} , and with entrance energy barriers or large products, both which increases τ_{diss} . Still radiative attachment tend to only be important for reactions where the reactants are very abundant and thus collisions plentiful, which in practice implies that one of the reactant is the most common element in the Universe, i.e. hydrogen in either atomic or molecular form (Herbst and Klemperer 1973). Compared to radiative association, associative detachment reactions are fast, but it plays a small role due to that it requires one of the reactants to be an anion and anions are generally rare (Millar et al. 2007).

Molecular bonds are destroyed through absorption of photons (photodissociation), collision with electrons (dissociative recombination), and in shocks through high-velocity collisions. Of these photodissociation dominates in UV exposed interstellar and circumstellar regions. Photodissociation is the process through which a molecular bond is cleaved following the absorption of a photon: $AB + h\nu \rightarrow A + B$. Typical covalent bond strengths are above >5 eV and UV photons are thus required. Most molecules can be directly photodissociated through the absorbance of a photon into a dissociative electronic state, and therefore by all photons above some energy threshold. H_2 and some other small molecules are dissociated through absorption of photons at specific frequencies, i.e. by resonance line photons. In these cases the photon absorption initially excites the molecule into an excited bound state, which can

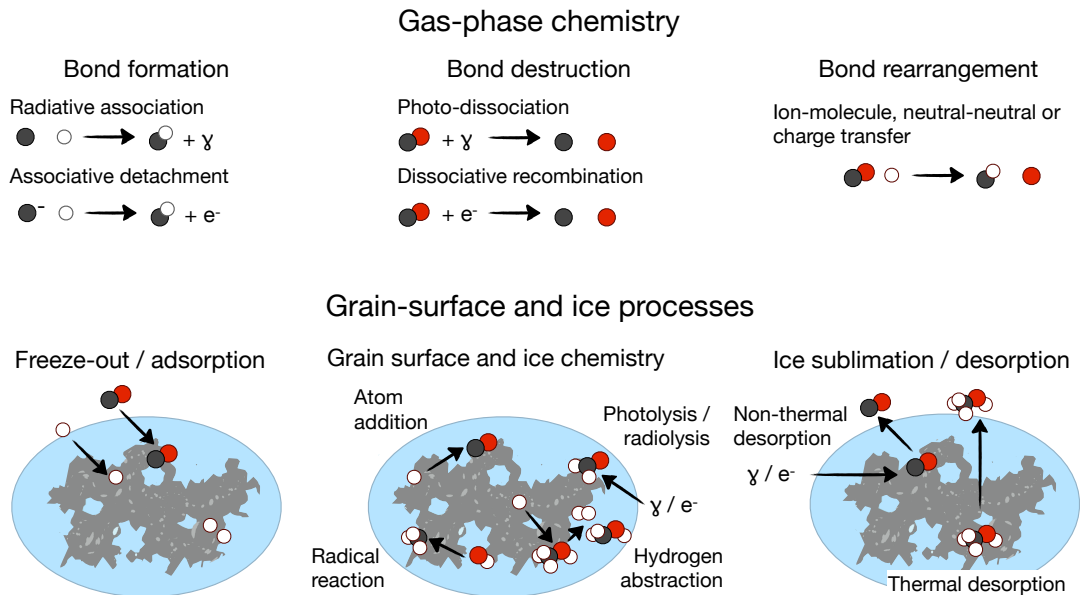


FIG. 3.— Common chemical reaction types in interstellar and circumstellar media. The top row lists reactions in the gas-phase that leads to bond formation, destruction and rearrangement, respectively, while the bottom row focuses on grain surface reactions and grain-gas interactions.

either cross over into a dissociative state (predissociation), or spontaneously decay into a dissociative state (spontaneous radiative dissociation) (van Dishoeck and Black 1988; Lee et al. 1996). For molecules that are only dissociated at discrete frequencies and abundant (especially H_2 and CO), self-shielding is often more important than shielding by dust. Photodissociation in an astrophysical context is described in detail by Hollenbach and Tielens (1999) and photodissociation rates and cross sections are found in Heays et al. (2017).

The final group of gas-phase reactions are those that result in a bond rearrangement, i.e. reactions of the type $AB + C \rightarrow A + BC$. Note that in this case there is no need to radiate away excess energy, since the net bond formation energy is carried away by A as kinetic energy. These reactions typically involve radicals or ions or both. The importance of ions for molecule formation and evolution in the dense interstellar medium was noted in the early 1970's by Herbst and Klemperer (1973). Ion-molecule reactions are typically exothermic, required at the low temperatures of most regions of interest to us, and reactions between ions and symmetric molecules with no permanent dipoles have a temperature-independent rate coefficient due to long-range charge interactions via an induced dipole which is modeled using the Langevin rate: $2\pi e\sqrt{\alpha/\mu}$ (for a complete chemical reference: Levine 2009). Here α is the molecular polarizability and μ the reduced mass. Higher, temperature-dependent, rates are found in the presence of a permanent dipole for the neutral molecule (Adams et al. 1985).

In diffuse media, and at the edges of dense clouds, surfaces of disks and other exposed regions, ions are produced through photoionization: $X^r + h\nu \rightarrow X^{r+1} + e^-$. The widespread presence of hydrogen atoms within the Galaxy means that UV photons with energies that exceed the hydrogen ionization threshold of 13.6 eV ($\lambda < 912 \text{ \AA}$) are largely absent. Photoionization of H and other atoms, and its balance with recombination is reviewed by Ferland (2003). In dense interstellar and circumstellar environments, the central molecule powering the gas phase chemistry is H_3^+ , which is a product of cosmic ray or X-ray ionization of H_2 (Graedel et al. 1982; Herbst and Leung 1989; Millar et al. 1991; Cleeves et al. 2013). The H_3^+ density generally regulates the gas-phase chemical timescale, and because the space density of H_3^+ is close to constant with density, so is the overall gas-chemical timescale (Lepp et al. 1987).

Though ion-molecule reactions are central in astrochemistry networks, there is also a large number of neutral-neutral reactions that have significant import. For example, the formation of water in hot ($T > 400 \text{ K}$) gas is powered via $\text{O} + \text{H}_2 \rightarrow \text{OH} + \text{H}$ followed by $\text{OH} + \text{H}_2 \rightarrow \text{H}_2\text{O} + \text{H}$ (Wagner and Graff 1987). A more general discussion of astrochemical reactions can be found in Herbst (1995) and Wakelam et al. (2010). In the past couple of years there has been increasing realization that neutral-neutral reactions govern some of the cooler astrochemistry, including the formation of some organic species (Shannon et al. 2013; Balucani et al. 2015).

A completely different set of chemical considerations are related to the presence of interstellar dust grains (e.g. Hasegawa et al. 1992; Hasegawa and Herbst 1993; Garrod et al. 2008). Grains are rare compared to gas-phase molecules, but play a large role in regulating astrochemical structures. First they act as sinks of gas-phase atoms and molecules. Grains are cool ($< 30 \text{ K}$) in most star and planet forming environments, and $< 10 \text{ K}$ in prestellar cores (Crapsi et al. 2007; Pagani et al. 2007). Atoms and molecules that collide with a cold grain, with the exception of H_2 and He, will adsorb or freeze-out/condense¹ onto the grain. Together with chemical reactions between adsorbed

¹ In the strict chemical sense, given the low pressures of interstellar space, the physical process involved for the vapor to solid transition is deposition. However, in the astrophysical and cosmochemical literature it is common to label this transition as condensation.

molecules and atoms on the grain surfaces, this freeze-out process results in the build-up of icy grain mantles.

The adsorption of gas-phase atoms and molecules can be described as a grain-atom/molecule collision as long as the sticking probability is high. The gas deposition timescale (and any timescale that depends on deposition/freeze-out) therefore has an inverse dependence on density:

$$\tau_{\text{gas-grain}} = 1/x_{\text{gr}}n_{\text{H}_2}\sigma_{\text{gr}}v_{i,\text{gas}} \quad (1)$$

In this equation x_{gr} is the abundance of cold grains, σ_{gr} their surface area, and $v_{i,\text{gas}}$ the thermal velocity of the particular molecule i . Interstellar grains are characterized with a size distribution that follows an powerlaw of size a distributed by $a^{-3.5}$ with sizes ranging from large molecules (~ 10 Å) to large grains with $a \sim 0.25$ μm (Mathis et al. 1977). Thus there is more surface area in small grains, while the mass resides in the larger grains (Draine 1995).

Once atoms/molecules are on the ices, the initial chemistry is dominated by H atom addition (Hasegawa et al. 1992). It has long been known that the most abundant molecule in space, H_2 , is required to form via grain surface catalytic chemistry (Gould and Salpeter 1963; Hollenbach and Salpeter 1971; Wakelam et al. 2017). H atom additions to heavier atoms such as O leads to the formation of water and other saturated species up to methanol (CH_3OH) in size (Tielens and Hagen 1982). Note that these reactions are effectively three-body reactions, with the grain acting as the third body, adsorbing the bond formation energy; i.e. the grain acts as a catalyst. Once CO, the most abundant molecule produced through gas-phase chemistry, begins to freeze out, there is also an important CO-mediated chemistry to form e.g. CO_2 .

Reactions on grain surfaces and in icy grain mantles can also produce more complex molecules. Figure 4 shows four proposed and experimentally verified pathways to complex organics originating in the ice mantles of interstellar grains. Radicals produced via UV or electron-mediated dissociation, or via hydrogen addition and abstraction, can recombine to produce more complex molecules (Garrod et al. 2008; Bennett et al. 2007; Öberg et al. 2009b; Chuang et al. 2017). These reactions can proceed at all temperatures between neighboring radicals, and throughout the ice if the grain is heated to above ~ 25 K, enabling radical diffusion. Oxygen insertion into hydrocarbons produces alcohols and aldehydes (Bergner et al. 2019b) in ices as cold as 10 K, and may produce complex organics in low-temperature environments. Finally, sublimated methanol ice can seed a complex gas-phase chemistry at a range of gas temperatures (Charnley et al. 1992; Balucani et al. 2015; Vasyunin et al. 2017).

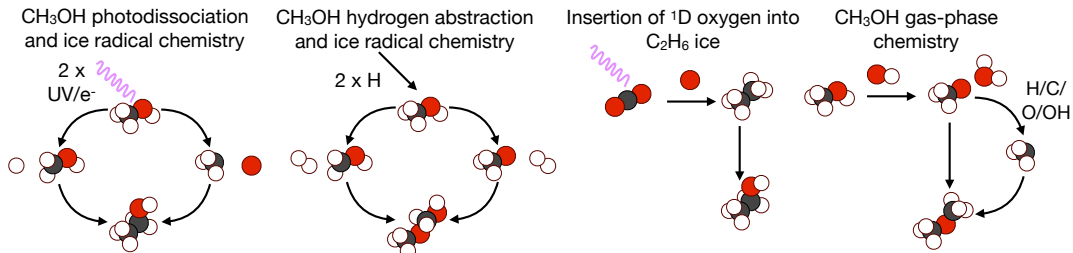


FIG. 4.— Four proposed pathways to forming O-rich organics during star and planet-formation. The multitude of pathways and a similar diversity in pathways to hydrocarbons and N-containing complex organics probably explains why complex organics are present in many kinds of interstellar and circumstellar environments. Note that a majority of the displayed chemistry is barrierless, but e.g. the radical ice chemistry is still faster at elevated temperatures because of faster radical diffusion through the ice.

Grain surface and ice species sublime through thermal desorption, photodesorption and electron stimulated desorption, release of chemical energy during a chemical reaction, grain-grain collisions and other energetic events. Thermal desorption tends to dominate the grain-gas balance in protostellar envelopes and other heated regions (Léger et al. 1985), while photodesorption regulates the gas-grain balance in UV exposed regions (Hollenbach et al. 2009). In cold, UV-shielded regions, desorption through release of chemical energy is suspected to be the dominant desorption mechanism (Garrod et al. 2007). Thermal desorption has been characterized for most common grain surface species (e.g. Fraser et al. 2001; Collings et al. 2004; Öberg et al. 2005), and found to be quite complex; the desorption barrier of some species is very sensitive to the details of the ice matrix (e.g. Fayolle et al. 2016). Based on information from laboratory, and the general physics behind physical adsorption, we can classify volatiles based upon their sublimation temperatures. CH_4 , CO and N_2 have the highest volatility with sublimation temperatures near 20-40 K (depending on the surface and pressure); these can be classified as hypervolatiles. Other species, such as water, CH_3OH , CO_2 , and NH_3 can be denoted as volatiles. Finally, of course, silicates and carbonaceous grains have the lowest volatility and are classified as refractories.

Of the different non-thermal desorption mechanisms, photodesorption has been most extensively explored via laboratory experiments in the past decade. Early experiments demonstrated that UV photodesorption is highly efficient (Westley et al. 1995; Öberg et al. 2007, 2009a,c), while molecular dynamics simulations (Andersson et al. 2006; Andersson and van Dishoeck 2008) revealed that the process can be quite complex and occur through several different channels, even for the same molecule. Most of the theoretically predicted channels have since been seen in experiments (Fayolle et al. 2011; Bertin et al. 2013). More recently, experiments on chemical desorption have begun to constrain this important process (e.g. Minissale et al. 2016).

1.3. Methods of astrochemistry

1.3.1. Astronomical observations

The nearest active star and planet forming regions are ~ 100 pc away and remote sensing is therefore the only option to obtain direct, empirical evidence of the chemistry that impacts planet formation. An important exception to this principle is the solar system, where the chemical composition of comets, asteroids, planets, and moons, all encode information about their formation conditions. Missions to comets, asteroids, and planets, along with remote observations of these same bodies, have provided invaluable information about their chemical make-up, which has then been used to map out the origins of their different constituents. For example the elevated D/H ratio found in terrestrial, asteroid and cometary water has been used to demonstrate that their water reservoirs to a large extent are inherited from the cold interstellar medium (Cleeves et al. 2014).

Yet most astrochemical observations are remote. A central limitation of these remote observations is the fact that H_2 is unemissive at the temperatures and densities characteristic of mass reservoirs throughout the phases of star and planet formation (Evans et al. 2003). To determine chemical abundances in each phase requires the use of calibrated probes, such as CO isotopologues and optically thin thermal continuum emission from dust grains, to determine the hydrogen content and therefore the total gas mass (for greater discussion see, Bergin and Williams 2017). More broadly, beyond H_2 and CO, there are a host of detectable emission lines arising from electronic, vibrational, torsional, and rotational states of hundreds of species, which together can be used to probe the physical and chemical characteristics of specific regions.

In principle, astrochemical observations are possible at all wavelengths where molecules emit and absorb photons at discreet energies, i.e. from UV to radio wavelengths. In practice the vast majority of astrochemical observations are, however, carried out at longer wavelengths, at infrared (IR), far-IR or Terahertz, sub-millimeter and millimeter, and radio wavelengths. Molecular spectral features at near and mid-IR wavelengths are generated by molecular vibrations, and are used to probe both gas-phase and solid-state compositions (van Dishoeck and Blake 1998; van Dishoeck 2006; Pontoppidan et al. 2014; Boogert et al. 2015). For gas-phase molecules, most studies have focused on warm enough gas that the lines are in emission. Solid-state compositional studies, are by contrast mainly carried out in absorption because ice mantles would sublime before they can be heated enough to emit at near to mid-IR ($< 20\mu\text{m}$) wavelengths (e.g., Boogert et al. 2015); emission is detectable at longer wavelengths (McClure et al. 2015; Min et al. 2016; Kamp et al. 2018). Some IR observations can be carried out from the ground, but complete IR spectral coverage is only possible from space, and the most recent IR mission is the Spitzer Space Telescope. Far-IR or Terahertz spectroscopy are exclusively possible from space (e.g. the Herschel Space Telescopes), or very high altitudes (SOFIA). These wavelengths give access to the fundamental rotational transitions of light hydrides such as H_2O (van Dishoeck et al. 2014), and HD (Bergin et al. 2013).

Moving to longer wavelengths, submillimeter and millimeter observations are possible from the ground, but the shorter wavelengths require exceptionally dry locations, motivating the placement of the Atacama Large Millimeter and submillimeter Array (ALMA), in the Atacama dessert. Most small and mid-sized molecules, including CO (Wilson et al. 1970), HCN and CH_3OH , have their fundamental transitions in this wavelength regime, and a majority of molecular observations make use of this wavelength regime. These transitions are sufficiently low energy to be excited even in the coldest interstellar and protoplanetary disk conditions, where temperatures are < 20 K. The longest wavelengths, beyond 3 mm enable accurate observations of large organic molecules (e.g. McGuire et al. 2018). Through these different kinds of astronomical observations more than 200 molecules have been identified in interstellar and circumstellar environments, the vast majority of which are organic (McGuire 2018).

Interpreting these observations relies on detailed radiative transfer codes, and other methods to estimate molecular abundances and excitation temperatures from molecular line observations. The reader is referred to the following references: Hogerheijde and van der Tak (2000), Brinch and Hogerheijde (2010), van der Tak (2011), Dullemond et al. (2012), and Shirley (2015)

1.3.2. Astrochemical models

Our theoretical understanding of astrochemical processes rely on a range of modeling techniques, each of which makes a different compromise between computational accuracy and computational speed. The different theoretical tools are reviewed in detail by Garrod and Widicus Weaver (2013), and Cuppen et al. (2013), and are briefly summarized here. The most computational expensive models are *ab initio* quantum mechanical calculations, which are employed in astrochemistry to calculate photodissociation cross sections, collisional excitation coefficients, reaction potentials, and some molecule-grain surface interactions (e.g. Heller 1978; Green and Chapman 1978; van Dishoeck and Black 1988; Schöier et al. 2005). Molecular dynamics (MD) simulations use these reaction potentials to calculate how molecules react on pico-second timescales using classically calculated trajectories (e.g. Andersson et al. 2006). Within astrochemistry, MD simulations has been used to uncover ice reaction mechanisms that can then be parametrically incorporated into higher-level modeling efforts.

Longer simulations require that reaction probabilities are parameterized, which is done through so called microscopic or kinetic Monte Carlo models. In these precise kinetic models, the motions of individual atoms, radicals and molecules are followed on top of and inside of ice mantles based on calculated probabilities. These models are typically employed to investigate specific grain-surface chemical processes, such as H_2 or CH_3OH formation. For grain surface processes this detailed treatment is important, since only considering the chemistry statistically can yield misleading results (e.g. Tielens and Hagen 1982; Cuppen et al. 2009). For larger networks consisting of more than a handful of species

and 10s of reactions, microscopic Monte Carlo simulations become intractable.

The next level of theory consists of macroscopic stochastic or rate equation models, both which are routinely employed to carry out comprehensive models of gas-phase and solid-state interstellar chemistry. In macroscopic Monte Carlo models, the master equation for the combined gas-phase and surface chemistry is solved using Monte Carlo techniques (Tielens and Hagen 1982; Charnley 1998; Vasyunin et al. 2009). These models employ averaged grain-surface reaction rates, and couple them with gas-phase chemistry, producing exact gas-phase and grain-surface populations for each chemical species, under the assumption that the detailed ice structure captured in the microscopic models is not important.

The most comprehensive astrochemistry models, in terms of number of species and reactions, exclusively use the rate equation approach or some modification of it. In these models a set of ordinary differential equations that describes the gas-and grain-phase chemical kinetics is solved to produce time dependent abundance information for each chemical species as the gas and ice are exposed to constant or changing physical conditions. Over the past 20 years detailed chemical networks have been constructed that are now widely applied to chemistry of dense cloud cores, planet-forming disks, and circumstellar envelopes (McElroy et al. 2013; Wakelam et al. 2015). Rate equation models have evolved in sophistication to compete in accuracy with macroscopic Monte Carlo methods (Garrod 2008). One important feature of most contemporary rate equation models is the treatment of ice surfaces separate from ice layers (Hasegawa and Herbst 1993), and so called three-phase models (ice mantle, ice surface and gas-phase) are now standard (Vasyunin and Herbst 2013; Garrod 2013). In addition, Cuppen et al. (2017) provide a detailed discussion of the inclusion of grain surface chemistry into networks.

The final class of chemical models are ones that link the gas-phase/gas-grain chemical evolution to the thermal properties of the gas and dust. Atomic (Dalgarno and McCray 1972) and molecular (Goldsmith and Langer 1978) emission are primary coolants for the gas in regions where the density is below where the gas and dust temperatures are decoupled; this occurs at densities of $\sim 10^5 \text{ cm}^{-3}$ for interstellar dust mixture and size distribution (Burke and Hollenbach 1983). Thus the chemistry can be intimately coupled to the resulting gas temperature. This class of models are labelled as thermochemical models and have been applied to the general interstellar medium (Wolfire et al. 1995), dense clouds exposed to enhanced radiation fields (Tielens and Hollenbach 1985; Sternberg and Dalgarno 1995; Kaufman et al. 1999; Le Petit et al. 2006), and protoplanetary disks (Gorti and Hollenbach 2004; Woitke et al. 2009; Kamp et al. 2010; Bruderer et al. 2012; Du and Bergin 2014).

1.3.3. Laboratory experiments

Most astrochemical processes cannot be calculated from first principles with sufficient precision. Rather, astrochemical models rely on laboratory experiments to anchor calculations of spectra of interstellar and circumstellar molecules, and of molecular and atomic excitations, and to predict the outcome of astrochemical reactions.

Spectroscopy. Molecular spectra cannot be calculated *a priori* to the precision required for identifications of interstellar spectral lines with specific carriers. Laboratory measurements of molecular spectra across the electromagnetic spectrum is a cornerstone for the astrochemical project (Widicus Weaver 2019). Spectral measurements of stable molecules are relatively straightforward in the gas-phase. Yet data-bases are far from complete, especially for isotopologues of common interstellar molecules (Müller et al. 2005). Spectra of radicals and ions are more cumbersome to obtain since they require the ionization or dissociation of a precursor. This produces a mixture of species due to multiple dissociation products and/or subsequent chemistry, and the resulting spectra need to be carefully analyzed to identify the lines belonging to the target molecule (e.g. McCarthy et al. 2006; Bizzocchi et al. 2017).

Spectra of ices are acquired in high or ultra-high vacuum chambers where thin (nm- μ m) ices are vapor-deposited before measuring their infrared or far-infrared spectra (e.g. Hagen et al. 1983). Ice spectroscopy differs from gas-phase spectroscopy in one important aspect, which is that the spectral band position, shape and strength depends on the nature of surrounding molecules. Detailed spectroscopic studies of the target molecule in different ice environments is therefore needed to characterize ice mantles in space (e.g. Gerakines et al. 1995; Ehrenfreund et al. 1996). There are multiple gas-phase and solid-state spectral databases serving the astrochemistry community, including the JPL spectral database, the Cologne Database for Molecular Spectroscopy (CDMS), Splatalogue, the Leiden ice database (<http://icedb.strw.leidenuniv.nl>) and the NASA Goddard Cosmic Ice Laboratory IR spectra database (<https://science.gsfc.nasa.gov/691/cosmicice/spectra.html>).

Molecular Excitation. Molecules can relax and release quantized amounts of energy via rotation/vibrational motions and electronic excitation. Transitions associated with rotational motions are powered by a rotating dipole corresponding to the lowest change in energy of tens to hundreds of Kelvins and are found at ($\Delta E = hc/\lambda$) mm/sub-mm wavelengths, while vibrational modes have $\Delta E \sim 0.1 \text{ eV}$ or 1000 K, observed in the infrared, and electronic transitions occur $\sim 10\text{eV}$ or 100,000 K corresponding to UV wavelengths. In star and planet forming regions most of the mass is at cold ($T < 100 \text{ K}$) temperatures, where only rotational transitions are excited. IR lines are also important, however, and are observed in absorption in cold regions, and in emission close to young stars. The reader is referred to the textbooks of the field to explore these questions more thoroughly from perspective of molecular physics (Herzberg 1950; Townes and Schawlow 1955; Gordy and Cook 1970).

In interstellar and circumstellar regions of interest to this review, the emission of atoms and molecules is generally excited via collisions with molecular hydrogen with temperature-dependent excitation cross-sections ($\langle \sigma v \rangle$) that are specific to H_2 (for details see, Flower 2012). In the densest interstellar and circumstellar regions, the details of the excitation process are not important, since local thermal equilibrium (LTE) can be assumed. In many, if not most,

'dense' astronomical regions the densities are not sufficient for LTE to hold, however and the collision rates are key to use molecular emission to derive molecular abundances, as well as to use molecular emission as tracers of gas densities and temperatures. The collision rate for molecule X is $n_X n_{H_2} \langle \sigma v \rangle$, and thus depend on H_2 space density, gas temperature and the collisional excitation cross section. For detailed discussion of this topic, and the methods used to determine the H_2 density and temperature, along with molecular abundance, the reader is referred to Evans (1999), Goldsmith and Langer (1999), Shirley (2015), and Mangum and Shirley (2015). The different techniques that have been developed to obtain collisional excitation data are summarized in a review by Smith (2011).

Gas-phase reactions. Smith (2011) also reviews experimental techniques for characterizing astrochemically relevant gas-phase reaction rates, and product branching ratios. The experimental apparatus used to obtain these depend on the reaction under investigation. Ion-neutral reactions where the neutral is a stable molecule are relatively straightforward to quantify using ion traps and flow tubes, and the experiments tend to agree with theoretical calculations within a factor of 3. Two important developments of the past few decades are the so called Selected Ion Flow Tube method where the reactant ion is mass selected and the reaction rate can therefore be measured with great precision (Martinez et al. 2008), and the CRESU apparatus, which enables the measurements of reaction rates at very low temperatures due to rapid, supersonic expansion of reactant gas (Sims et al. 1993). Low temperature measurements are important since it is difficult to predict the temperature dependence of reaction rates at low temperatures based on room temperature experiments.

Neutral-neutral reactions are more challenging to characterize, especially between unstable species, due to difficulties in mass-selecting neutral molecules and radicals. A small number of reaction systems have, however, been explored using either the flow tubes and the CRESU method. A key discovery from these experiments is that the rate coefficients of many neutral-neutral reactions increase with decreasing temperature, often in contradiction with pre-existing calculations. This characteristic has resulted in a re-evaluation of the importance of neutral-neutral reactions in cold interstellar and circumstellar environments (Smith 2011).

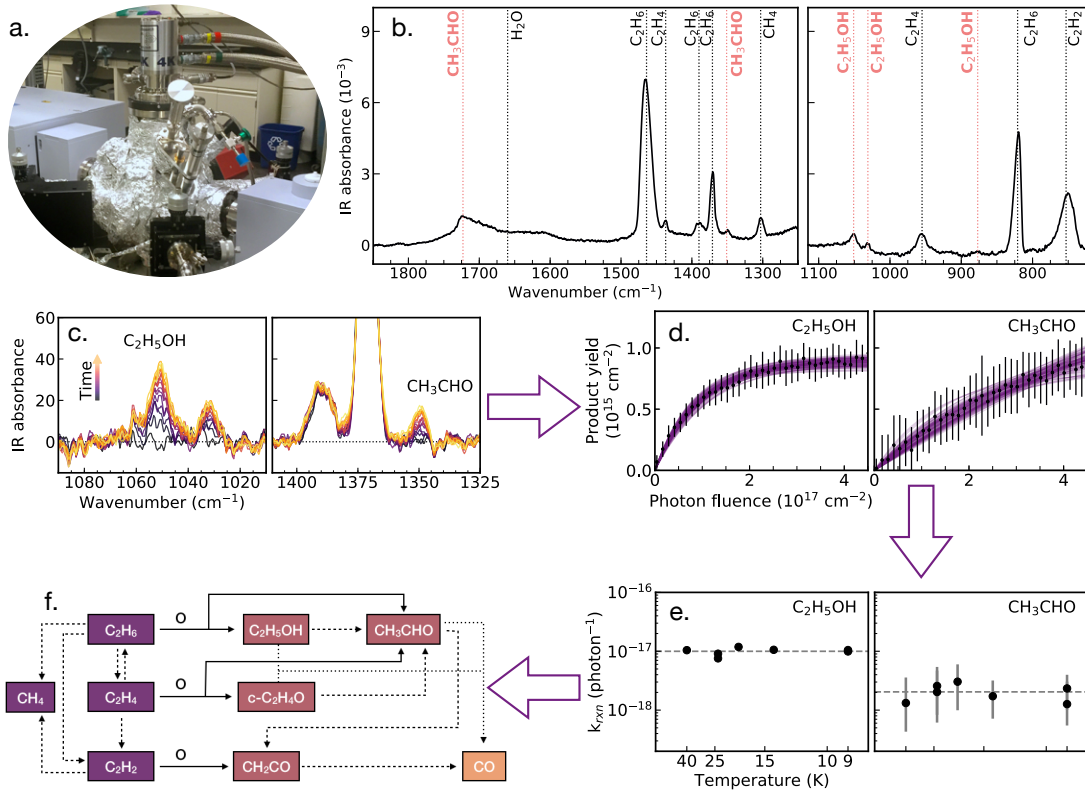


FIG. 5.— Flowchart for a typical astrochemistry solid-state experiment, using data from Bergner et al. (2019b). Experiments are carried out in vacuum chambers (a), where an initial ice is deposited on a substrate. The ice is exposed to atoms, heat or energetic processing and the chemical products are identified using spectroscopy (b), or mass spectrometry following ice desorption. If the ice products are monitored over time (c), product growth curves can be modeled (d) to obtain rate coefficients. By comparing rate coefficients obtained at different ice temperatures, the reaction barrier can be determined (e). This quantitative information, together with a qualitative identification of reaction products in different ice experiments can then be used to assemble astrochemically relevant reaction networks (f).

Solid-state reactions. The chemical abundances on the surface of interstellar grains depend on a combination of adsorption, desorption, diffusion and surface chemical reactions. These are characterized using surface-science ap-

paratuses designed to mimic the high vacuum and range of temperatures (down to 4 K) characteristic of interstellar environments. Three kinds of experimental domains can be identified, those dealing with warm grains where chemisorption is important, those dealing with bare grains, and those dealing with ice covered grains. The first kind of experiment addresses e.g. H_2 formation in the warm, diffuse interstellar medium, where the residence time of any atom would be too short unless chemical binding between the incoming atom and the surface is invoked.

In the first family of experiments, graphite analogs are exposed to (H) atoms followed by mass-spectrometric or microscopic monitoring of reaction kinetics (e.g. Rauls and Hornekær 2008). Experiments on cold bare grains are most commonly simulated by exposing cryo-cooled silicate and graphite surfaces to atomic beams followed by temperature programmed desorption experiments (TPD) where the surface is rapidly heated up while the chamber is monitored mass-spectrometrically (e.g. Katz et al. 1999). Finally, as illustrated in Fig. 5, experiments aimed at understanding the chemistry of ice covered grains typically proceed by exposing a cryo-cooled metal or glass surface to a molecular beam of water vapor or another common interstellar gas (mixture) to build up a thin (nm to 10s of nm) ice. This ice is then exposed to atoms, UV photons, electrons, X-rays, energetic particles or heat, and ice desorption, restructuring, and chemistry is monitored using infrared spectroscopic and mass-spectrometric techniques (e.g. Watanabe and Kouchi 2002; Öberg et al. 2015).

2. SETTING THE CHEMICAL TRAJECTORY: THE CHEMISTRY OF PLANET FORMATION BEGINS IN MOLECULAR CLOUDS AND CLOUD CORES

There is growing evidence that the chemistry present in planet-forming disks is intimately linked to the coupled physical and chemical processes that regulate chemistry in the interstellar medium. It is in interstellar clouds, and even during their assembly, that the major volatile carriers of oxygen, carbon and nitrogen form: H_2O , CO , and N_2 . These carriers remain the major ones through the later star and planet-forming phases, and their relative volatility and chemical reactivity are key to understand how the chemistry evolves during planet formation. The first objective of this section is to review why so much oxygen, carbon and nitrogen become incorporated into just these three carriers. The volatile reservoirs of two other elements, sulfur (S) and phosphorous (P), should also be established in the dense cloud stage. Our understanding of the S and P chemistry is much less mature, however, and apart from a short section in § 4.4, we do not treat these two prebiotically important elements in detail in this review. The reader is instead referred Vidal et al. (2017); Vastel et al. (2018); Laas and Caselli (2019); Le Gal et al. (2019a) and Lefloch et al. (2016); Ziurys et al. (2018); Jiménez-Serra et al. (2018); Bergner et al. (2019c); Rivilla et al. (2020) for some recent developments in our understanding of S and P astrochemistry, respectively.

Molecular clouds and cloud cores are also the formation sites of the most abundant volatile organics during planet formation – CH_4 and CH_3OH (Mumma and Charnley 2011) – as well as the pre-biotically interesting NH_3 . These are the building blocks of any proceeding complex organic chemistry and their initial abundance may effectively limit how many large organic molecules can form in the later protostellar and protoplanetary-disk stages. The second objective of this section is to review the chemistry responsible for NH_3 , CH_4 and CH_3OH production in clouds and how it relates to the formation of the major oxygen, carbon, and nitrogen carriers H_2O , CO , and N_2 .

Finally, molecular clouds and cloud cores are sites of isotopic fractionation, the fingerprint of which is seen today in solar system water (as one example). Deuterium enrichments that can be linked to low-temperature fractionation processes are found in the Earth’s ocean, as well as in cometary ices, and they represent our most important evidence connecting solar system chemistry to interstellar chemistry. There are several chemical processes through which molecules can become enriched or depleted in heavy, stable isotopes, and the final objective of this section is to review the physics and chemistry behind interstellar isotopic fractionation, especially how it pertains to deuterium fractionation in cold cloud cores.

Before treating these specifics it is useful to consider the overall chemical structure of molecular clouds. In the molecular cloud stage, key quantities that influence the overall chemical trajectory are the radiation field (cosmic rays, X-rays, UV radiation), gas and dust temperature, and gas density. These quantities are both time and location dependent. As clouds compact they become denser, and therefore colder and less permeable to radiation, while in an already compact, dense cloud, the exposed edges are warmer and more irradiated than the shielded interiors. In both the time-dependent and cloud-depth dependent description of cloud chemistry, the chemical structures initially (or closer to the cloud surface) depend on an interplay of photon-mediated processes (photoionization, photodissociation, photon-heating, and photodesorption), and molecular formation through gas and dust surface chemical processes. In the more shielded cloud regions (or later times) the chemistry instead becomes regulated by a competition between gas-phase chemistry, and increasing freeze-out of molecules from the gas-phase onto dust grains.

Figure 6 shows an illustration of the resulting chemical structures of clouds, where the x-axis reflects depth into a cloud. In astronomy, such UV-exposed molecular cloud edges are traditionally characterized as Photo-Dissociation Regions or PDRs (Tielens and Hollenbach 1985; Hollenbach and Tielens 1999). When viewed edge-on, these regions display characteristic chemical layers associated with increasing UV attenuation. Indeed, Fig. 6 illustrates the chemical depth-dependent transitions for the most abundant elements (except for He), i.e. H/H_2 , $\text{C}^+/\text{C}/\text{CO}/\text{CO}(\text{gr})$, $\text{O}/\text{CO}+\text{H}_2\text{O}(\text{gr})$, $\text{N}/\text{N}_2/\text{N}_2(\text{gr})$, where (gr) marks a species that has frozen out on a grain surface. The same kind of chemical transitions are expected in all interstellar and circumstellar regions that are externally illuminated, and classical PDR chemistry are therefore also considered model systems for understanding chemical layering in planet forming disks (van Zadelhoff et al. 2001; Le Gal et al. 2019b). We note that Fig. 6 would look qualitatively the same if the x-axis instead reflected time during cloud assembly and compaction (Bergin et al. 2004b; Glover and Mac Low 2007). We can therefore use this classical PDR framework to explain the chemical trajectory present during cloud

formation and core condensation, and in particular to address our three objectives to explain oxygen, carbon and nitrogen carriers throughout star formation, origins of common organics, and the presence of high levels of isotopic fractionation.

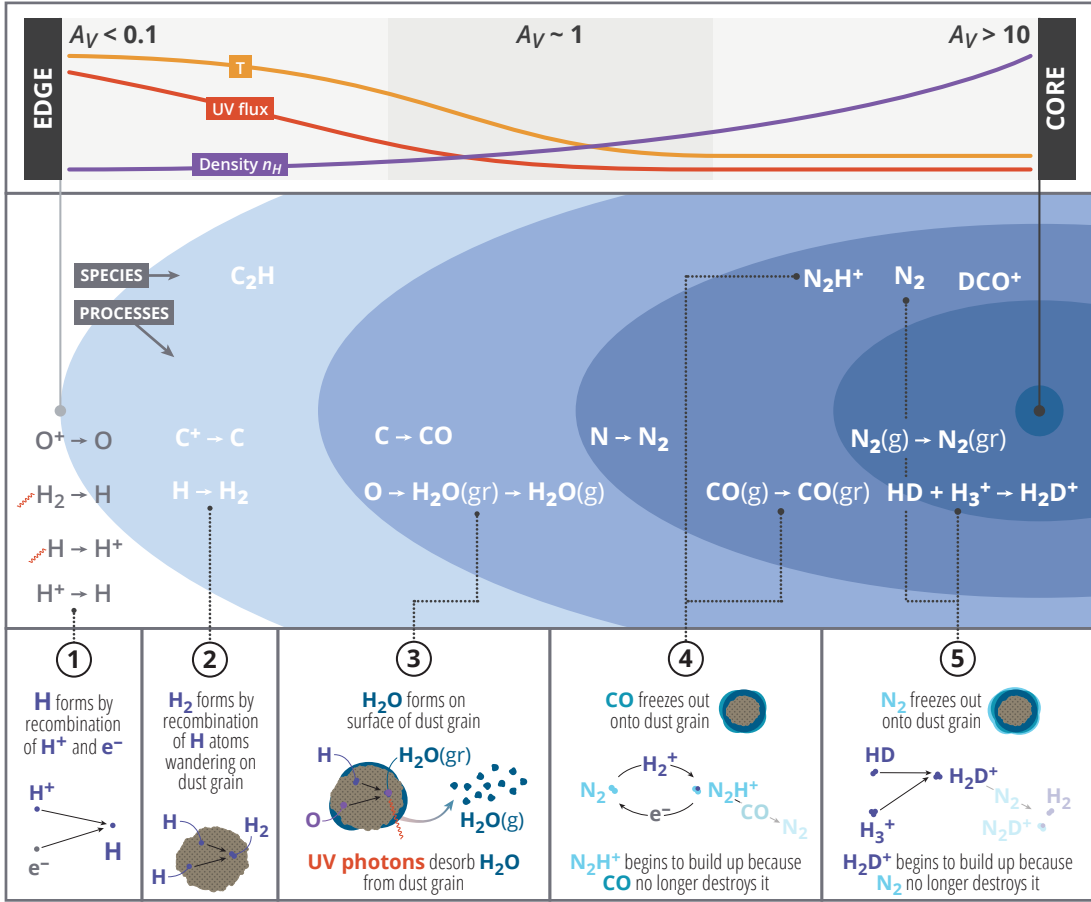


FIG. 6.— Illustration of the chemical structure of a molecular cloud from the UV exposed cloud edge (left) to the protected cloud core (right), where cloud depth is parameterized by extinction (measured in visual magnitudes A_V). At the cloud edge, the most energetic UV photons, capable of ionizing H and O have already become fully absorbed. In the outer cloud layers carbon transitions from atomic ions to neutral atoms, and hydrogen from atoms to molecules. In the inner surface layer carbon is rapidly converted to CO, effectively locking in most of the volatile carbon budget. In the same cloud layer the remaining oxygen is mainly incorporated into the much less volatile water. Most nitrogen is expected to become incorporated into the hypervolatile N_2 , but a substantial amount may also be present as NH_3 , already in the water formation zone. In the deepest molecular cloud region, all molecules except for H_2 , H_3^+ and their isotopologues rapidly freeze-out onto grains, resulting in a volatile-depleted gas, and efficient deuterium fractionation. While this cartoon primarily presents a static view of the cloud chemical structure, it also illustrates what happens as a function of time (going from left to right), when a package of diffuse cloud material compacts to form a dense cloud. Image credit: K. Peek, after the PDR illustration presented in Tielens and Hollenbach (1985).

2.1. Origins of Major Oxygen, Carbon and Nitrogen Volatiles: Photodissociation vs Formation

The major volatile carriers of oxygen, carbon, and nitrogen form in molecular clouds. Why some species and not others end up dominating the oxygen, carbon, and nitrogen budget primarily depends on an interplay between photodissociation and gas-phase formation, and secondarily, how readily the products of this initial gas-phase chemistry can be converted into other molecules.

As introduced above, the interstellar regions where photodissociation regulates the chemistry are referred to as PDRs. PDRs are most readily identified at the edges of dense clouds that face massive stars and are thus exposed to high levels of UV radiation. Indeed these are typically referred to as ‘Classical PDRs’, and a famous example is the Horsehead Nebula, whose chemical structure is shown in Fig. 7. Molecular clouds that are not directly exposed to massive stars still always experience some level of irradiation and their outer structures too are determined by photoprocesses. In both scenarios, photons with energies higher than 13.6 eV become fully absorbed by atomic hydrogen at some distance from the cloud edge, resulting in a H^+/H transition (Fig. 6). Other species that require photons >13.6 eV, e.g. atomic oxygen, also transition to their neutral form at this boundary between a predominantly ionized and neutral medium. Species that have lower ionization energies, i.e. carbon, remain largely ionized.

The second major transition is between H and H_2 , which occurs when H_2 formation on grains out-competes H_2 photodissociation, which has a threshold of 11.2 eV. As described above, H_2 efficiently self-shields and this boundary

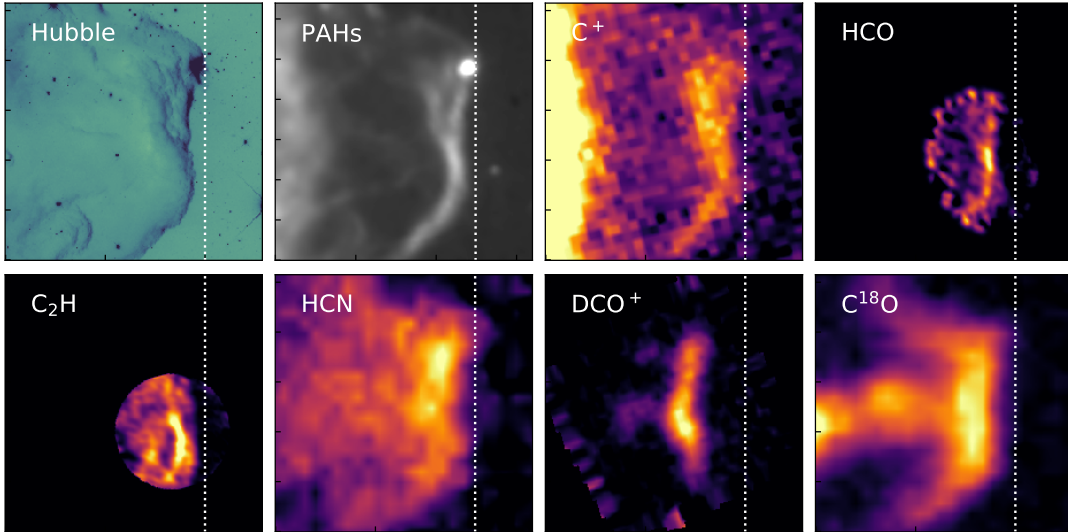


FIG. 7.— Observations of the Horsehead nebula in infrared light from HST’s WFC3 infrared camera (Hubble legacy archive), PAHs (Abergel et al. 2003), C^+ (Bally et al. 2018), and five different molecular tracers: HCO, C_2H , HCN, DCO^+ , and $C^{18}O$ (Gerin et al. 2009; Pety et al. 2005, 2007, 2017). The dotted line shows the edge of the C_2H emission in all panels, denoting the edge of the molecular layer in the PDR. Note the different chemical layers probed by different species, i.e. C^+ and polycyclic hydrocarbons (PAHs) emit close to the surface, most molecules somewhat further into the cloud, and DCO^+ deep into the cloud core. Image credit: V. Guzmán

is obtained when a certain hydrogen column is between the cloud and the ionizing source. This boundary marks the edge of the dense molecular cloud (Narayanan et al. 2008). Concomitant with the selective shielding of UV photons by H_2 , a combination of self-shielding and overall UV attenuation by dust results in a slow transition between C^+ and C. C is a starting point of an efficient oxygen-poor organic chemistry resulting in e.g. the build-up of C_2H in these outer cloud layers. At this point most oxygen, carbon, and nitrogen are in their atomic form, and what happens next is what determines the different chemical trajectories and reservoirs of these three elements.

Interior to the H-to- H_2 transition layer, CO formation becomes efficient enough to build up sufficient CO column density to self-shield against the still pervasive interstellar radiation field (van Dishoeck and Black 1988). The ability of CO to self-shield effectively locks up most of the available carbon into CO, making it the main volatile carbon reservoir from this stage and onwards. The rapid conversion of carbon into CO, and the very slow conversion of CO into other molecules up until the disk stage, makes it an excellent tracer of gas mass, and it is indeed the most common tracer of gas mass through most stages of star and planet formation (see Bergin and Williams 2017, and references therein).

In the same PDR layer, oxygen is efficiently converted into water ice through hydrogen addition to oxygen atoms, and oxygen molecules on the surfaces of dust grains. This process is efficient enough that a majority of the available volatile oxygen goes into water ice, resulting in comparable water ice and CO vapor abundances (Hollenbach et al. 2009). This process also starves the gas-phase of available oxygen which stunts the subsequent gas-phase formation of water vapor and O_2 (Bergin et al. 2000) as evidenced by measured low abundances of water vapor and systemic non-detections of O_2 towards nearly all² lines of sight (Snell et al. 2000; Goldsmith et al. 2000; Pagani et al. 2003; van Dishoeck et al. 2011; Caselli and Ceccarelli 2012; Wirström et al. 2016).

It is an interesting question why CO and H_2O become the dominant carriers of carbon and oxygen rather than say CH_4 , which can form from hydrogen addition to atomic carbon on grain surfaces, and O_2 , which can form through gas-phase chemistry. Some CH_4 certainly does form through grain-surface chemistry, but its abundance is low, a few %, compared to water. The inefficiency of this chemistry can be understood from a delicate balance between rapid conversion of C into CO, just as radiation attenuation becomes high enough to allow for build-up of molecules on grain surfaces – slightly closer to the cloud surface, where C is more abundant than CO, any molecule formed on the grain surface is rapidly photodesorbed and/or photodissociated. Some O_2 also likely forms in this PDR layer, but compared to CO it faces two important disadvantages: it does not self-shield efficiently and is therefore photodissociated deeper into the cloud, and O_2 is relatively easy to convert into water once it adsorbs onto a grain surface, resulting in water ice (Ioppolo et al. 2008).

The case of nitrogen likely mirrors that of carbon, but with some important distinctions. Like CO, molecular nitrogen, N_2 , forms in the gas-phase and it is expected, though not directly proven, that this is the major reservoir of nitrogen (van Dishoeck et al. 1993; Maret et al. 2006; Daranlot et al. 2012; Furuya et al. 2018). N_2 self-shields (Heays et al. 2014), which limits its photodissociation, but because nitrogen has an intrinsically lower abundance than carbon, the self-shielding only becomes effective deeper into the cloud. In addition, N_2 formation chemistry is initiated by slow neutral-neutral reactions (Pineau des Forets et al. 1990; Gerin et al. 1992), and its formation is therefore slower than

² O_2 has surprisingly high abundance in one object, the ρ Oph cloud (Liseau et al. 2012).

ion-molecule fostered production of CO. As a result, nitrogen transitions from N to N₂ at deeper cloud layers. Once N₂ has formed it is chemically very stable, and effectively locks up the nitrogen through the remainder of the star and planet formation process. Because the nitrogen remains atomic for longer than carbon, a substantial portion of N may react with hydrogen on grain surfaces to form NH₃ (Fedoseev et al. 2015), analogous to water formation from atomic oxygen. NH₃ is detected in the icy mantles of interstellar grains, but not at very high abundances (Boogert et al. 2015). It has been suggested, however, that a substantial amount of the NH₃ is hidden as ammonium salts, and that together NH₃ and NH₄⁺ may constitute an appreciable nitrogen reservoir (Boogert et al. 2015; Altwegg et al. 2020).

2.2. Ice formation, and O/C/N budgets

In the previous sub-section, we described how H₂O, CO and N₂ become the most abundant volatile carriers of O, C and N, in molecular clouds, the building material of planetary systems. We now turn to the other important carriers O, C, and N, and how they together set the complete O, C and N budgets.

In molecular clouds, we can observe the sequential build-up of icy grain mantles, which at the onset of star formation constitute the main reservoir of volatiles (except for H₂ and He). Observations of ices in clouds and cloud envelopes surrounding protostars have been previously reviewed by Gibb et al. (2004), Öberg et al. (2011a), and Aikawa et al. (2012), and more recently by Boogert et al. (2015). In addition formation of different ice constituents has been studied experimentally and theoretically. CH₃OH formation from CO was the first system to be investigated in detail (Hiraoka et al. 1998), followed by H₂O from O, O₂ and O₃ (Hiraoka et al. 2002; Watanabe and Kouchi 2002), and CO₂ from CO and OH (Ioppolo et al. 2008; Miyauchi et al. 2008; Mokrane et al. 2009; Dulieu et al. 2010). By now there are experimentally verified atom-addition pathways to all major ice constituents (Ioppolo et al. 2011a). Note that additional ice chemistry may be needed to explain specific aspects of the observed ice morphology, such as the small amount of CO observed to be mixed with water ice (Mennella et al. 2004).

Here we briefly review the observational and laboratory/theoretical results most pertinent for establishing the composition and morphology of typical icy grains during star and planet formation, and the relative importance of different volatile and non-volatile O, C, and N carriers. Figure 8 shows ice spectra observed towards protostars in ρ -Oph F, and how the ice composition changes with distance from the central dense core (Pontoppidan et al. 2008b). As established in the previous sub-section, water ice forms early, and therefore shows up throughout the cloud. The other two major ice constituents, CO and its derivative CO₂, increase in abundance with respect to H₂O towards the cloud core, increasing the C/O ratio in the ice. The rate of increase for CO and CO₂ are quite different, with CO increasing much more rapidly, which suggests that a substantial amount of CO₂ co-forms with the water ice.

Based on these kinds of ice mapping observations as well as detailed characterizations of ice spectra (Pontoppidan et al. 2004, 2008a; Boogert et al. 2008), the initial icy grain mantles are composed mainly of H₂O and CO₂. The early-forming water-dominated ice layer should also be the main host of CH₄ and NH₃, which are expected to form mainly from atomic carbon and nitrogen before N and C are completely converted into CO and N₂, respectively (Tielens and Hagen 1982; Garrod and Pauly 2011). The preference for CO₂ to co-exist with H₂O is explained by its major formation pathway through CO+OH (Ioppolo et al. 2011b; Garrod and Pauly 2011). The OH forms in the ice through H addition to O, and can then either form H₂O through the addition of a second H, or CO₂ through a reaction with a CO molecule residing on the grain surface. The relative mixing ratio of H₂O and CO₂ in this ice layer will depend on the relative reaction rates between OH+H and OH+CO, which in its turn will depend on the gas-phase abundances of CO and H, as well as their different mobilities on grain surfaces.

Closer to the cloud core, elevated densities result in a CO freeze-out rate that is too high for H-atom activated grain-surface reactions to keep up, resulting a mainly CO-containing outer ice mantle. Depending on the exact conditions, some portion of the deposited CO does react with H atoms, produced through cosmic ray interactions with molecular hydrogen even in the densest part of the cloud, to form CH₃OH. Figure 8 (lower panels) illustrates this aspect of layered ice formation, while the upper panels show the rapid increase in CO-ice content deeper into the ρ Oph F core (Pontoppidan 2006). We expect that N₂ is either mixed in with the CO ice or frozen out on top since the N₂ freeze-out and sublimation characteristics closely resemble that of CO – it is only about 10% more volatile (Öberg et al. 2005; Bisschop et al. 2006; Nguyen et al. 2018). The resulting ice morphology is important for the chemistry of planet formation for two reasons: 1) it regulates what kind of organic chemistry can take place in the ice since not all ice reactants are mixed together, and 2) it allows for many of the hyper-volatiles residing in the CO-dominated ice, such as CO and N₂ to readily sublime when the ice is heated, while other hyper-volatiles, such as CH₄ may be more difficult to dislodge from within the water ice lattice. The latter is key to estimate the O/C/N ratio of solids residing at different temperatures in protoplanetary disks.

To date, icy mantle and gas-phase volatile compositions have been estimated in 10s of lines of sight. In Figure 9, we combine these constraints with observations of solar system comets to estimate the O, C and N reservoirs at the onset of star formation. To start with, substantial parts of the O, C, and N budgets are refractory. In the case of O, this is mainly silicate grain cores, whose abundance can be estimated from observations (Whittet 2010), which constitutes about a quarter of the O budget assuming a Solar O abundance (Asplund et al. 2009). Water, CO₂ and organic (CH₃OH and CH₄) ices make up another 13%, and CO another 20% (adopting a total CO gas + CO ice abundance of 10⁻⁴ with respect to n_H, the number of hydrogen nuclei). The remaining ~40% of oxygen is unaccounted for and this is a major mystery in interstellar studies (see also, Poteet et al. 2015; Jones and Ysard 2019). There is some evidence for a hidden water ice reservoir; in Orion, much of the oxygen not carried by CO, CO₂, and interstellar dust is found in water vapor (Neill et al. 2013), which suggests that water ice is under-counted in interstellar ice studies,

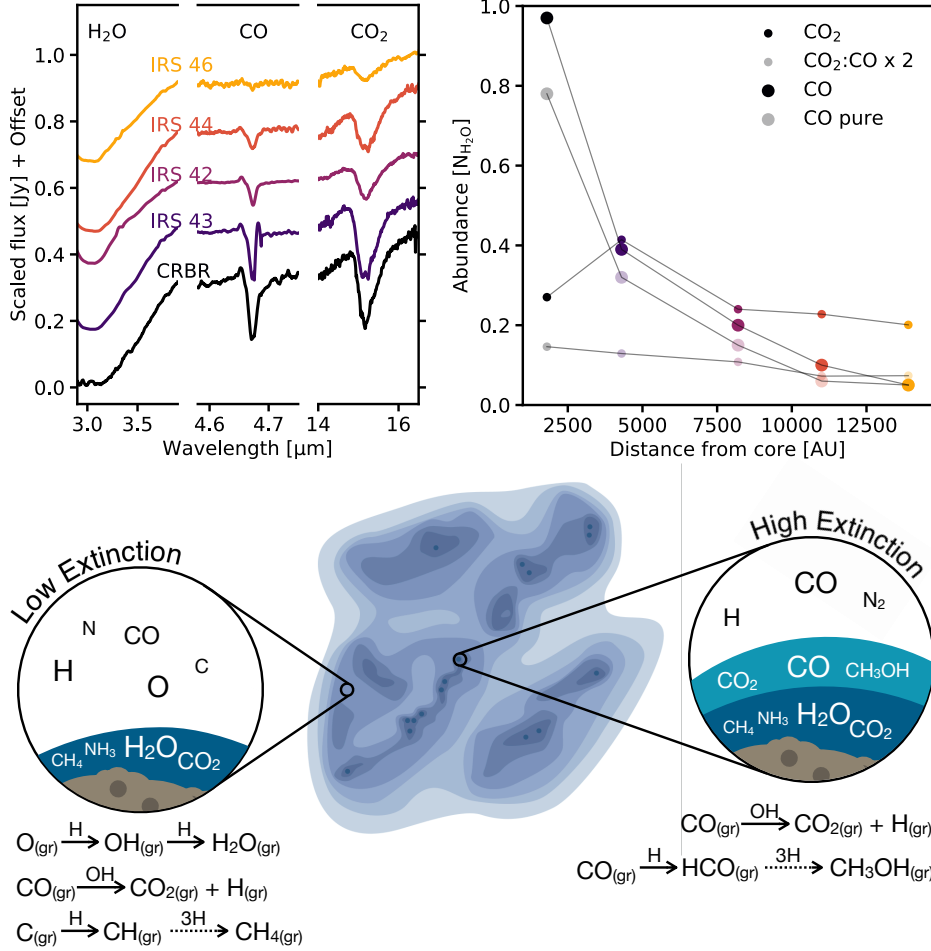


FIG. 8.— Observations of sequential formation of ices. (*Top:*) Ice spectra (top-left) and a radial profile of CO and CO₂ ices (top-right) obtained from spectra towards background sources that lie behind the ρ Oph F cloud core. All ice abundances are relative to water ice and are given at the projected distance from the center of the core. CO itself is listed as “CO pure” (CO in CO-dominated ice) and as “CO”, which is the total CO ice content. Similarly we show the total CO₂ abundance, and the abundance of CO₂ in the CO-dominated ice layer. (*Bottom:*) Schematic of ice layers and ice chemistry at Low Extinction where temperatures are warmer ($T > 10$ K) and the UV radiation is diluted but present and High Extinction where the gas and dust are cold with UV radiation extinguished. Data from Pontoppidan (2006). Image credit K. Peek.

but this requires further investigation. For carbon, the accounting is somewhat easier as there are only four major carriers, CO, CO₂, organics, and refractory carbon. About half of the carbon is thought to be refractory based on observations of carbon depletion in the diffuse interstellar medium (Mishra and Li 2015), which implies that carbon is almost equally split between refractory and volatile material. Of the volatiles, a majority is hypervolatile, i.e. CO. In the case of nitrogen, only a small part of the budget is directly observed in the form ammonia (Boogert et al. 2015), and N-containing volatile organics (Rice et al. 2018). Based on solar system comets, a substantial portion of N may be in more refractory organics and salts (Altwegg et al. 2020). The majority of N is unobserved, and is likely present in the form of N₂.

2.3. Building up the organic reservoir

In addition to dividing up O, C, and N into its major volatile reservoirs, the molecular cloud phase is responsible for forming the first generation of organic molecules, which constitute the feedstock of organic chemistry during the later stages of star and planet formation. This generation zero of organics (Herbst and van Dishoeck 2009) forms through a combination of gas-phase and ice-phase chemistry and is observed through ice infrared absorption spectroscopy, and through rotational spectroscopy of gas-phase molecules both at the UV-exposed edges of clouds, and deep into cloud cores.

On grain surfaces the two most common organic molecules are CH₃OH and CH₄, which form through H addition chemistry as outlined above. Observationally there is a clear connection between catastrophic CO freeze-out and the gas-phase appearance of CH₃OH in cloud cores (Caselli et al. 1999; Bizzocchi et al. 2014), which likely originates from low levels of non-thermal sublimation of CH₃OH ice formed from CO ice. CH₃OH and CH₄ are also abundant in comets Mumma and Charnley (2011), highlighting the persistence of the molecular cloud organic reservoir from cloud

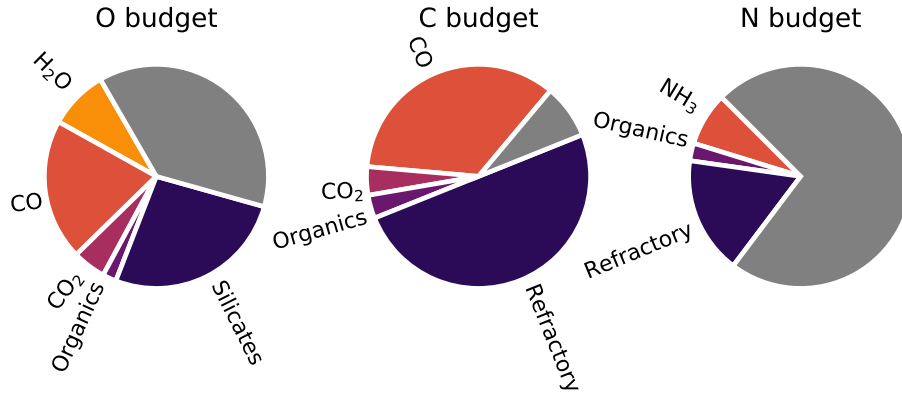


FIG. 9.— The O, C, and N budgets at the onset of star and planet formation, based on observations of ice abundances (Boogert et al. 2015), standard assumptions about CO, silicate and refractory carbon abundances, and solar system comet measurements of refractory nitrogen. Grey indicates an unknown component, which in the case of N is likely mainly N₂, while the nature of the missing O carrier is unclear.

collapse to planetesimal formation. In addition to CH₃OH and CH₄, HNC also seems to form through ice chemistry and is detected in the ice in its ionized form (OCN⁻). There is, furthermore, observational evidence for that some of this initial organic ice reservoir is converted into more complex organics in interstellar clouds (Öberg et al. 2010; Bacmann et al. 2012; Cernicharo et al. 2012; Vastel et al. 2014; Jiménez-Serra et al. 2016; Scibelli and Shirley 2020). Different low-temperature ice pathways, and ice-dependent gas-chemistry pathways to complex organic molecules were reviewed in §1.2, and it is currently unclear which one is the most important for complex organic molecule formation in clouds. There is some evidence for a changing complex organic chemistry between cloud core and cloud edges, which suggests that different pathways may drive the growth of complexity at different stages of cloud and core evolution (Jiménez-Serra et al. 2016). In either case, the conversion efficiency is expected to be low, and we expect that the organic ice reservoir in molecular clouds mainly consists of CH₃OH and CH₄.

Another pathway to organic molecules is through gas-phase ion-molecule and neutral-neutral reactions. Such pathways are responsible for small common organics like HCN, as well as for larger unsaturated organics such C₄H (Herbst and van Dishoeck 2009). With water vapor and molecular oxygen absent from the gas phase, the gas has C/O \gtrsim 1 (with most of the gas-phase carbon and oxygen carried by CO, since water is frozen on grain surfaces), which is at least in part responsible for the oxygen-poor nature of these organics (see, e.g., Langer et al. 1984). Gas phase chemistry is also implicated in the formation of benzene, benzene derivatives, and small polycyclic hydrocarbons in molecular clouds (McGuire et al. 2018). Compared to complex organic molecules formed in the ice, large organic molecules formed in the gas-phase tends to be oxygen and hydrogen poor. They therefore constitute an almost orthogonal reservoir of organic molecules that can become incorporated into planetesimals if they survive through cloud collapse and disk formation. Such survival is quite likely if the molecules freeze-out, which is expected in the dense parts of clouds where freeze-out time scales are short, and become embedded in the icy grain mantles.

Complex organic molecules are also detected in classical PDRs. The organic chemistry there seems to favor hydrocarbons and nitrogen-containing organics over oxygen-bearing molecules (Le Gal et al. 2017). It is currently unclear whether this is due to an efficient gas-phase organic chemistry operating under elevated C/O conditions, due to oxygen lock-up in water ice and /or photoinduced carbon-grain destruction enriching the gas in carbon, or whether we are there witnessing the products of an oxygen-starved grain-surface organic chemistry (Guzmán et al. 2015a; Le Gal et al. 2019b). In either case, the organic composition found in PDRs demonstrates that there are more pathways to organic complexity in the molecular cloud stage than has traditionally been assumed. Thus even if the most abundant organics are small at the onset of star formation, there are already more complex organics present, and their nature will depend on the contribution from ice, gas, and PDR organic chemistry.

2.4. Isotopic fractionation

A final aspect of molecular cloud chemistry of importance to decode the chemical environment within which planets form is isotopic fractionation, and the resulting isotopic imprints in hydrogen, carbon, nitrogen, and oxygen. The isotopic composition of a molecule is set at its formation, and because most isotopic fractionation processes are very sensitive to either photon flux, or gas or grain temperatures, the D/H, ¹³C/¹²C, ¹⁵N/¹⁴N, and ¹⁸O/¹⁶O ratios in molecules can be used to pinpoint when and where they formed. This is famously used to constrain the origin of the Earth’s oceans. It is more generally, a tool to understand the origins of volatile reservoirs in the solar system, as well as in disks where exoplanetary systems are currently assembling. In this sub-section we review major isotopic fractionation pathways for H, C, N, and O in molecular clouds and how they are predicted and observed to affect the isotopic compositions of volatiles formed at this evolutionary stage. The review is by necessity brief, and for more detailed descriptions of isotopic fractionation chemistry in interstellar and circumstellar environments we refer the reader to Aikawa and Herbst (2001), Visser et al. (2009), Aikawa et al. (2012), Persson et al. (2013), Ceccarelli et al. (2014), Heays et al. (2014), Roueff et al. (2015), Furuya et al. (2015), and Furuya et al. (2018).

2.4.1. Hydrogen

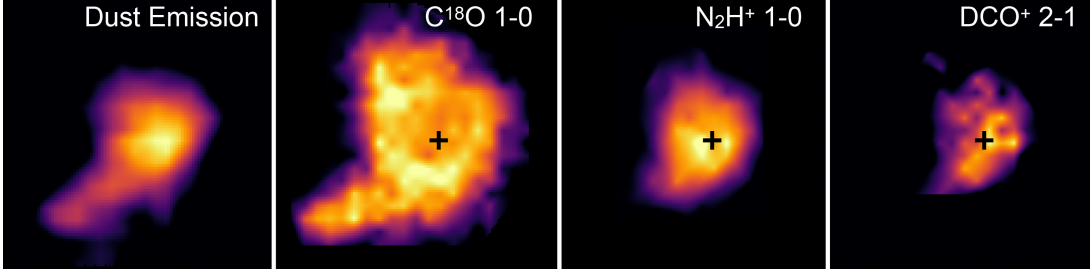


FIG. 10.— Montage of mm-wave emission distributions of dust thermal continuum and molecular emission lines within the Barnard 68 prestellar core. Dust emission is the 850 μm flux from Bianchi et al. (2003), C^{18}O 1–0 and N_2H^+ 1–0 from Bergin et al. (2002), and DCO^+ 2–1 from Maret and Bergin (2007). The cross shown in molecular emission line images for C^{18}O , N_2H^+ 1–0, and DCO^+ 2–1 denotes the location of the dust continuum flux peak or the center of the core traced by the maximum of the dust column.

Deuterium is formed as part of big bang nucleosynthesis (Boesgaard and Steigman 1985; Galli and Palla 2013) with an abundance of $\text{D}/\text{H} \sim 2.5 \pm 0.2 \times 10^{-5}$. Deuterium fractionation occurs at cold temperatures due to zero-point energy differences between hydrogenated and deuterated ions; because of its larger mass, D forms slightly stronger bonds than H, which makes it favorable to transfer D from HD into ions and molecules with strong bond interactions. The primary reactions within the deuterium fractionation chemical networks are (Millar et al. 1989; Roueff et al. 2015):



If the temperature is cold ($< 30 \text{ K}$ for H_3^+ and $< 300 \text{ K}$ for CH_3^+) the forward reaction is favored and the back channel is inactive. This is slightly more complicated as the endothermicity of the back reaction depends on the spin states of the products in particular that of H_2 (Pineau des Forets et al. 1991; Pagani et al. 1992; Flower et al. 2006; Sipilä et al. 2015). Once H_2D^+ or CH_2D^+ has formed they can efficiently transfer a deuteron to a range of other molecules, e.g. to CO to form DCO^+ (e.g., Turner 2001). Some fractionation could thus be expected throughout cloud regions that are $< 30\text{--}300 \text{ K}$. Observationally, large abundances of deuterated molecules like DCO^+ are only observed in the coldest, densest, and most well shielded parts of molecular clouds (Figure 10), i.e. in molecular cloud cores, which suggests that something in addition to low temperatures is needed to substantially deuterate molecules. This something is CO depletion. Figure 10 shows that the dense core, here traced by dust emission, is associated with depletion of CO gas (as traced by its rare C^{18}O isotopologue), and excess DCO^+ . The reason CO depletion is needed for efficient deuterium fractionation, is that the chemistry depends directly or indirectly on the abundance of the H_3^+ ion, and this ion is rapidly destroyed by gas-phase CO ($\text{H}_3^+ + \text{CO} \rightarrow \text{HCO}^+ + \text{H}_2$) (Lepp et al. 1987; Caselli et al. 2002).

CO depletes from the gas-phase through freeze-out onto grains in cloud cores when grain temperatures are $< 18 \text{ K}$ (Bisschop et al. 2006) if CO mainly binds to other CO molecules, and at somewhat higher grain temperatures if CO freezes out on top of water ice (Collings et al. 2003; Fayolle et al. 2016). Cloud cores are colder than this, and the level of depletion in a given core therefore depends on the depletion time scale, which is a direct function of core density (Bergin et al. 1995; Caselli et al. 1999). Figure 11 shows that for typical core densities the freeze-out time is less than 10^5 years. This is smaller than the free-fall time scale and we can therefore expect CO to be frozen out and an efficient deuterium chemistry activated by the time a cloud core collapses to form a star and planetary system. This is further illustrated in the right-hand panel of Fig. 11, which shows that for temperatures $< 17 \text{ K}$, the forward deuterium fractionation reaction pushes the D into H_2D^+ such that $\text{H}_2\text{D}^+/\text{H}_3^+ \gg \text{HD}/\text{H}_2$, often by orders of magnitude (Millar et al. 1989).

For the chemistry of planet formation, the most important lasting effect of this fractionation process is a by-product; elevated $\text{H}_2\text{D}^+/\text{H}_3^+$ result in an excess of atomic deuterium in the gas ($\text{D}/\text{H} \gg \text{HD}/\text{H}_2$) because in dense cloud cores D and H atoms are produced through recombinations between deuterated and protonated molecules and electrons. Excess H_2D^+ therefore naturally produces excess D atoms. These D atoms collide with grain surfaces and participate in chemical reactions that lead to D enrichments in the molecular ices for both water and organics (Tielens 1983; Taquet et al. 2013). All ices discussed in the previous sub-section that form through hydrogen addition will be fractionated in D if they form in a cloud (core) region where $\text{D}/\text{H} > \text{HD}/\text{H}_2$.

Based on observations and theory, different ice components form at different times, and therefore at different cloud temperatures and densities, which should result in different levels of deuterium fractionation (Caselli and Ceccarelli 2012). Most water forms prior to core formation and should therefore be less deuterated than molecules like CH_3OH , which forms in the dense cloud core. Still, substantial H_2O deuterium fractionation is expected (Furuya et al. 2015, 2016), which explains why all water in the solar system is enriched in water (e.g., Cleaves et al. 2014). CH_3OH and

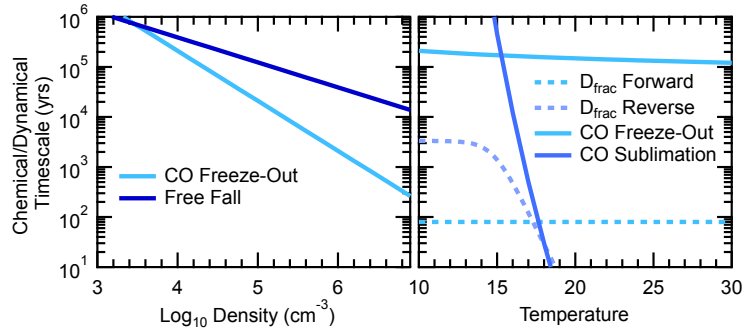


FIG. 11.— Chemical and dynamical timescales as a function of density (assuming $T_{gas} = T_{dust} = 10$ K), and temperature (assuming $n_{H_2} = 10^4$ cm^{-3}). CO freezeout using formalism of Hollenbach et al. (2009) and sublimation using the CO binding energy measured by Fayolle et al. (2014). For deuterium fractionation the timescales refer to the forward and reverse of the following reaction: $H_3^+ + HD \leftrightarrow H_2D^+ + H_2 + 232$ K. We use the rates given by Hugo et al. (2009) and assume that the o/p ratio of the reactants and products are set by equilibrium at the specific temperature using the approximations described by Lee and Bergin (2015). Under these assumptions the reverse reaction begins to activate near 17 K, but this transition temperature will depend sensitively on the history of ortho and para H_2 during cloud and core formation (Flower et al. 2006; Pagani et al. 2013; Furuya et al. 2015).

organics forming from CH_3OH should have higher levels of deuteration than H_2O , and this is indeed observed (Parise et al. 2002; Coutens et al. 2012; Persson et al. 2014; Taquet et al. 2019). Whether these high D/H levels in organics are preserved during planet formation is less clear than in the case of water, and is the subject of ongoing studies. Elevated D/H ratios in organics in comets and carbonaceous chondrites compared to water (Alexander et al. 2007, 2010; Altwegg et al. 2019) suggest that the interstellar D/H patterns persist throughout planet formation, but disk chemistry models also show that a disk *in situ* origin of the observed organic deuterium fractionation cannot be excluded (Cleeves et al. 2016).

2.4.2. Carbon, Nitrogen, and Oxygen

The chemical fractionation via ion-molecule reactions with low endothermicity discussed above for H is also present for C, and N, and perhaps also for O; a similar zero-point energy difference exist between the heavy isotopologues containing ^{13}C , ^{18}O , and ^{15}N , and the normal isotopologues, but the relative mass differences are smaller and the expected fractionations are therefore less. For carbon, a central reaction in the ion-molecule chain that powers fractionation is $^{13}C^+ + ^{12}CO \leftrightarrow ^{12}C^+ + ^{13}CO + 35$ K; this does lead to a slight excess of ^{13}CO in cold regions (Langer and Penzias 1990; Milam et al. 2005). A similar set of reactions are found in the nitrogen pool that again favor heavy element enrichment at low temperature (Terzieva and Herbst 2000); however, the overall efficacy of various pathways are currently a matter of debate (Roueff et al. 2015; Wirström and Charnley 2018). For oxygen, Langer and Graedel (1989) demonstrated that there is little ion-molecule powered fractionation in major oxygen carriers such as CO, while Loison et al. (2019) finds that there may be effect for other, less abundant species.

For C, N and O there also exists another, often more important isotope fractionation pathway: isotopic selective photodissociation. Both CO (main carrier of C and O) and N_2 (main carrier of N) are dissociated via molecular bands or lines in discrete regions of the UV spectrum as opposed to continuous photodissociation cross-sections from 912 to ~ 2000 Å. These spectral lines can saturate ($\tau \gg 1$) and any molecules downstream from the source of radiation will remain safely shielded from molecule-destroying UV radiation. As the radiation transfer is limited by absorption via electronic-state transitions, the optical depth of a given line, τ , has a direct dependence on the molecular abundance. Lesser abundant isotopologues (^{13}CO , $C^{18}O$, $C^{17}O$, ^{15}NN) have lower line optical depth and, hence, the onset of self-shielding is found in successively deeper layers than more abundant isotopologues. As a result, there will a deficit in the heavy, less abundant molecular isotopologues, and an excess of the heavier (less abundant) elemental atoms in the outer surface layers of clouds. For example, for oxygen, $^{12}C^{16}O$ self-shields prior to the onset of $^{12}C^{18}O$ self-shielding. In gas layers that lie between these two self-shielding transitions there is an excess of ^{18}O . Similar effects are seen for nitrogen (Heays et al. 2014; Visser et al. 2018; Furuya et al. 2018) and carbon (Röllig and Ossenkopf 2013).

This isotopic stratification will affect the isotopic patterns of ices formed from atomic O, C and N. In particular, water ice that forms early and therefore in UV exposed regions of molecular clouds should be enriched in ^{18}O because of isotope specific photodissociation. If these ices survive the star and planetesimal formation process, we would expect to see ^{18}O enrichments in bodies that formed volatile-rich (Yurimoto and Kuramoto 2004; Lee et al. 2008). Indeed isotopic selective photodissociation is a prominent theory for the origin of heavy element enrichments detected in meteorites for both O and N (Clayton 1993; Marty 2012). Such an enrichment could also be due to isotope-specific photodissociation in planet-forming disks, since similar to clouds, disks too have a UV exposed PDR layer where this process should be important (Lyons and Young 2005; Visser et al. 2018), and it is currently unclear whether this isotopic signature is a sign of volatile inheritance or not.

2.5. Summary: Setting the Chemical Trajectory

At the onset of cloud formation, the chemistry is constrained by the locking up of $\sim 1/4$ of the oxygen and $\sim 1/2$ of the carbon in refractory material. During cloud formation, the remaining carbon, oxygen and nitrogen become mainly incorporated into CO, water and N₂, respectively. The prominence of these C, N, and O carriers appear universal across star forming regions, and across time during star and planet formation. Since water ice, and the unidentified oxygen carrier(s), are significantly less volatile than CO or N₂ this means that for much of the cloud-chemical evolution, the gas-phase elemental budgets have C/O ~ 1 , and N/O ~ 0.2 (i.e. excess C and N with respect to O). Though many details remain uncertain about this chemical evolution, we can say with confidence that at the beginning of cloud collapse to form a star and planetary system, the carriers of the C, N, and O elemental pools are already established.

In addition to establishing the main volatile carriers, dense cloud chemistry is responsible for producing the organic feedstock molecules that drive a more complex organic chemistry at later evolutionary stages. Ammonia, methane, and methanol all form on the surfaces of interstellar grains and are incorporated into the icy grain mantles. Finally clouds and cloud cores are seats of efficient isotopic fractionation. At cloud edges, CO and N₂ self-shielding results in a build-up of the main isotopologue and a relative depletion in the minor isotopologues. In the cold cloud cores heavier isotopologues are instead favored due to small differences in zero-point energies between normal and main isotopologues. This is especially important for deuterium fractionation, which leaves imprints on organics and water that can still be seen in solar system volatiles today.

3. CHEMICAL INHERITANCE AND TRANSFORMATION DURING THE PROTOSTELLAR STAGE

Protostars form through the collapse of cloud cores. In our understanding of the chemistry of planet formation, this stage plays a key role because, first, it is during the warm-up of infalling cloud material towards the central protostar that much of the icy molecular cloud chemistry described in the previous section is revealed. Second, warm-up of interstellar grains in the protostellar envelope activates new chemical pathways that changes the compositions of the future solid building blocks of planetesimals and planets. Third, the protostellar disk that forms at this stage is the precursor to the planet-forming disks treated in the next section, and the balance between preservation or inheritance and reset at this stage provides the initial chemical conditions for planet formation. In this section we review the protostellar organic chemistry, and the chemistry of protostellar disks, after a brief review of the chemical structures of low-mass protostars (analogs to the protosun) and their surrounding environment.

3.1. *The chemical structure of Solar-type protostars*

Low-mass or Solar-type protostars ($< 2M_{\odot}$, from now on simply referred to as protostars) present multiple distinct chemical environments, which are not present during the earlier stages of star formation (Caselli and Ceccarelli 2012). Figure 12 illustrates the rather complex and dynamical structure characteristic of protostars. The central protostar is surrounded by a large envelope of infalling cloud material, which has an inward temperature gradient due to heating from the central protostar. At large distances, 1000s of AU, the gas and dust temperatures are low (< 20 K), and the chemistry is initially a continuation of the processes found in molecular cloud cores. As gas and dust warm up above 20–30 K, multiple chemical changes occur at once. First the ice-gas equilibrium for the most volatile species such as CH₄, CO and N₂ changes, resulting in substantial sublimation of hypervolatiles not trapped in the water ice mantle. This changes the availability of reactants in the gas-phase, and especially the sublimation of CH₄ at these intermediate distances has been proposed to drive a warm carbon-chain chemistry (Sakai et al. 2008). Second, at 20–30 K, some molecules and radicals begin to diffuse in ice mantles, resulting in a wave of ice organic chemistry (Garrod et al. 2008).

Closer to the protostar, grains heat up above 100 K resulting in complete ice sublimation and the seeding of the gas-phase with water and a range of ice-produced organic molecules, forming a so called hot corino³, which may then chemically evolve further (Herbst and van Dishoeck 2009; Caselli and Ceccarelli 2012). At similar scales as the hot corino we expect, and sometimes observe, the formation of a protostellar disk (e.g., Tobin et al. 2012). The envelope-disk interface can result in mild shocks and therefore shock-driven sublimation of ices, again seeding the gas with ice-chemistry products, and gas-phase chemistry (Aota et al. 2015; Miura et al. 2017). In the disk itself, densities are high compared to cloud and envelope densities, enabling new kinds of gas-phase chemistry, possibly even 3-body reactions close to the protostar.

Finally, protostars generate outflows at a range of velocities, and the interaction of these outflows with the remnant envelope produces shocks that sublimate icy grain mantles, sputter the grain core, enables hot gas phase chemistry, and produces UV fronts that result in PDR like chemistry along the outflow cavity walls (e.g. Arce et al. 2008).⁴ The prevalence of water vapor in outflowing gas is believed to be partially induced by the activation of neutral-neutral reactions with activation barriers that when overcome lead to rapid water production (Wagner and Graff 1987; Kaufman et al. 1999). A similar chemistry regulates the water vapor abundance in the hot gas close to the star in protoplanetary disks (Pontoppidan et al. 2010; Bethell and Bergin 2011).

3.2. *An increasing organic complexity*

Molecular cloud and cloud core chemistry is responsible for the production of organic feedstock molecules during star and planet formation, while protostellar envelopes are organic chemistry factories that transform a large fraction of this feedstock into more complex, but still fairly volatile, complex organic molecules (Herbst and van Dishoeck

³ Chemically rich “hot cores” around massive protostars have been known for a long time. The name “hot corino” was introduced by Bottinelli et al. (2004) to classify the low-mass or protosun analog of a hot core.

⁴ There are several seminal references regarding shock physics and the reader is referred to these for more information (Draine and Salpeter 1979; Hollenbach and McKee 1979; Flower et al. 1985; Hollenbach and McKee 1989; Neufeld and Dalgarno 1989; Kaufman and Neufeld 1996).

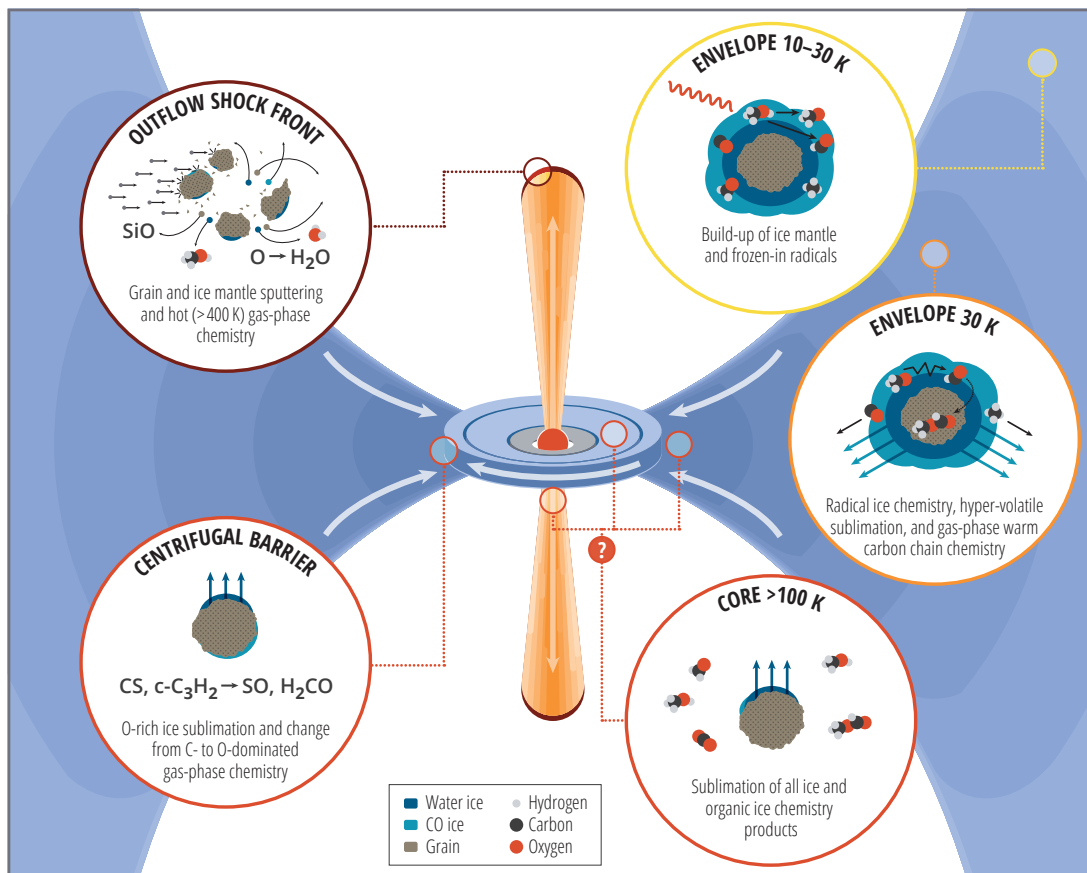


FIG. 12.— The main structural elements of a protostar are the core, envelope, disk, and outflow. The envelope presents a radial temperature gradient, which results in a radially dependent gas and grain surface chemistry regulated by sublimation, radical ice chemistry, and temperature-dependent gas chemistry. The disk and the disk-envelope interface presents its own set of specific chemical conditions, including weak accretion shocks. Along the outflow we expect to see both shock and UV driven chemistry. Image credit: K. Peek

2009). This transformation is the subject of this sub-section. Before reviewing this process, it is important to remind ourselves that there is mounting evidence for a limited complex organic chemistry in cloud cores and at the UV-exposed edges of clouds. The importance of this chemistry for the organic inventory during planet formation is not yet clear. The current mainstream view, which is what is described here, is that it is minor compared to the organic chemistry activated during protostellar formation. This view may change, however. Observations of COMs in outflow shocks, which may originate from sublimation of interstellar ices (Arce et al. 2008), and of PAH formation in clouds (McGuire et al. 2018) suggest that substantial amounts of complex organics may form in clouds prior to the onset of star formation. There are also theoretical models that suggest that complex molecules can form in icy grain mantles at very low temperatures (e.g. Shingledecker et al. 2018), and the reader is encouraged to closely monitor further developments.

The chemical transformation associated with protostars begins at the early stages of protostellar formation when icy grains streaming towards the contracting and increasingly hot core begin to heat up. The first important temperature threshold is around 25-30 K. At these temperatures, the most volatile ice constituents CO, N₂ and CH₄ begin to sublimate. The rapid increase of CO around protostars due to this process has been observationally confirmed (Jørgensen et al. 2002). The release of CH₄ into the gas-phase has been proposed by Sakai and Yamamoto (2013) to fuel an efficient warm carbon chain chemistry resulting in high abundances of e.g. C₄H and other unsaturated hydrocarbons in the envelopes of protostars (Law et al. 2018). These carbon chains have a lower volatility than CH₄ and may freeze out on the grains increasing its inventory of unsaturated organics. There is evidence for that some such unsaturated organics, whether they originate from the molecular cloud or the protostellar envelope, survive incorporation into the planet-forming disk and further into planetesimals, based on their presence in comets (Altwegg et al. 2020).

Around 20-30 K, there are also new chemical pathways activated in the icy grain mantles, which enable the transformation of organic ices produced in earlier phases (e.g. CH₄ and CH₃OH) into a wide range of larger and more complex organic material. The onset of this second generation of ice chemistry is powered by two factors: the build-up of radicals in cold ices, and diffusion of these radicals at slightly elevated ice temperatures (Garrod and Herbst 2006; Garrod et al. 2008; Garrod 2013). Radicals form in ices through incomplete hydrogenation (Chuang et al. 2016, 2017), and through energetic processing by photons, electrons of cosmic rays of pre-existing ices (Greenberg 1983; Öberg et al. 2017). Cosmic rays are present throughout molecular clouds, and in addition to their direct interaction with icy

grains, they also produce secondary electrons, and a dilute UV field (Prasad and Tarafdar 1983). Energetic processing of especially CH_3OH ice is expected to be highly efficient at producing organic radicals such as CH_3 , CH_3O and CH_2OH . At 10 K these are frozen into the ice. In the protostellar phase, initial grain heating to 20-30 K enables radical diffusion, resulting in a productive radical-radical chemistry, where e.g. ethanol forms from $\text{CH}_3 + \text{CH}_2\text{OH}$ (Bennett et al. 2007; Öberg et al. 2009b).

Most ice-produced COMs are expected to survive until the bulk of ice sublimates around 100 K, 10-100 AU away from the central protostar. Models implementing such a scheme have been successful at explaining complex organic abundances following sublimation (described next), but it is important to note that we are not able to observe the complex organics as they form in the ice. Beyond CH_3OH , CH_4 , HNCO , H_2CO and HCOOH , organics have abundances below the $\sim 1\%$ (relative to H_2O) threshold for detection via current infrared absorption studies (Boogert et al. 2015), and are thus hidden from view until they sublimate and become possible to detect via gas phase spectroscopic techniques (Widicus Weaver 2019). Perhaps our best view of pristine icy organics that have not experienced temperatures beyond 30 K will come from in-depth observations of protostellar outflow shock fronts. Some outflow shocks are associated with complex molecule detection and the interpretation is that these originate from rapidly sublimating ices as a protostellar outflow slams into the protostellar envelope (Arce et al. 2008; Lefloch et al. 2017). We note that there are ongoing programs such as SOLIS (Seeds of Life In Space) to map out how the ice organic chemistry revealed through outflow shocks may differ from the organic ice chemistry revealed in hot corinos (Ceccarelli et al. 2017).

As icy grains continue to flow towards the central protostar they continue to warm up. When they reach 100–200 K, the bulk water ice sublimates, and most of the organic ice will co-desorb resulting in a hot, organic-rich core, i.e. a hot corino, since we are here interested in a Solar-like protostar. Hot corinos are observationally characterized by dense spectra at millimeter wavelengths due to the large abundances of warm, mid-sized organic molecules, which each has a large partition function and therefore a multitude of rotational transitions. The most well-known example of such a protostellar hot corino is IRAS 16293-2422, a protostellar multiple system, whose mm spectrum is shown in Fig. 13. The spectrum is incredibly rich at mm, sub-mm, and far-infrared wavelengths, with most of the detected lines associated with organics and water (van Dishoeck et al. 1995; Zernickel et al. 2012; Crockett et al. 2014; Jørgensen et al. 2016).

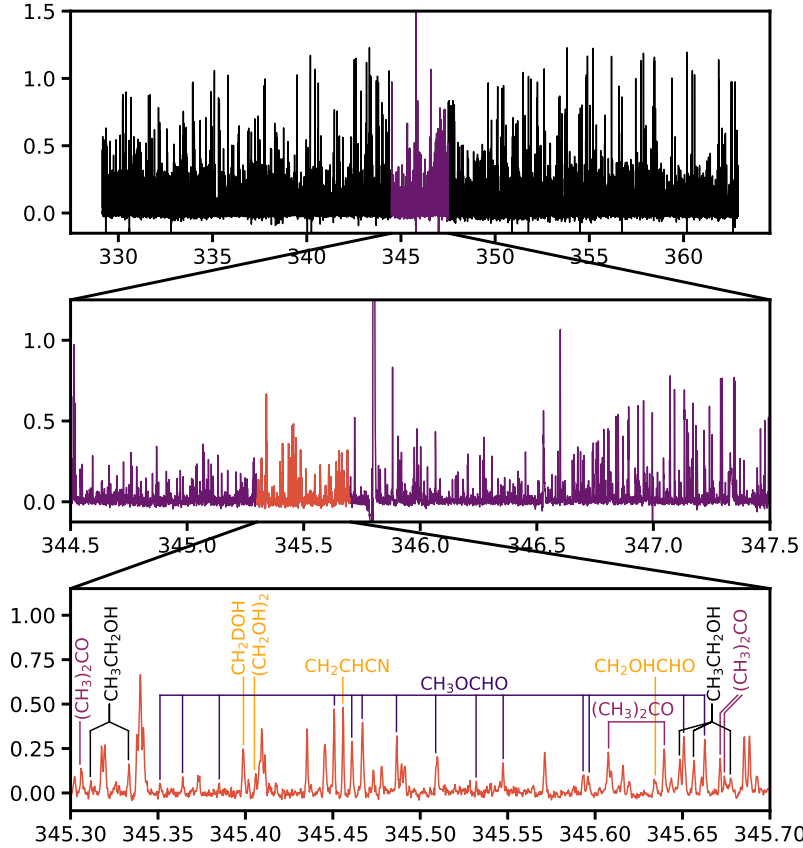


FIG. 13.— 40 GHz of the spectrum towards the Solar-mass protostars IRAS 16293-2422 from Jørgensen et al. (2016). The spectrum is acquired with ALMA at the organic ‘sweet spot’ next to source A in this binary star, approximately 50 AU from the source center. IRAS 16293 is one of a growing number of protostars that display a rich complex organic spectrum, which can be traced back to a hot molecular core in the vicinity of the protostar, where rapid ice sublimation enriches the gas-phase with complex ice chemistry products, as well as feeds a hot gas-phase organic chemistry.

Over ~ 40 organic molecules with 8 atoms or more have been detected in hot corinos, revealing a rapid growth in organic complexity in the evolutionary stage immediately preceding the formation of planet forming disks (McGuire 2018). Some of the organics may originate from hot gas chemistry close to the protostar (Charnley 1997), but a majority of the inventory can be traced back to ice chemistry. Both water (Jacq et al. 1988; Persson et al. 2013) and complex organics (Charnley et al. 1997; Belloche et al. 2016) in hot corinos are highly deuterated, which, as discussed in the previous section, can be traced back to the formation conditions of water and CH_3OH in molecular clouds and cloud cores (Aikawa et al. 2012). If the hot corino molecules were mainly produced through gas phase chemistry, the chemical kinetics would rapidly push the D/H ratio back to $\sim 10^{-5}$ in $\sim 10^4$ years (Rodgers and Millar 1996).

One new aspect revealed by high-resolution images down to tens-of-au scales by ALMA, regards the geometry of the hot corino itself. In general, the organics are assumed to lie in an evaporation zone extending into the heated envelope surrounding a young hot protostellar disk (Fig. 12). In Figure 14, right panel, we show that protostellar disks may be important contributors to the complex organic emission at these scales. In the displayed source, complex organic molecular emission is visibly associated with the surface of a disk rather than the surrounding envelope. Methanol (CH_3OH) and more complex organic molecules, including ethanol, CH_3OCH_3 and HCOOCH_3 , have been detected towards a number of protostars with confirmed disks or disk candidates (Sakai et al. 2014b; Lee et al. 2017; Codella et al. 2018; Lee et al. 2019; van 't Hoff et al. 2018; Martín-Doménech et al. 2019; Bergner et al. 2019b). These are the same kind of molecules that are signatures of hot corinos (Herbst and van Dishoeck 2009). Furthermore, the organic molecules in these disk sources are generally observed to be warm or hot, fulfilling commonly used criteria for hot corino emission. Whether there is a general causal connection between protostellar disk formation and hot corinos is currently unclear.

In summary, protostellar envelopes are sites of chemical transformation of initially simpler organic molecules into more complex ones. The chemistry mainly takes place in icy grain mantles, but is only observable following ice sublimation close to the protostar, or in outflow shocks. The icy grains that become incorporated into protostellar disks, pre-cursors of planet-forming disks, should be expected to contain a rich organic inventory, with organic molecules ranging in complexity from methanol to volatile complex organic molecules, and further to more refractory organics. Understanding this organic inventory is key to map out the initial organic chemistry on planets. We note, however, that despite the impressive spectra produced by mid-sized complex organic molecules, these molecules do not constitute a major elemental reservoir. Accounting of organic carriers of C and N within the complete spectrum of the best studied hot core in Orion (Crockett et al. 2014) suggests that volatile and semi-volatile organics carry only $\sim 1\%$ of interstellar carbon (Bergin et al. 2014), a \sim few percent of total nitrogen (Rice et al. 2018), and less than a percent of the oxygen. The main elemental carriers at this stage remain the same as in the molecular cloud and cloud core (e.g. H_2O , N_2 , CO , CO_2).

3.3. Protostellar disk chemistry: Reset and Inheritance

Disks form during star formation to preserve angular momentum during the collapse and accretion of interstellar cloud material onto the central protostar (e.g. Terebey et al. 1984). The initial stages of disk assembly close to the protostar are expected to be hot, and may result in complete atomization, removing any recollection of the chemistry of previous stages. As this material viscously spreads outward, it will seed the outer and cooler disk regions with the resulting chemical products, which may be quite different compared to the interstellar inventory (Lynden-Bell and Pringle 1974; Cuzzi et al. 1993; Ciesla 2010). Throughout disk formation, infalling material is further subject to irradiation (Visser et al. 2009) and accretion shocks (Neufeld and Hollenbach 1994; Visser and Dullemond 2010; Aota et al. 2015; Miura et al. 2017), which may also alter the chemical composition of material that accretes during later, less energetic phases, see, e.g. Lunine et al. (1991). However, as disk formation proceeds, the centrifugal radius where infall is being supplied to the disk rapidly moves outwards (Shu 1977). Thus there is substantial material supplied at large distances where any chemical reprocessing of supplied material will be minimal. The central question then becomes whether the disk chemical composition is best described by chemical reset or by inheritance from the interstellar medium and protostellar envelope.

The solar system record provides evidence for both a chemical reset, and substantial inheritance. The volatility trend seen in elements in certain meteoritic classes (Davis 2006) and in the Earth's lithosphere, where there is a correlation between the elemental abundance (normalized to Mg and CI chondrite) to the “half-mass condensation temperature”⁵ (McDonough and Sun 1995; Wood et al. 2019), suggest a complete ablation of ices and refractory grains at temperatures above 2000 K, followed by condensation of minerals through a sequence defined by equilibrium chemistry (Grossman 1972). On the other hand, *all* solar system water carries a deuterium enrichment. This requires chemistry active below 30 K (Millar et al. 1989) and cold storage at temperatures below the water ice sublimation temperature to maintain the enrichment. Efficient low-temperature production of H_2O is only possible in molecular clouds, which strongly indicates that most of the solar system's water was inherited (Cleeves et al. 2014). In addition, the volatile organic inventories in Comet 67/P and the protostar IRAS 16293-2422 are remarkably similar, further suggesting that much of the solar system organics were inherited as well (Drozdovskaya et al. 2019). Neither a complete reset nor a complete inheritance scenario can explain the full solar system record and the only remaining answer is that both must have played a role during formation of the protosolar disk (e.g. Ciesla 2010).

⁵ The half-mass condensation temperature is defined through a sequence of equilibrium condensation for a given element assuming an atomic gas of solar composition that is cooling from temperatures >2000 K. For example, from Lodders (2003), the majority of Mg removal from the gas coincides with the condensation of forsterite (Mg_2SiO_4) and enstatite (MgSiO_3) and 1/2 of the mass of Mg is removed from the gas and placed into a solid mineral at 1336 K.

This mixed model is also supported by observations of protostellar disks. Figure 14 shows two recent spectacular ALMA images of molecular emission emerging from edge-on protostellar disks around precursors to Sun-like stars in nearby star forming regions (Lee et al. 2017, 2019; Louvet et al. 2018). Towards HH30 (left panel), CO 2–1 emission is clearly observed to be coincident with the dust disk. Since CO is main reservoir of carbon these and similar observations enable us to address whether a substantial amount of CO has been converted into other molecules during the protostellar disk phase, or whether this interstellar reservoir of carbon is preserved intact. Zhang et al. (2020) finds that CO is preserved, while Anderl et al. (2016) and Bergner et al. (2020) find some evidence for CO depletion in evolved protostellar disks/sources, indicative of that while CO is being incorporated intact into the disk, there are some disk processes that over time convert CO into other species, such as CO₂ and organics, potentially changing the balance between different C and O carriers (Bergin et al. 2014; Reboussin et al. 2015; Schwarz et al. 2016; Eistrup et al. 2018; Schwarz et al. 2018; Bosman et al. 2018).

The hot (> 1000 K) disk phase inferred from the inner (< 2.5 au) solar system volatility trend has not been directly observed (Persson et al. 2016; Aso et al. 2017; van ’t Hoff et al. 2017; Artur de la Villarmois et al. 2019; van’t Hoff et al. 2020), which suggests that a “hot” reset phase must occur fairly early (\sim first 100,000 years) during disk formation. By the time protostellar disks are observable they appear too cold even for substantial water vapor (Harsono et al. 2020), implying that water is present as ice throughout most of the disk. This is consistent with models of chemical processing during protostellar collapse by e.g. Visser et al. (2009), which suggests that most water ice is supplied to the disk from the protostellar envelope unaltered (see also: Yoneda et al. 2016). However, there are observations of crystalline ice in some disks, which only forms when water ice is heated close to its sublimation point, or first sublimates and then reforms (McClure et al. 2015), which shows that also the record of external protostellar disks require a combination of chemical reset and inheritance. This conclusion is supported by observations revealing thermal processing of small silicate particles in disks (Waelkens et al. 1996; Malfait et al. 1998; van Boekel et al. 2004; Watson et al. 2009).

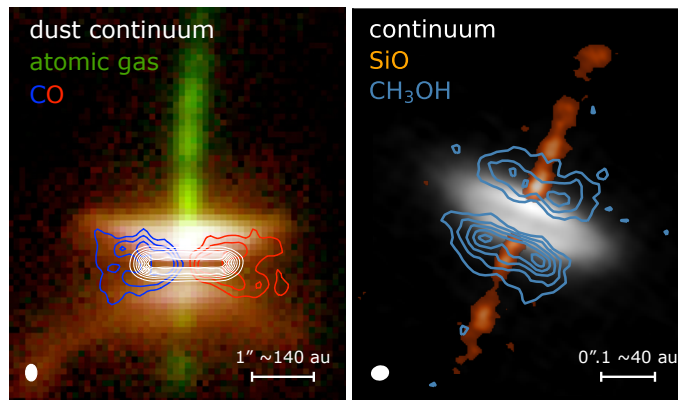


FIG. 14.— *Left*: HST image of HH30 (credit: Chris Burrows (STScI), the WFPC2 Science Team and NASA/ESA) overlaid with ALMA observations of dust continuum (white contours) and blue and red-shifted CO 2–1 emission from Louvet et al. (2018), revealing a molecular disk. *Right*: ALMA observations of dust continuum from the HH 212 protostellar disk (white), SiO emission tracing the protostellar jet, and CH₃OH emission, which appears to originate from the disk surface (Lee et al. 2017, 2019). In both panels the synthesized beams for the continuum are shown in the bottom left corner – the molecular lines were observed at a comparable spatial resolution.

Beyond CO, there are few observations of the chemical inventory in the protostellar disk interior. By contrast there is a growing number of observations showing interesting chemical structures at the edges and surfaces of protostellar disks. Figure 14 shows that disk surfaces may present the same kind of complex organics traditional associated with hot corinos (*cf.* Bergner et al. (2019a)). This discovery may be related to other observations of sharp chemical gradients from a carbon-rich, as traced by small hydrocarbons and CS, to an oxygen-rich chemistry, as traced by H₂CO and SO, at the centrifugal barrier where the gravitational pull of the nascent star is balanced by the centrifugal force (Sakai et al. 2014a,b). At this radius, infalling material is expected to experience a shock, which may result in partial sublimation of icy interstellar grains (Aota et al. 2015; Miura et al. 2017). This ice sublimation may increase the gas-phase O/C ratio since ice mantles are O-rich, pushing the chemistry towards forming O-containing molecules at the expense of hydrocarbon destruction. A difference between C-rich envelopes and SO-rich (O-rich?) protostellar disks are also seen in surveys of protostellar disks (e.g., Artur de la Villarmois et al. 2018), suggesting that chemical gradients across the centrifugal radius may be universal. They do not appear to always be associated with a rich organic chemistry, however, which suggests that such a chemistry is either a transient phenomenon, or sensitive to the abundance of organic feed-stock molecules inherited from the prestellar core stage.

3.4. Summary: Chemistry in Protostellar Envelopes and Disks

The protostellar stage is characterized by a combination of preservation of the major interstellar volatile C, N, and O carriers, by a transformation of a portion of simple interstellar organics into more complex ones, and by a partial chemical reset during the earliest stages of disk formation. As a result, predicting the disk composition at the outset of planet formation is complicated and far from a solved problem. All protoplanetary disks will likely be marked by a

combination of interstellar, protostellar and disk chemical processes, but the relative importance of the three may vary between different disks dependent on the details of the protostellar collapse and disk formation (Aikawa et al. 2012; Drozdovskaya et al. 2016). More in depth studies of protostellar disks, further model exploration on the combined effects of chemistry and dynamics, as well as a better understanding of the volatile content of the young solar system are all key to map out the ‘typical’ initial conditions of planet formation, and how they depend on the protostellar disk formation dynamics.

4. PROTOPLANETARY DISK CHEMISTRY AND PLANET FORMATION

In the final stage of forming a planetary system, the now pre-main sequence star has dispersed its envelope, and is only surrounded by a disk of gas and dust. There are several lines of evidence that planet formation is well underway in these disks and they are therefore commonly referred to as protoplanetary disks or planet-forming disks (Williams and Cieza 2011; Andrews et al. 2018; Andrews 2020). The chemical structures of protoplanetary disks impact several aspects of planet formation. The time dependent radial and vertical distribution of molecules determines what material is available to planets forming at different disk locations and at different times. The division of molecules, and therefore volatile elements, between gas and solids constrains what material is available for incorporation into rocky planet cores versus primary atmospheres. The interplay between snowlines, grain compositions, and grain fragmentation and coagulation properties regulate pebble size distributions across the disk and therefore planetesimal and planet growth rates. Finally the locations of water and organic reservoirs in disks constrain how easy or difficult it is for young terrestrial planets to access these reservoirs. These different aspects of the chemistry of planet formation are reviewed in the following sub-sections.

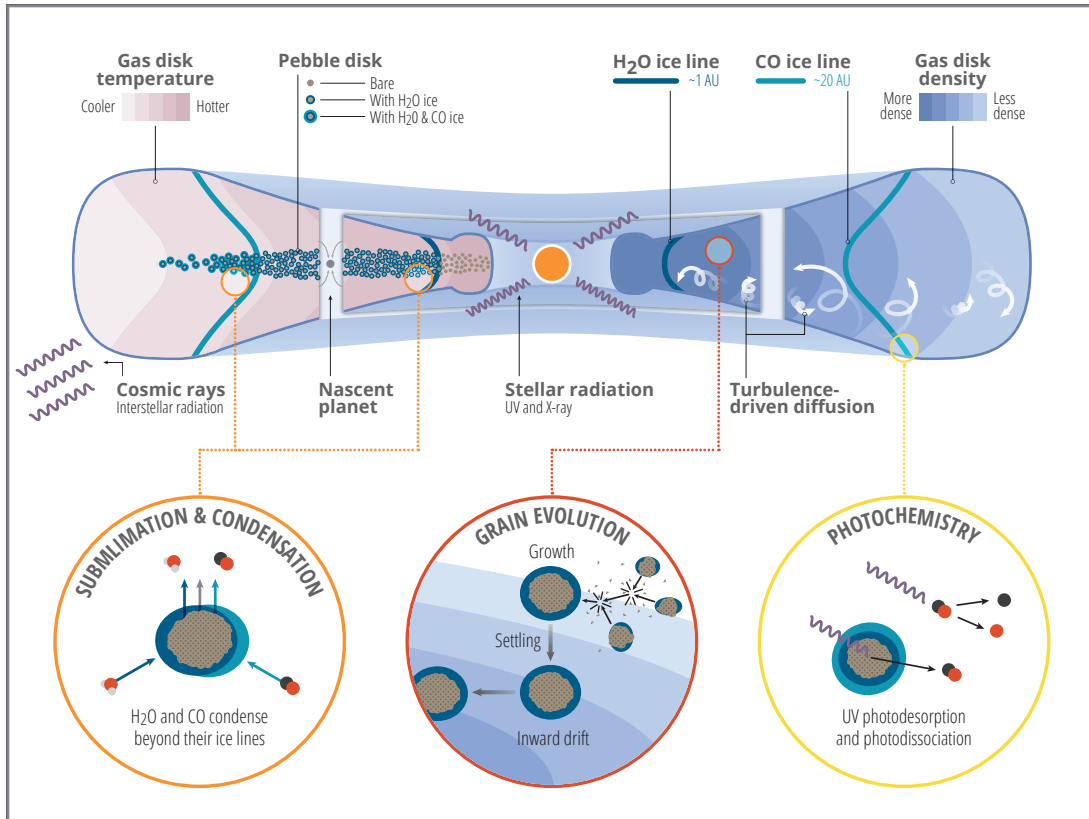


FIG. 15.— Cartoon of protoplanetary disk chemistry and its coupling to different gas and grain dynamical processes. Note the temperature gradient inward and upward (pink shading) resulting in a series of snowlines, as well as the inward and downward density gradient (blue shading). Disk surfaces are characterized by photon processes and display PDR-like chemistry. Disk midplanes are by contrast cold and UV-poor, and the main volatile reservoirs (other than H₂ and He) are in icy grain and pebble mantles.

Before addressing the interplay between disk chemistry and planet formation, it is useful to review our current understanding of chemical and dynamical processes in protoplanetary disks as illustrated in Fig. 15. There has been several reviews in recent years that have treated protoplanetary disks and their chemistry. We refer the reader to Henning and Semenov (2013) for a review of disk chemistry and especially disk chemistry theory but there are also other numerous salient contributions (e.g. Aikawa and Herbst 1999; Gorti and Hollenbach 2004; Nomura and Millar 2005; Woitke et al. 2009; Kamp et al. 2010; Walsh et al. 2010; Bruderer et al. 2012; Wakelam et al. 2016; Schwarz et al. 2019, as a small sample). Absent dynamical redistribution of material, the disk radial and vertical chemical structure is mainly set by gradients in temperature and ionizing radiation away from the central star, and down towards the

midplane. This is analogous to clouds, and different disk regions can be profitably compared with interstellar structures that we have already discussed. The disk atmosphere resembles a PDR, while the disk midplane chemistry has many similarities with pre-stellar cores. The analogies are not perfect, however, because dynamical redistribution is not, in fact, absent, and because grain growth result in thermal and dynamical decoupling of dust and gas (D’Alessio et al. 2001; Jonkheid et al. 2004; Aikawa and Nomura 2006; Nomura and Nakagawa 2006; Nomura et al. 2007). Once grains grow they settle towards the midplane and drift inwards (Blum and Wurm 2008), which can result in substantial redistribution of volatiles both vertically and radially (Cuzzi and Zahnle 2004; Ciesla and Cuzzi 2006; Meijerink et al. 2009; Krijt et al. 2016, 2018). Turbulent diffusion may also result in large-scale volatile transport.

A major question is how efficient the chemical-dynamical evolution of disks is at resetting the chemistry, or whether chemical products inherited from previous stages of star and planet formation survive. The answer is complicated. Crudely, chemical time scales decrease inwards and upwards in disks, and we therefore expect inheritance to play the major role in the outer disk midplane, *in situ* chemistry in disk atmospheres, and a mixed behavior in intermediate regions. Dynamical transport of material from one region to another may change this picture dramatically, however, and we are only beginning to explore the effects of such transport on disk chemical structures during the epoch of planet formation (e.g. Semenov and Wiebe 2011).

With these caveats in mind, we here review aspects of disk chemistry of especial interest to predicting planet formation outcomes. We first discuss how the disk chemical structure can affect the planet formation process due to changes in grain growth and grain concentrations across volatile condensation/sublimation fronts or snowlines. Second we explore how snowlines combine with *in situ* disk chemistry and disk dynamics to set the distribution of volatile elements C, N and O during planet formation. Third we describe the distribution of organics during planet formation, and its dependence on inheritance and disk chemistry. Finally we review solar system constraints on the distribution of volatile elements during planet formation, and how water and organics can be incorporated into nascent, temperate and rocky planets, i.e. the kind of planets likely most hospitable to life.

4.1. Snow lines and planet formation

The dichotomy between dry terrestrial planets in the inner solar system, and water- and volatile-rich gas/ice giants and comets in the outer solar system has long be ascribed to a transition of water vapor to the solid state across the solar nebular snowline. There are several potential mechanisms through which snowlines regulate planet formation, some which apply only to the water snowline, and some which would also be active at the snowlines of other major volatiles such as CO, CO₂, CH₄, NH₃, and N₂. At the most basic level, snowlines always influence planet formation, since they determine the elemental content of solids and gas at different disk locations. This is reviewed in the next section. In this section we instead focus on whether and through which mechanisms snowlines can alter the efficiency at which planets form, resulting in preferred planet locations, and in predictable distributions of planet sizes.

There are at least four mechanisms through which snowlines can affect the planet formation process by speeding up the growth of pebbles, the building blocks of planets and planet cores. First, across the snowlines the solid material surface density increases. This effect will be the largest for the most abundant volatiles. Exact numbers are unclear, but some estimates increases the column density of condensates (silicate rocks + ices) by $\gtrsim 3$ compared to right inside the snowline (Hayashi 1981). This alone might mean that solids grow to larger sizes beyond the water and CO snow lines.

Second, diffusive flows of vapor across snowlines may both increase the column density of solids exterior to the snowline and result in preferential growth of larger particles. Stevenson and Lunine (1988) suggested that diffusive flow of water vapor outwards would result in condensation and accumulation of water ices via a so-called “cold trap” or “cold finger” effect. This effect can be greatly enhanced by the presence of radial drift of particles across the snowline (Ciesla and Cuzzi 2006; Ros and Johansen 2013): in the presence of a radial pressure gradient the gas orbits at sub-Keplerian velocities for a given radius (Whipple 1972; Weidenschilling 1977), resulting in a drag force on the solids, which induces radial drift of intermediate-sized (mm–m) grains and pebbles towards the pressure maximum. Diffusive flows are also expected in the vertical direction, where vertical temperature gradients produce snow surfaces that extend across the disk (Willacy et al. 2006; Meijerink et al. 2009; Semenov and Wiebe 2011). Exterior to the volatile snowline, vapor would diffuse downwards and be caught in the overall grain evolution (growth and settling) (van Dishoeck et al. 2014; Blevins et al. 2016; Ros et al. 2019), further enhancing the midplane ice density (Krijt et al. 2016). Lower than expected water and CO vapor abundances beyond their respective snowlines support the presence of efficient vertical volatile flows towards the midplane (Chapillon et al. 2008; Hogerheijde et al. 2011; Favre et al. 2013; Krijt et al. 2016, 2018). This mechanism should operate along all major snowlines.

Third the material properties changes across snowlines, which may increase (or decrease) stickiness and fragmentation thresholds, both of which aid (or quench) transforming initially sub-micron-sized particles into mm/cm-sized pebbles via coagulation (Güttler et al. 2010; Pinilla et al. 2017). Both theory (Dominik and Tielens 1997; Wada et al. 2013) and experiments (Gundlach and Blum 2015) find that the velocity at which a grain-grain collision causes fragmentation, as opposed to growth, is an order of magnitude *higher* for water-ice coated grains as opposed to bare silicates. Thus water ice coated grains are expected to readily grow to pebble sizes beyond the water snowline, while growth may be limited to sub-cm sizes in the innermost disk regions (Birnstiel et al. 2010). This break in dust size should be observable at mm-wavelengths because of the link between dust size population and the shape of the dust spectral emission as a function of wavelength (Banzatti et al. 2015). Such a break has been detected in one object, V380 Ori, which is undergoing a burst in its luminosity, likely tracing a temporary water snowline in the outer disk, which is resolvable by ALMA, due to an accretion event (Cieza et al. 2016). Further out in the disk where volatiles like CO₂ and CO

freezes, the grain material properties change again, but this time perhaps destructively, resulting in diminished growth as a snowline is crossed (Musiolik et al. 2016; Pinilla et al. 2017). This mechanism thus depends strongly on the kind of snowline.

Fourth, major snowlines may operate as localized regions of enhanced pressure that reverses the overall pressure gradient in a disk. The local pressure gradient will operate as a trap to drifting dust leading to a localized dust density enhancement and enhanced dust growth (Cuzzi and Zahnle 2004).

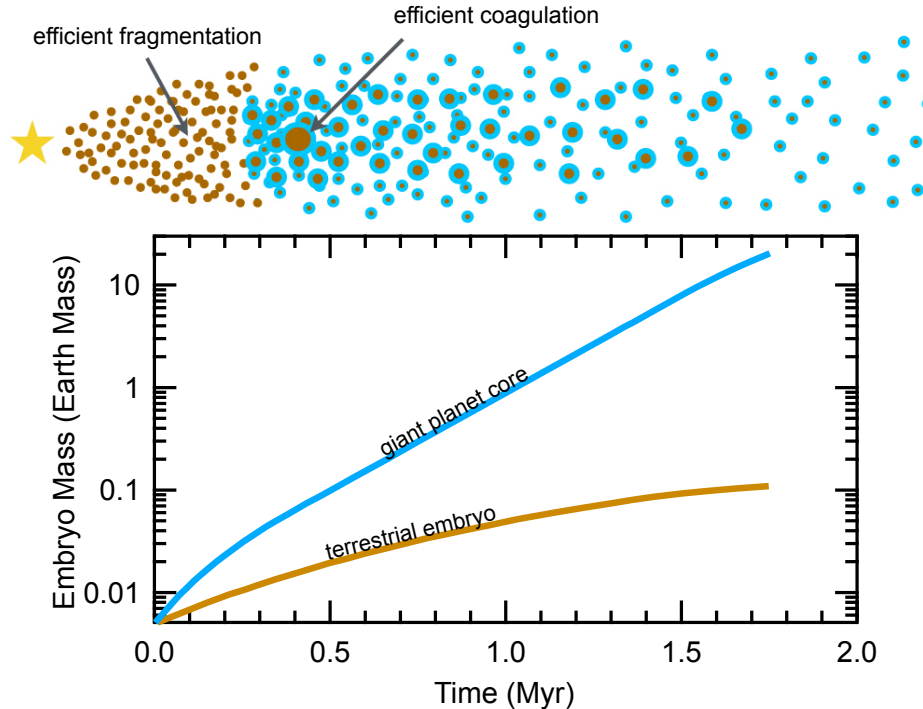


FIG. 16.— (*Top:*) Schematic of grain growth across the water snowline according to experimental results and theory. Schematic taken from Banzatti et al. (2015). (*Bottom:*) Mass growth due to pebble flux for two simulations: one inside the water snowline, shown as a brown line, and another outside the water snowline, given as the blue line. Figure taken from Morbidelli et al. (2015). Based on the work of Lambrechts and Johansen (2014) the 20 Earth mass embryo will capture nebular gas and become a giant planet.

What might all this mean for planet formation near the snowline of the most abundant volatiles? Morbidelli et al. (2015) explored planetary growth via pebble accretion (e.g., Johansen and Lambrechts 2017) assuming that pebbles are few cm-sized beyond the water snowline and mm-sized interior to the snowline. The resulting growth of planetary bodies is shown in Fig. 16. Beyond the ice line the larger mass of cm-sized pebbles allows for growth of a giant planet core within a few Myr, while only a Mars-sized embryo forms inside the snow line. Several other models also find a change in planet formation at the water snowline (Armitage et al. 2016; Schoonenberg and Ormel 2017; Drazkowska and Alibert 2017), which together with a recent observational coincidence between the outer edge of the H₂O emission region and the 13 au dark lane identified by ALMA in HL Tau (ALMA Partnership et al. 2015), suggest that the water snowline is important for regulating planet growth in disks (Salyk et al. 2019).

A central question is whether we should only expect preferential dust growth and planet formation at the water snowline, or also at the snowlines of other major volatiles, such as CO, CO₂ or N₂, as posited e.g. by Cuzzi and Zahnle (2004). Zhang et al. (2013) suggested that this might be the case based on a comparison of one realization of the midplane temperature profile and observations of significant symmetric sub-structure (rings/gaps) within the dust emission towards HL Tau (see also Pinilla et al. 2017). They argued that this substructure was indicative of a change in dust properties due to localized grain growth at snowlines. More recent comparisons of dust sub-structure in many disks do not find a link of substructure with the inferred sublimation temperature of key volatiles (Huang et al. 2018; Long et al. 2018). At face value, this suggests that the snowlines of volatiles such as CO, CO₂, N₂, etc are not inducing significant dust evolution. However, for most disks we still lack direct observations of snowline locations (see below), and laboratory data suggest that they may appear at quite different temperatures in different disks because the ice sublimation temperatures depend sensitively on ice composition and morphology (Fayolle et al. 2016).

Direct observations of the water snowline is hard because water sublimates close to the star limiting our ability to spatially resolve emission (Notsu et al. 2016; Carr et al. 2018; Notsu et al. 2019). Instead, the best constraints exist for CO. The CO snowline is easier to observe than the other snowlines because it occurs at large distances, which makes it easier to resolve, and because there are multiple potential molecular tracers of CO midplane freeze-out: optically thin CO isotopologues, H₂CO and N₂H⁺. Figure 17 shows examples of snowline tracers towards three disks, TW Hya, HD 163296 and LkCa 15. Direct observations of CO isotopologues is the conceptually most straightforward method of

detecting CO snowlines; at the location of the CO midplane snowline there should be a sharp decrease in CO emission. This appear to be the case for TW Hya and other systems (Zhang et al. 2017; Qi et al. 2019; Zhang et al. 2019), but it can be difficult to distinguish between a drop in CO and overall gas column density. N_2H^+ emission should trace CO snowlines because it is only observable in disk regions where CO is depleted from the gas phase (Qi et al. 2013), while H_2CO should trace CO freeze-out because it readily forms from hydrogenation of CO ice (Öberg et al. 2017). The two chemical snowline tracers can also be difficult to interpret, however, because their identifications with CO freeze-out are not unique; N_2H^+ can also trace CO-poor disk atmospheres (van 't Hoff et al. 2017), and H_2CO can also form through gas-phase chemistry that is independent of CO freeze-out. The community is still working out for which kind of disk which method provides the most accurate CO snowline radius estimate (e.g. Zhang et al. 2019; Qi et al. 2019), and how to extend the lessons learned from CO to other molecules (Qi et al. 2019).

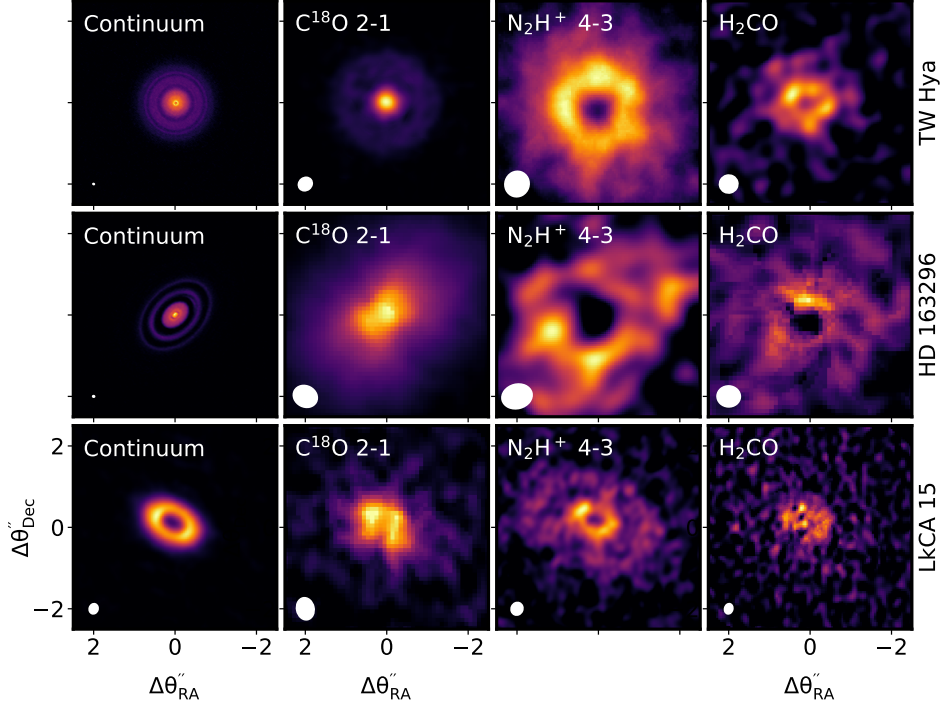


FIG. 17.— ALMA gallery of observed CO snowline tracers towards three disks, shown together with their millimeter continua images (left panel). *2nd panel:* C^{18}O emission is expected to be optically thin in outer disk regions and provides constraints on radial CO depletion. *3rd panel:* N_2H^+ is readily destroyed by CO gas and should trace midplane regions where CO is frozen out, i.e. the inner rim of the N_2H^+ ring should coincide with the CO snowline. *4th panel:* H_2CO forms through CO ice hydrogenation, among other pathways, and should be present in excess exterior to the CO snowline. The synthesized beams are shown in the lower left corner of each panel. Data are taken from (Huang et al. 2018; Andrews et al. 2018; Zhang et al. 2017; Pegues et al. 2020; Qi et al. 2013, 2019; Öberg et al. 2017)

4.2. Disk volatile structures and budgets

The distributions and abundances of abundant volatile elements in the disk regulates the bulk compositions of gas giants, as well as the volatile inventories of terrestrial worlds (e.g., Öberg et al. 2011b; Bergin et al. 2015). In a static disk the elemental distribution is fundamentally set by a combination of chemistry, which determines the main carriers of O, C, N, S, and P, and the freeze-out temperatures of these carriers. The compositions of inner disk volatiles has been reviewed by Pontoppidan et al. (2014), and we focus here on the outer disk, i.e. the disk exterior to the water snowline. Based on models and comparisons between cloud and cometary abundances (Cleeves et al. 2013; Drozdovskaya et al. 2019), the volatile composition exterior to the water snowline in disks is to a large extent inherited from the molecular cloud, and interstellar cloud chemistry may therefore be more important than disk chemistry to understand the main reservoirs of volatiles in disks. Given the chemical composition outlined in Fig. 9, molecular condensation/freeze-out temperatures then determines where in the disk the elements are in solid form and available for incorporation into planetesimals and planet cores, and where it is in gas and can only become incorporated into planets through nebular gas accretion.

Figure 18 shows that using a model of the Solar Nebula (Öberg and Wordsworth 2019), and assuming that the division of O, C and N between different volatile carriers established in the molecular cloud stage survives disk formation, the gas and solid state C/N/O ratios change across the disk because of different sublimation temperatures of major carriers of O, C and N. In particular, the difference in sublimation temperature of water (a major O carrier), and the hypervolatile CO and N_2 (major C and N carriers, respectively) cause the gas-phase C/O and N/O ratios to

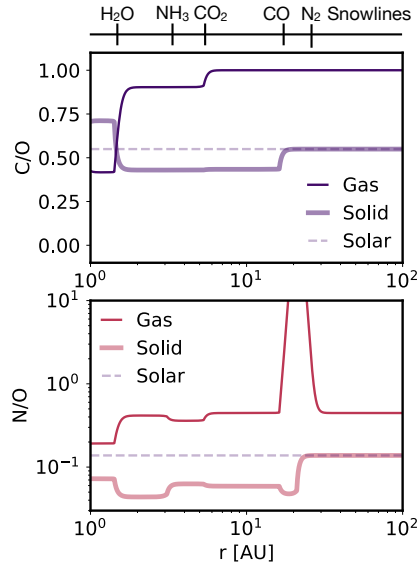


FIG. 18.— The sequential freeze-out of volatile carriers of O, C and N in protoplanetary disks results in radially dependent C/O and N/O ratios in gas and solids. For this model we used the distribution of O, C and N carriers shown in Fig. 9, assuming that the unknown O is equally divided between water and refractories, and that the unknown N is in N_2 . Beyond the CO and N_2 snowline we assume that a small amount of CO and N_2 (10^{-3}) is maintained in the gas through non-thermal desorption.

increase with disk radius (Öberg et al. 2011b; Piso et al. 2016). As a result a Gas Giant forming exterior to the water snowline should initially have a O-rich core and a O-poor atmosphere, though subsequent mixing between the phases may change this picture (Helled and Guillot 2018; Öberg and Wordsworth 2019). Whether such planets are common will be tested by upcoming exoplanet missions, most notably by observations by JWST.

There are several dynamical processes that are active in disks that complicate the simple scenario outlined above, with static, narrow snowlines regulating the distribution of volatiles. First, snowline locations are fundamentally set by the disk thermal profile, which is regulated by stellar radiation and accretion, both which decrease over the lifetime of the disk. Simultaneously the disk mass decreases, however, increasing the efficiency at which it can be heated. The net result is a complex dependence of snowline locations on disk age (Dodson-Robinson et al. 2009). Second, sublimation time scales are often similar to grain drift timescales due to angular momentum transfer between Keplerian solids and sub-Keplerian gas. This can result in that snowlines are effectively moved inwards by as much as 50% of their ‘static’ radius (Ciesla and Cuzzi 2006; Piso et al. 2015). Third, diffusive flows from interior of the snowline to the volatile poor exterior can deplete the gas in regions substantially inward of the snowline, while not changing the location where ice formation begins (Ros and Johansen 2013). Pebble drift can also redistribute volatiles from the inner to the outer disk (Cuzzi and Zahnle 2004; Öberg 2016; Krijt et al. 2018). Finally all these dynamical processes occur together with a chemical evolution that can change the nature of the disk volatiles, e.g. converting substantial amounts of CO into CO_2 and/or CH_3OH . This does not *per se* change snowline locations, but rather it changes which snowlines matter for setting the C/N/O ratios in solids and gas across the disk (Meijerink et al. 2009; Reboussin et al. 2015; Schwarz et al. 2016, 2018; Bosman et al. 2018; Eistrup et al. 2018).

These complications aside, the expected preferential sequestration of O and, to some extent, C into solids in outer disk regions should have observable effects on the gas phase chemical composition, which should become increasingly O and C poor. This has been verified by cold water observations by Herschel towards two nearby disks, DM Tau and TW Hya (Bergin et al. 2010; Hogerheijde et al. 2011), supplemented by a survey (Du et al. 2017). However, to everybody’s surprise water was not just depleted in the disk midplane (as expected), but also high up into the disk atmosphere where UV radiation from the central star should be able to maintain some of the water in the gas-phase if it had been present at normal abundances in icy grain mantles. The inferred water ice depletion in disk atmospheres from far-IR observations is roughly consistent with observed water ice features at infrared wavelengths (Debes et al. 2013; Honda et al. 2016). More recent observations have revealed an underabundance of CO in disk atmospheres indicative of that carbon is also more depleted from the gas than expected from passive freeze-out alone (Favre et al. 2013; Schwarz et al. 2016; Miotello et al. 2016; Cleeves et al. 2018). By contrast nitrogen does not appear to be depleted in disk atmospheres (Cleeves et al. 2018; Anderson et al. 2019), which likely reflects both the volatile nature of the main nitrogen carrier, N_2 , and the difficulty of converting N_2 into more refractory species on disk time scales. There is mixed evidence for C-depletion interior to the CO snowline (Salyk et al. 2011; Bosman et al. 2017; Zhang et al. 2017; Bosman et al. 2019a; Zhang et al. 2019), and mapping out the C/O and N/O ratios at scales of 10s of au and less is an observational frontier (Najita et al. 2013).

Several possible removal mechanisms have been proposed to explain the missing O and C in disk atmospheres, including grain settling, diffusive flows, and chemical conversion of CO into more refractory species (e.g. Reboussin et al. 2015; Krijt et al. 2016; Yu et al. 2017; Eistrup et al. 2018; Schwarz et al. 2018; Bosman et al. 2018). The latter

explanation may only be possible to explore by observing the volatile composition inside the water snowline where all volatiles, including potential CO derivatives, such CH₃OH should return to the gas. Meijerink et al. (2009), Salyk et al. (2011), and Blevins et al. (2016) used data from Spitzer, and in some cases Herschel (see also summary in Pontoppidan et al. 2014) to model water vapor emission at radii commensurate with its snowline. These models are consistent with water returning to the gas-phase at \sim ISM abundance levels inside the water snow line. However, there is some uncertainty because water emission is optically thick, JWST is needed both to establish the water abundance, and the composition of any co-sublimating organic ice.

4.3. Disk organic chemistry

The distributions of organic molecules in disks are of special interest because of their connection to complex organic molecules in comets and asteroids (Ehrenfreund and Charnley 2000; Altwegg et al. 2019), and therefore possible connection to prebiotic chemistry on planets following asteroid and comet bombardment (Pearce et al. 2017; Howard et al. 2013). A range of organic molecules have been observed in protoplanetary disks: HCN, CN, C₂H₂, C₂H, *c*-CH₃H₂, H₂CO, CH₃OH, HCOOH, HC₃N, H₃CN, CS and H₂CS. Most of these have been detected at millimeter and sub-millimeter wavelengths (Dutrey et al. 1997; Aikawa et al. 2003; Thi et al. 2004; Chapillon et al. 2012; Öberg et al. 2015; Walsh et al. 2016; Favre et al. 2018; Le Gal et al. 2019a), but HCN is also observed at IR wavelengths, and C₂H₂ is only observed at these shorter wavelengths due to its lack of a permanent dipole moment (Carr and Najita 2008; Salyk et al. 2008; Najita et al. 2010). In most cases IR and mm observations probe upper disk layers, and the connection between observed organic inventories to those of planet-forming material in disk midplanes is not straightforward. There is both chemical and kinematic evidence for a dynamical link between midplane and disk atmosphere chemical abundances, however. First, observations of complex organic molecules such as CH₃CN are only reproduced in models where cold icy grains are lifted up into the disk atmosphere (Öberg et al. 2015). Second, Teague et al. (2019) recently showed that there are meridional flows in at least one disk, which would effectively circulate disk material between the atmosphere and midplane. While we currently lack models that can quantify the importance of this link for the organic composition of forming planetesimals, a first step is a detailed understanding of the organic inventory where we can observe it, and this is reviewed below.

Constraints on the organic reservoirs in inner disk regions, commensurate with formation zones of habitable planets comes from IR observations; observations at longer wavelengths are confined to larger disk radii with existing facilities. Such IR observations of HCN and C₂H₂ have revealed that small organic molecules are abundant in the inner disk atmosphere (Pontoppidan et al. 2014). There is a curious difference in composition between disks around Solar-type and cool stars – the latter generally lack HCN (Pascucci et al. 2009). There are several possible explanations for this difference, with different implications for the organic content of planet-forming pebbles and boulders around different kinds of stars. If HCN is produced *in situ* in the inner disk gas, the observed differences in HCN/C₂H₂ ratio may simply be due to different radiation fields around Solar-type and cool stars, and may not be informative about the organic composition of planet-forming organic solids in the two kinds of disks. While this explanation remains a possibility it is not supported by current astrochemical disk models (Walsh et al. 2015).

A second possible explanation is that the observed chemistry depends on disk dynamics, which depends on disk mass, which in its turn correlates with stellar mass (Andrews et al. 2013). Najita et al. (2013) found that the HCN-water ratio depends on disk mass, which is explained by regulation of the C/O ratio by drift, or the lack thereof, of water-rich pebbles into the inner disk, which in its turn regulates the HCN gas-phase production. A third possible explanation for the observed differences in HCN/C₂H₂ between disks around cool and Solar-type stars is that this reflects a difference in organic composition of inward drifting pebbles, i.e. that the organic chemistry in the outer disk depends on the stellar mass and luminosity. Supporting this scenario is the similarity between HCN/C₂H₂/H₂O abundance ratios in disks around Solar-type stars and solar system comets (Pontoppidan et al. 2014; Altwegg et al. 2019). This would imply that planets form in chemically very different environments around different kinds of stars, which may drive substantially different prebiotic chemistries.

Spectrally resolved millimeter and sub-millimeter observations probe disk chemical compositions at larger disk radii, typically beyond 10s of au. Spatially resolved observations of organic molecules exist towards samples of \sim 10 disks, and Fig. 19 shows radial profiles of four organic molecules towards a subset of these disks. The molecules have been chosen as representatives of the four families of organic molecules observed in disks: hydrocarbons (C₂H), O-containing organics (H₂CO), nitriles and iso-nitriles (HC₃N), and S-containing organics (CS). Based on these profiles alone, (1) organics are not evenly distributed across disks, (2) there are multiple kinds of organic distributions and by extension organic chemical pathways present in each disk (compare e.g. the distribution of C₂H and H₂CO in V4046 Sgr), and (3) a single molecule can be distributed differently in different disks. This entails that if the observed chemical distributions trace or influence planetesimal compositions, the planetesimal organic compositions will strongly depend both where and around which star the planetesimals formed.

A number of disk chemical models have been developed to predict and explain the kind of observations introduced above. Henning and Semenov (2013) provides a quite recent review of these models. Some patterns that are emerging is that it is difficult to explain the relative abundances of nitrogen and oxygen bearing organics unless the disk atmospheres are C-rich and/or O-poor (Bergin et al. 2016; Kama et al. 2016; Cleeves et al. 2018; Le Gal et al. 2019b), that O-bearing organics are present at lower abundances than expected (Walsh et al. 2016), and that grain-surface chemistry is needed to reproduce both O and N-bearing complex organic abundances (Walsh et al. 2016; Loomis et al. 2018).

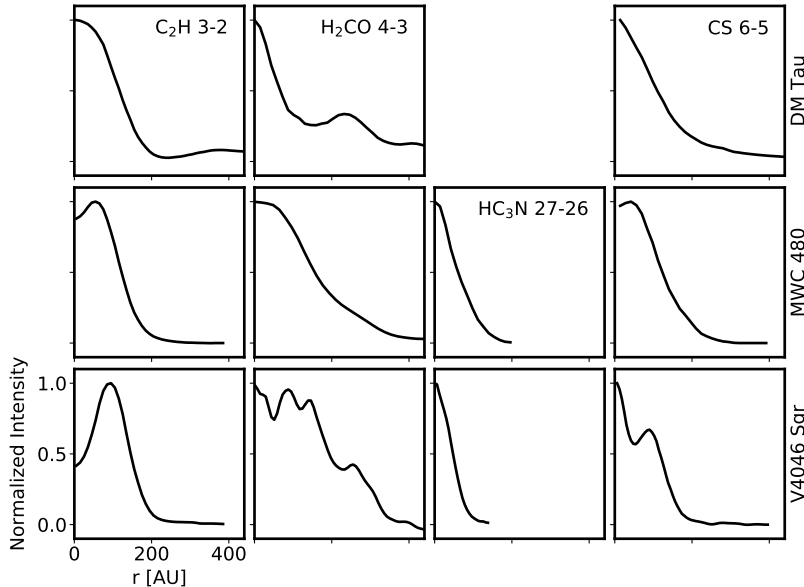


FIG. 19.— Radial profiles of four commonly observed organic molecules towards three representative protoplanetary disks: the young T Tauri disk DM Tau, the Herbig Ae disk MWC 480, and the old T Tauri disk V4046 Sgr. The four molecules, C_2H , H_2CO , HC_3N , and CS , are examples of the hydrocarbons, O-, N-, and S-containing organics. Note that the distribution of organic molecules differ both between disks, and between different kinds of organics. The origins of most variations are currently highly speculative, but are thought to be connected to differences in C and O depletions across and between disks, snowline locations, and dust sub-structure. Data from (Bergner et al. 2019a; Le Gal et al. 2019a; Pegues et al. 2020).

4.4. Elemental Accounting in the Solar System

Much of the existing connective tissue between astronomical composition and exoplanet composition links measurements of C/H and O/H (C/O) in planetary atmospheres, such as summarized by Madhusudhan (2019), to disk observations and planet formation theory. Fig. 18 is a prime motivator for this work. In our solar system, Jupiter and Saturn appear to be enriched in both C and N with values above that of the proto-Sun (Wong et al. 2004; Atreya et al. 2020). This has been posited to be the result of volatile enrichment in the gas via pebble drift (Cuzzi and Zahnle 2004; Öberg 2016) but see also Helled and Guillot (2018). The N enrichment for Jupiter has been suggested to be the result of formation of Jupiter beyond the N_2 iceline followed by migration (Öberg and Wordsworth 2019; Bosman et al. 2019b). The uncertain disposition of oxygen in this context is critical as the C/O ratio is a useful link to the formative conditions, but oxygen is difficult to probe in gas and ice giants (e.g., Cavalié et al. 2020). In Jupiter, Juno measured $\text{O}/\text{H} = 2.7^{+2.4}_{-1.7}$ times protosolar (Li et al. 2020), potentially consistent with enrichment, but this needs to be measured at different latitudes to determine if this represents the bulk composition.

Elemental accounting within the rocky/icy bodies are also of use and in Fig. 20 we provide an accounting of the budgets of the volatile elements O, C, and N in key solar system objects dominated by rocks and ices. We continue our focus C, O, and N as they are the most abundant and well-characterized of the volatile elements, but see below for a brief discussion of sulfur and phosphorous. We do not mention H, which is carried terrestrial worlds via H_2O and giant planets via H_2 . There are some distinctions in terms of the accounting in Fig. 20 that are worth mentioning. For isotopic ratios, we note which species we are referring to, e.g. H_2 or H_2O . For comets we provide the accounting within volatile ices and the total content which includes refractory material and the ices. Finally, CI Chondrites refer to a class of meteorites that are the least altered; hence they represent most primitive sampling of rocky material available (Weisberg et al. 2006).

Inside the water snowline, the fate of the C and N that was initial locked up into refractory material is a puzzle. For oxygen it is certain that any O locked in silicates in the ISM finds its way into solar system rocks, since silicates are only destroyed very close to the star where temperatures rise above ~ 1500 K (Dullemond and Monnier 2010), and this is consistent with the compositions of Earth and carbonaceous chondrites. But, materials provided to the disk also had large content of C and N carried in refractory form, which does not appear to have survived. The Earth acquired as little as 1 in 10,000 carbon atoms available at formation (Table 20 Finocchi et al. 1997; Lee et al. 2010; Pontoppidan et al. 2014) and CI chondrites, which formed in the inner Solar Nebula, are significantly carbon-depleted (Geiss and Reeves 1972; Bergin et al. 2015; Rubin et al. 2019). By contrast, substantial refractory and volatile carbon is found in comets, which perhaps best reflect the initial inventory of the solar system. Nitrogen exhibits even more extreme depletions in inner solar system solids, and is also under-abundant in comets (consistent with N_2 being a major nitrogen carrier), though comets still retain some more refractory nitrogen content (Altwegg et al. 2020).

It is important to state that constraints on the Earth are somewhat uncertain due to possible sequestration of a significant amount of carbon (or nitrogen) deep within the Earth (Dasgupta et al. 2013). Regardless, it is clear that

there is a gradient in the carbon and nitrogen content of solids from the inner to outer solar system; both carbon and nitrogen must have been primarily in volatile forms during early formative stages of pre-cursor materials inside of, at least, ~ 3 au. This may be a generic result in planet formation as the remnants of other rocky planetary systems currently accreting onto white dwarfs are also carbon-poor (Jura et al. 2015; Xu et al. 2019). Various theories have been proposed to account for this disposition (Gail 2002; Lee et al. 2010; Bergin et al. 2015; Anderson et al. 2017; Gail and Trieloff 2017; Klarmann et al. 2018).

Sulphur and Phosphorus are two other abundant volatile elements of import to biology. For sulphur, there is a puzzle in the interstellar medium as the main carrier remains unidentified (Kama et al. 2019, and references therein). In the solar system, the accounting is clearer: C I chondrites contain a nearly solar abundance of S (Lodders 2010), and so does the comet 67P/Churyumov–Gerasimenko Calmonte et al. (2016). Kama et al. (2019) used photospheric abundances of B stars, which have radiative envelopes with longer mixing timescales, to infer that in the accreting disk material, $\sim 89 \pm 8\%$ of sulphur resides in refractory material. In the case of 67P, sulfur is present in refractory, semi-refractory and volatile (H_2S) comet phases, however Calmonte et al. (2016), and it is possible that the volatility of sulfur reservoir changes between the inner and outer disk regions.

Similar to sulphur, chondritic and solar composition are in close agreement for P/Si, indicative of that most phosphorous was refractory in the inner Solar Nebula (Lodders 2010; Wang et al. 2019). Also similar to sulfur, there is potential tension between this finding and the identification of a substantial volatile phosphorous reservoir in comets. Most notably, phosphorous is detected in the coma of comet 67P, indicative of that at least some phosphorous is present in more volatile form during planet formation (Altwegg et al. 2019). Rivilla et al. (2020) identified the volatile phosphorous in 67P with PO, and found that the P/O abundance was consistent with solar, indicative of a low fraction of refractory P in the comet-forming zone, in direct contrast with the conclusion drawn from meteoritic abundances. It is currently unclear whether there is a gradient in refractory and volatile phosphorous carriers across disks, or whether 67P presents an unusual phosphorous abundance pattern. The solar system measurements can be compared with interstellar observations: PO and PN have been detected in the vicinity of protostars, most often in shocked outflow regions (Caux et al. 2011; Yamaguchi et al. 2011; Rivilla et al. 2016; Lefloch et al. 2016; Rivilla et al. 2020; Bergner et al. 2019d). Their abundances are well below solar phosphorous abundances, indicative of that most phosphorous in the dense ISM is solid and hidden from view. This could be consistent with either the meteoritic or cometary inferences, and more data is needed to identify the nature, and especially the volatility, of phosphorous and sulfur carriers during the early stages of star and planet formation.

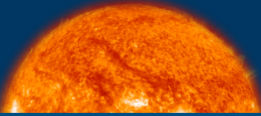
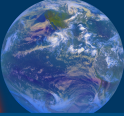




	Sun	Earth	Primitive Meteorites	Comets		
						
	Sun	Earth	CI Chondrites	Comets (Refractory)	Comets (Ice)	Comets (Total)
D/H	(H): 2.5×10^{-5}	(H ₂ O): 1.56×10^{-4}	(H ₂ O): $0.6\text{-}1.0 \times 10^{-4}$	—	(H ₂ O): $1.6\text{-}5.2 \times 10^{-4}$	—
¹⁴ N/ ¹⁵ N	(N): 441^{+33}_{-33}	(N ₂): 272	(Bulk): 261^{+2}_{-3}	—	(HCN): 100-150	—
O/Si	$15.6^{+2.8}_{-2.8}$	$1.8^{+0.1}_{-0.1}$	$7.5^{+0.8}_{-0.8}$	$5.4^{+8.5}_{-4.1}$	$10.5^{+0.6}_{-0.6}$	16^{+19}_{-4}
C/Si	$7.2^{+0.7}_{-0.7}$	$1.0^{+0.2}_{-0.2} \times 10^{-3}$	$0.7^{+0.1}_{-0.5}$	$5.4^{+9.2}_{-4.8}$	$0.9^{+0.3}_{-0.3}$	$6.3^{+9.2}_{-4.8}$
N/Si	$2.1^{+0.7}_{-0.7}$	$2.5^{+0.5}_{-0.5} \times 10^{-5}$	$0.042^{+0.11}_{-0.11}$	$0.19^{+0.37}_{-0.19}$	$0.09^{+0.03}_{-0.03}$	$0.28^{+0.37}_{-0.19}$

FIG. 20.— Volatile element budget and isotopic composition in select Solar System objects. (Sun): Image credit SeekPNG. Protostellar D/H ratio as determined by Geiss and Reeves (1972) and nitrogen isotopic ratio of the solar wind from Genesis (Marty et al. 2011). Atomic elemental abundance ratio of O, C, and N to Si are solar system abundances from 4.56 Gyr ago as estimated by Lodders (2010). (Earth): Image credit NOAA. D/H ratio of Earth water is set by Vienna Standard Mean Ocean Water. Atomic ratios are taken from Wang et al. (2018) for O and from Bergin et al. (2015) for C and N. (CI Chondrites:) Image Isotopic and atomic ratios for CI chondrites as given by Wänke and Dreibus (1988) and Wang et al. (2019). Errors represent the range in the samples. D/H ratio for water are from Alexander et al. (2012). (Comet:) Image of Comet ISON by Waldemar Skorupa. Comet water D/H and HCN nitrogen isotopic ratios represent the range detected in both Oort Cloud and Jupiter family comets (Mumma and Charnley 2011; Lis et al. 2019). Bulk elemental abundance atomic ratios are from Comet 67P/Churyumov-Gerasimenko as provided by Rubin et al. (2019) for a dust/ice ratio of unity.

4.5. Delivery of water and organics to temperate planets

The supply of water and organic material to Earth and other temperate terrestrial worlds during their formative stages, is a central question for habitability. How do key ingredients of life that originate in interstellar space affect the surface compositions of worlds that lie within the habitable zone, and make them chemically habitable. Based on the discussion in the earlier sections it is clear that the Earth, and many other rocky worlds, formed within their respective snowlines. This does not mean that these planets formed dry, as our own planets composition tells us; rather the supply of both water and organic material is likely part of the formation process. Below we will describe the theories that have been proposed to account for the origin of Earth's water and, by extension, its organics, and how lessons learned from Earth can be extended to other habitable planets.

When elucidating this process we will especially consider the D/H and $^{14}\text{N}/^{15}\text{N}$ isotopic ratios of Earth's volatiles. The D/H ratio hints at Earth's water history via a simple fact. Earth's water, and indeed all solar system water (Cleeves et al. 2014), has an excess of deuterium relative to hydrogen above that within the main deuterium repository HD. The same is also the case for interstellar water. As discussed above deuterium fractionation reactions for water proceed provided the gas temperature is less than 30 K. The opposite is also true: any deuterium enrichment, formed at cold temperatures and released to the gas via sublimation, will be redistributed back into HD on a timescale of few $\times 10^5$ yr or less depending on the strength of radial and/or vertical motions (Drouart et al. 1999; Furuya et al. 2013). The expected temperature of Earth's building blocks was clearly in excess of the sublimation temperature of water ice (~ 150 – 200 K). At these temperatures the deuterium signature would be destroyed and the resulting water would not be D-enriched. Thus, Earth's water received a contribution in full or in part from water ice beyond the snowline where the cold temperatures kept water frozen in the ices and the deuterium enrichment intact.

Nitrogen isotopic enrichments constitute another tool that has been used to explore the origin of Earth's volatile content (Marty 2012). Tracing the origin of this enrichment to particular locations in the ISM or in the solar nebula is difficult as there are multiple pathways to ^{15}N enrichments, through low temperature reactions and N_2 isotopic self-shielding, which could have been active at multiple stages during the pre-Solar, proto-Solar and Nebular stages (Wirström and Charnley 2018; Furuya et al. 2018; Visser et al. 2018). Still, $^{14}\text{N}/^{15}\text{N}$ similarities and differences between the Earth and different solar system volatile reservoirs can be used to constrain the origin of the Earth's nitrogen within the solar system (Table 1), though more work needs to be done to understand the origin of the ^{15}N excess (e.g., Hily-Blant et al. 2019).

There are (at least) three theories for the origin of water on a dry world – in situ, inward motion of the water snowline, and dynamical supply from beyond the ice line – and here we evaluate them in light of the Earth's isotopic enrichment patterns:

1. *In Situ*: In general, it is thought that interstellar molecules are bound to grain surfaces via physical adsorption and, for water, via H-bonds. However, interstellar grains are likely complex with more fractal like surfaces as seen in laboratory experiments of coagulation (Blum and Wurm 2008). These surfaces themselves may present sites where water might be chemisorbed onto dust grains or grouped into more resistant clusters, leading to a dilute water presence on dust grains even above the nominal evaporation temperature (Stimpfl et al. 2006; Muralidharan et al. 2008; King et al. 2010). The water vapor needed for this model is typically assumed to originate from a complete reset of the chemistry in the hot (>2000 K) cooling nebula model that is suggested for numerous inner solar system solids (see, e.g., McDonough and Sun 1995; Lodders 2010). D'Angelo et al. (2019) explored this question and demonstrated that hydrated minerals (phyllosilicates) could form and provide 0.5-10 Earth oceans worth of water to forming terrestrial worlds even at 300 K. This would essentially mean that the Earth formed wet. At face value this solution would provide water, but it is not certain whether carbon/nitrogen would also be provided at the same time. We note, that absent a high-temperature D-enrichment pathway such as suggested by Thi et al. (2010), the water would carry no deuterium enrichment in this scenario, which would require additional, substantial delivery of cold material, to match the Earth's D/H ratio.
2. *Snowline evolution*: During the early stages of nebular evolution the midplane is viscously heated via accretion, keeping the nebular snowline beyond 1 AU. However, the accretion rate decays with age (Hartmann et al. 2016), and when it falls below $\sim 10^{-8} M_{\odot}/\text{yr}$ the snowline is predicted to move interior to 1 AU (Garaud and Lin 2007; Oka et al. 2011). At this time (~ 1 Myr) the disk is clearly dominated by mm/cm sized pebbles (Andrews et al. 2018). Sato et al. (2016) and Ida et al. (2019) show that if sufficiently large planetary embryos ($\sim 0.1M_{\oplus}$) exist at 1 AU after the snowline moves inwards, then these embryos can grow via accretion of ice-coated pebble as the pebbles drift inwards. In addition to water, these pebbles would contain some carbon, and nitrogen, and likely carry the isotopic signatures of chondritic material. Thus, this scenario could be consistent with the isotopic evidence. However, Morbidelli et al. (2016) suggested that if Jupiter were to form before the water snowline moved interior to 1 AU, it would effectively stop icy-pebble drift leaving the inner nebula mostly dry. For systems with giant planets present, such as our own, this scenario may then not provide an explanation of Earth's enrichment in water and other volatiles. By contrast, in systems that lack Jupiter-analogs at 3 – 7 au, and they are estimated to constitute $>90\%$ of planetary systems (Wittenmyer et al. 2020), water and organics will likely be present in high abundance during early stage of terrestrial planet formation (Raymond and Morbidelli 2020).
3. *Dynamical Supply*: This is the traditional model for water delivery to habitable planets in systems similar to our own. In the solar system, there is a close connection between planetesimal bombardment of terrestrial planets and the presence of Jupiter, and its interaction with the gaseous and planetesimal disk. It is currently unclear whether

planetary systems that lack a Jupiter analog could use this scenario to deliver volatiles to habitable worlds. In the context of the Earth, the appeal of this scenario, is that provides a natural supply of water and organics from the outer asteroid belt, and match isotopic constraints. There are two comprehensive reviews in the recent literature that explore these models within the context of water supply and the reader is referred to these references (O’Brien et al. 2018; Raymond and Morbidelli 2020).

Of course, these different theories need not be exclusive and it is possible that combinations contribute. Further, here we only discuss the initial supply for water and C/N/S/P bearing organic/silicate material. In subsequent planet-evolutionary stages, there are a number of potential loss mechanisms that would modify the original volatile inventory. A brief (and not exhaustive) list of such mechanisms include ^{26}Al heating dehydration (Lichtenberg et al. 2019), impact-driven atmospheric loss (Schlichting et al. 2015), thermal metamorphism (Hashizume and Sugiura 1998), and core formation (Bergin et al. 2015; Grewal et al. 2019). In all, the assembly of habitable planets starts with basic physical and chemical principles that drive the formation of abundant water ice and organic material in interstellar space, but the implementation of these principles is complex and a research frontier.

4.6. Disk Chemistry Summary

Planets form in disks around pre-main sequence stars and the volatile composition of disks therefore directly impacts the volatile composition of planets. Over the past decade direct observations of disk gas have provided important clues about the disk volatile inventory, revealing e.g. that outer disk regions are oxygen depleted in the gas, and therefore, presumably, oxygen-enriched in its solids. This points to an active disk chemistry and a changing volatile composition during planet formation. These changes cannot be too large, however, since the similarity between cometary and interstellar ice compositions, as well as the water deuterium record in the solar system point to substantial inheritance of interstellar volatiles. Figuring out the exact balance between inheritance and disk chemistry is a key question for the next decade.

Within disks the distribution of volatiles may affect how efficiently planet formation proceeds. Snowlines are thought to change the grain growth process, through differential sticking and fragmentation, diffusive flows, and induced pressure traps. Snowlines also change the division of elements between gas and solids, and therefore regulate the initial composition of cores and atmospheres on planets, including their elemental C/N/O ratios. In this regard, bulk composition is a key tool to link planet formation to both gas giants and terrestrial worlds.

In addition to bulk compositions, we have paid special attention to the distribution of water and organics across disks, and the likelihood that they may become incorporated into or delivered to terrestrial planets. Disk do present a rich organic chemistry, and likely inherit much of the complex organic chemistry that is observed in protostellar envelopes. These potential precursors of prebiotic molecules are widely distributed across disks, but there is growing evidence that the organic composition varies both across and between different disks, indicating that planets may form with a diverse set of initial organic chemical conditions. How water and organic molecules do become part of the surface layers of planets, and populate their atmospheres and hydrospheres is not yet a solved problem. In the solar system impact delivery appears to have played an important role, but how important is debated. It is also unclear how easy it is to transfer this mechanism of enriching terrestrial planets in water and organics to exoplanetary systems without an analog to our outer solar system.

5. REVIEW SUMMARY AND FUTURE OUTLOOK

In this contribution we have explored how the chemistry of interstellar space influences the composition of planetary systems. Our focus has been on the elemental pools of the most abundant volatile elements C, O, N and H, on water, and on organics.

The chemical trajectory begins during the transition from diffuse to dense clouds, when the ultraviolet (UV) radiation exposure of all cloud material decreases, but the decrease is more dramatic towards the cloud center, resulting in temporal and spatial chemical gradients. During this process, the chemistry relevant for future planet formation shifts from the gas-phase, which regulates CO and N₂ formation, to the grain surface, where water and feedstock organics form. Importantly, at this stage most volatile carbon become locked into CO, most N into N₂, and most volatile O into CO and H₂O. The majority of these volatiles appears to survive the star formation process and become incorporated into planet-forming disks intact. The bulk volatile composition is thus set long before planet formation begins. *A key mystery at this stage is that one third of the oxygen is unaccounted for, which affects e.g. C/O ratio predictions throughout the protostellar and planet-forming stages.*

Organics represent a small portion of the overall elemental inventory, but their proposed connection to prebiotic chemistry motivates a detailed understanding of their formation and transformations during star and planet formation. The initial organic feed-stock molecules are formed in cold cloud regions through gas-phase chemistry (unsaturated organics) and grain-surface processes (saturated organics). During cloud collapse, heating by protostars and shock-induced grain heating, increases the mobility of ice constituents, resulting in a rich and complex organic chemistry. This chemistry is qualitatively quite well understood, but a lack of quantitative experimental and computational data on chemical reaction probabilities and rates limits the predictive capability of existing models. *Ice experiments, comprehensive surveys of protostellar chemistry, and theoretical models that fully couple the dynamics and time-dependent chemistry constitute frontiers in protostellar organic chemistry.*

Models predict that most of the bulk volatile composition, as well as the organic chemistry developed in the protostellar stage is incorporated into the planet-forming disk. Within the disk some alteration is expected, especially in the

inner disk, and at disk surfaces. In the latter regions, there is clear evidence for substantial oxygen depletion, some carbon depletion, and no nitrogen depletion, which must affect the elemental make-up of pebbles and planetesimals in the planet-forming disk midplane. The balance between inheritance and chemical processing is currently being explored theoretically, through comparisons between solar system and interstellar/protostellar observations, and through direct observations of disks with ALMA and other millimeter and sub-millimeter facilities. A difficulty in establishing this balance is that it certainly depends on a coupling between time-dependent chemistry and disk dynamics, especially mixing between disk surfaces and midplanes, and radial volatile transport through diffusive flows, accretion flows, and pebble drift. *There are several ongoing efforts to connect chemical theory and dynamics, and we expect rapid model improvement in the next few years. These models will be tested by forthcoming observations of disk gas by ALMA, and with JWST observations of midplane ices, and inner disk surface gas.*

The final step is how to connect chemical compositions of gas and pebbles in disks with the compositions of young planets. This requires a better understanding of disk midplane compositions (see above), but also on how volatiles can be added to planets post-formation. The latter is especially important to predict the water and organic content of temperate, Earth-like planets. *It is currently not clear under which conditions Earth-like planets can sample volatiles formed or preserved in outer disk regions, beyond the water snowline.* More in-depth cometary studies are key to assess their formation zones, as well as their relationship to terrestrial volatiles. A frontier in the connection between astrochemistry and planet composition regards the carbon content of inner disks; in the ISM, 50% of carbon resides in refractories, which appears preserved in comets, but seems to have been lost in the inner solar system. Depending on the nature of the refractory carbon removal mechanism, terrestrial planets may be generally carbon-poor, and depend on impacts both for water and organic delivery.

Finally, we note that Astrochemistry is an inherently interdisciplinary field. Its past and future successes depend on a combination of astronomical observations, chemical physics laboratory experiments, quantum calculations, molecular dynamics theory, and astrochemical models. We are entering an exciting era where astrochemistry is connecting with planetary and exoplanetary science to explore the formation of planets and the evolution of their hydrospheres and atmospheres. While the chemistry of planet formation sets the initial conditions of planets, the atmospheric chemistry and geochemistry determines how these initial conditions develop, and how often we may expect the complex chemistry we believe preceded life here on Earth.

EAB acknowledges support from NSF AAG Grant (#1907653) and the following grants from NASA’s Exoplanetary Research (80NSSC20K0259) and Emerging Worlds (80NSSC20K0333) programs. KIÖ acknowledges support from the Simons Foundation (SCOL #321183) and an NSF AAG Grant (#1907653). The authors are grateful to Viviana Guzmán, Romane Le Gal, Jennifer Bergner, Jamila Pegues, Chunhua Qi, and Chin-Fei Lee for contributing to the figures. The authors are also deeply appreciative to Henrick Beuther, Geoff Blake, Paola Caselli, Cecilia Ceccarelli, Ilse Cleeves, Rachel Freisen, Robin Garrod, Maryvonne Gerin, Viviana Guzmán, Javier Goicoechea, Eric Herbst, Pierre Hily-Blant, Romane Le Gal, Klaus Pontoppidan, Evelyne Roueff, Nami Sakai, Ian Sims, Vianney Taquet, Ewine van Dishoeck, Qizhou Zhang for providing input on the content of the review.

REFERENCES

- Abergel, A., Teyssier, D., Bernard, J.P., Boulanger, F., Coulais, A., Fosse, D., Falgarone, E., Gerin, M., Perault, M., Puget, J.L., Nordh, L., Olofsson, G., Hultdtgren, M., Kaas, A.A., André, P., Bontemps, S., Casali, M.M., Cesarsky, C.J., Copet, E., Davies, J., Montmerle, T., Persi, P., Sibille, F., 2003. ISOCAM and molecular observations of the edge of the Horsehead nebula. *A&A* 410, 577–585. doi:doi:10.1051/0004-6361:20030878.
- Adams, N.G., Smith, D., Clary, D.C., 1985. Rate coefficients for the reactions of ions with polar molecules at interstellar temperatures. *ApJ* 296, L31–L34. doi:doi:10.1086/184543.
- Aikawa, Y., Herbst, E., 1999. Molecular evolution in protoplanetary disks. Two-dimensional distributions and column densities of gaseous molecules. *A&A* 351, 233–246.
- Aikawa, Y., Herbst, E., 2001. Two-dimensional distributions and column densities of gaseous molecules in protoplanetary disks. II. Deuterated species and UV shielding by ambient clouds. *A&A* 371, 1107–1117. doi:doi:10.1051/0004-6361:20010416, arXiv:arXiv:astro-ph/0202062.
- Aikawa, Y., Momose, M., Thi, W., van Zadelhoff, G., Qi, C., Blake, G.A., van Dishoeck, E.F., 2003. Interferometric Observations of Formaldehyde in the Protoplanetary Disk around LkCa 15. *PASJ* 55, 11–15. arXiv:arXiv:astro-ph/0211440.
- Aikawa, Y., Nomura, H., 2006. Physical and Chemical Structure of Protoplanetary Disks with Grain Growth. *ApJ* 642, 1152–1162. doi:doi:10.1086/501114, arXiv:astro-ph/0601230.
- Aikawa, Y., Wakelam, V., Hersant, F., Garrod, R.T., Herbst, E., 2012. From Prestellar to Protostellar Cores. II. Time Dependence and Deuterium Fractionation. *ApJ* 760, 40. doi:doi:10.1088/0004-637X/760/1/40, arXiv:1210.2476.
- Alexander, C.M.O., Bowden, R., Fogel, M.L., Howard, K.T., Herd, C.D.K., Nittler, L.R., 2012. The Provenances of Asteroids, and Their Contributions to the Volatile Inventories of the Terrestrial Planets. *Science* 337, 721. doi:doi:10.1126/science.1223474.
- Alexander, C.M.O.D., Fogel, M., Yabuta, H., Cody, G.D., 2007. The origin and evolution of chondrites recorded in the elemental and isotopic compositions of their macromolecular organic matter. *Geochim. Cosmochim. Acta* 71, 4380–4403. doi:doi:10.1016/j.gca.2007.06.052.
- Alexander, C.M.O.D., Newsome, S.D., Fogel, M.L., Nittler, L.R., Busemann, H., Cody, G.D., 2010. Deuterium enrichments in chondritic macromolecular material—Implications for the origin and evolution of organics, water and asteroids. *Geochim. Cosmochim. Acta* 74, 4417–4437. doi:doi:10.1016/j.gca.2010.05.005.

- ALMA Partnership, Brogan, C.L., Pérez, L.M., Hunter, T.R., Dent, W.R.F., Hales, A.S., Hills, R.E., Corder, S., Fomalont, E.B., Vlahakis, C., Asaki, Y., Barkats, D., Hirota, A., Hodge, J.A., Impellizzeri, C.M.V., Kneissl, R., Liuzzo, E., Lucas, R., Marcelino, N., Matsushita, S., Nakanishi, K., Phillips, N., Richards, A.M.S., Toledo, I., Aladro, R., Broguiere, D., Cortes, J.R., Cortes, P.C., Espada, D., Galarza, F., Garcia-Appadoo, D., Guzman-Ramirez, L., Humphreys, E.M., Jung, T., Kamenoi, S., Laing, R.A., Leon, S., Marconi, G., Mignano, A., Nikolic, B., Nyman, L.A., Radiszcz, M., Remijan, A., Rodón, J.A., Sawada, T., Takahashi, S., Tilanus, R.P.J., Vila Vilaro, B., Watson, L.C., Wiklind, T., Akiyama, E., Chapillon, E., de Gregorio-Monsalvo, I., Di Francesco, J., Gueth, F., Kawamura, A., Lee, C.F., Nguyen Luong, Q., Mangum, J., Pietu, V., Sanhueza, P., Saigo, K., Takakuwa, S., Ubach, C., van Kempen, T., Wootten, A., Castro-Carrizo, A., Francke, H., Gallardo, J., Garcia, J., Gonzalez, S., Hill, T., Kaminski, T., Kurono, Y., Liu, H.Y., Lopez, C., Morales, F., Plarre, K., Schieven, G., Testi, L., Videla, L., Villard, E., Andreani, P., Hibbard, J.E., Tatematsu, K., 2015. The 2014 ALMA Long Baseline Campaign: First Results from High Angular Resolution Observations toward the HL Tau Region. *ApJ* 808, L3. doi:doi:10.1088/2041-8205/808/1/L3.
- Altwegg, K., Balsiger, H., Fuselier, S.A., 2019. Cometary Chemistry and the Origin of Icy Solar System Bodies: The View After Rosetta. *ARA&A* 57, 113–155. doi:doi:10.1146/annurev-astro-091918-104409, arXiv:1908.04046.
- Altwegg, K., Balsiger, H., Hänni, N., Rubin, M., Schuhmann, M., Schroeder, I., Sémon, T., Wampfler, S., Berthelier, J.J., Briois, C., Combi, M., Gombosi, T.I., Cottin, H., De Keyser, J., Dhoghe, F., Fiethe, B., Fuselier, S.A., 2020. Evidence of ammonium salts in comet 67P as explanation for the nitrogen depletion in cometary comae. *Nature Astronomy*, 3doi:doi:10.1038/s41550-019-0991-9, arXiv:1911.13005.
- Anderl, S., Maret, S., Cabrit, S., Belloche, A., Maury, A.J., André, P., Codella, C., Bacmann, A., Bontemps, S., Podio, L., Gueth, F., Bergin, E., 2016. Probing the CO and methanol snow lines in young protostars. Results from the CALYPSO IRAM-PdBI survey. *A&A* 591, A3. doi:doi:10.1051/0004-6361/201527831, arXiv:1604.05121.
- Anderson, D.E., Bergin, E.A., Blake, G.A., Ciesla, F.J., Visser, R., Lee, J.E., 2017. Destruction of Refractory Carbon in Protoplanetary Disks. *ApJ* 845, 13. doi:doi:10.3847/1538-4357/aa7da1, arXiv:1707.08982.
- Anderson, D.E., Blake, G.A., Bergin, E.A., Zhang, K., Carpenter, J.M., Schwarz, K.R., Huang, J., Öberg, K.I., 2019. Probing the Gas Content of Late-stage Protoplanetary Disks with N_2H^+ . *ApJ* 881, 127. doi:doi:10.3847/1538-4357/ab2cb5.
- Andersson, S., Al-Halabi, A., Kroes, G.J., van Dishoeck, E.F., 2006. Molecular-dynamics study of photodissociation of water in crystalline and amorphous ices. *J. Chem. Phys.* 124, 064715–064715. doi:doi:10.1063/1.2162901, arXiv:astro-ph/0512596.
- Andersson, S., van Dishoeck, E.F., 2008. Photodesorption of water ice. A molecular dynamics study. *A&A* 491, 907–916. doi:doi:10.1051/0004-6361:200810374, arXiv:0810.1916.
- Andrews, S.M., 2020. Observations of Protoplanetary Disk Structures. arXiv e-prints, in press. arXiv:2001.05007.
- Andrews, S.M., Huang, J., Pérez, L.M., Isella, A., Dullemond, C.P., Kurtovic, N.T., Guzmán, V.V., Carpenter, J.M., Wilner, D.J., Zhang, S., Zhu, Z., Birnstiel, T., Bai, X.N., Benisty, M., Hughes, A.M., Öberg, K.I., Ricci, L., 2018. The Disk Substructures at High Angular Resolution Project (DSHARP). I. Motivation, Sample, Calibration, and Overview. *ApJ* 869, L41. doi:doi:10.3847/2041-8213/aaf741, arXiv:1812.04040.
- Andrews, S.M., Rosenfeld, K.A., Kraus, A.L., Wilner, D.J., 2013. The Mass Dependence between Protoplanetary Disks and their Stellar Hosts. *ApJ* 771, 129. doi:doi:10.1088/0004-637X/771/2/129, arXiv:1305.5262.
- Andrews, S.M., Wilner, D.J., Zhu, Z., Birnstiel, T., Carpenter, J.M., Pérez, L.M., Bai, X.N., Öberg, K.I., Hughes, A.M., Isella, A., Ricci, L., 2016. Ringed Substructure and a Gap at 1 au in the Nearest Protoplanetary Disk. *ApJ* 820, L40. doi:doi:10.3847/2041-8205/820/2/L40, arXiv:1603.09352.
- Aota, T., Inoue, T., Aikawa, Y., 2015. Evaporation of Grain-surface Species by Shock Waves in a Protoplanetary Disk. *ApJ* 799, 141. doi:doi:10.1088/0004-637X/799/2/141, arXiv:1412.1178.
- Arce, H.G., Santiago-García, J., Jørgensen, J.K., Tafalla, M., Bachiller, R., 2008. Complex Molecules in the L1157 Molecular Outflow. *ApJL* 681, L21–L24. doi:doi:10.1086/590110, arXiv:0805.2550.
- Armitage, P.J., Eisner, J.A., Simon, J.B., 2016. Prompt Planetesimal Formation beyond the Snow Line. *ApJ* 828, L2. doi:doi:10.3847/2041-8205/828/1/L2, arXiv:1608.03592.
- Artur de la Villarmois, E., Jørgensen, J.K., Kristensen, L.E., Bergin, E.A., Harsono, D., Sakai, N., van Dishoeck, E.F., Yamamoto, S., 2019. Physical and chemical fingerprint of protostellar disc formation. *A&A* 626, A71. doi:doi:10.1051/0004-6361/201834877, arXiv:1904.13161.
- Artur de la Villarmois, E., Kristensen, L.E., Jørgensen, J.K., Bergin, E.A., Brinch, C., Frimann, S., Harsono, D., Sakai, N., Yamamoto, S., 2018. Chemistry of a newly detected circumbinary disk in Ophiuchus. *A&A* 614, A26. doi:doi:10.1051/0004-6361/201731603, arXiv:1802.09286.
- Aso, Y., Ohashi, N., Aikawa, Y., Machida, M.N., Saigo, K., Saito, M., Takakuwa, S., Tomida, K., Tomisaka, K., Yen, H.W., 2017. ALMA Observations of the Protostar L1527 IRS: Probing Details of the Disk and the Envelope Structures. *ApJ* 849, 56. doi:doi:10.3847/1538-4357/aa8264, arXiv:1707.08697.
- Asplund, M., Grevesse, N., Sauval, A.J., Scott, P., 2009. The Chemical Composition of the Sun. *ARA&A* 47, 481–522. doi:doi:10.1146/annurev.astro.46.060407.145222, arXiv:0909.0948.
- Atreya, S.K., Hofstadter, M.H., In, J.H., Mousis, O., Reh, K., Wong, M.H., 2020. Deep Atmosphere Composition, Structure, Origin, and Exploration, with Particular Focus on Critical in situ Science at the Icy Giants. *Space Sci. Rev.* 216, 18. doi:doi:10.1007/s11214-020-0640-8.
- Bacmann, A., Taquet, V., Faure, A., Kahane, C., Ceccarelli, C., 2012. Detection of complex organic molecules in a prestellar core: a new challenge for astrochemical models. *A&A* 541, L12. doi:doi:10.1051/0004-6361/201219207.
- Bally, J., Chambers, E., Guzman, V., Keto, E., Mookerjee, B., Sandell, G., Stanke, T., Zinnecker, H., 2018. Kinematics of the Horsehead Nebula and IC 434 Ionization Front in CO and C^+ . *AJ* 155, 80. doi:doi:10.3847/1538-3881/aaa248.
- Balucani, N., Ceccarelli, C., Taquet, V., 2015. Formation of complex organic molecules in cold objects: the role of gas-phase reactions. *MNRAS* 449, L16–L20. doi:doi:10.1093/mnras/slv009, arXiv:1501.03668.
- Banzatti, A., Pinilla, P., Ricci, L., Pontoppidan, K.M., Birnstiel, T., Ciesla, F., 2015. Direct Imaging of the Water Snow Line at the Time of Planet Formation using Two ALMA Continuum Bands. *ApJ* 815, L15. doi:doi:10.1088/2041-8205/815/1/L15, arXiv:1511.06762.
- Belloche, A., Müller, H.S.P., Garrod, R.T., Menten, K.M., 2016. Exploring molecular complexity with ALMA (EMoCA): Deuterated complex organic molecules in Sagittarius B2(N2). *A&A* 587, A91. doi:doi:10.1051/0004-6361/201527268, arXiv:1511.05721.
- Bennett, C.J., Chen, S.H., Sun, B.J., Chang, A.H.H., Kaiser, R.I., 2007. Mechanical Studies on the Irradiation of Methanol in Extraterrestrial Ices. *ApJ* 660, 1588–1608. doi:doi:10.1086/511296.
- Benson, P.J., Myers, P.C., 1989. A Survey for Dense Cores in Dark Clouds. *ApJS* 71, 89. doi:doi:10.1086/191365.
- Bergin, E., Calvet, N., Sitko, M.L., Abgrall, H., D'Alessio, P., Herczeg, G.J., Roueff, E., Qi, C., Lynch, D.K., Russell, R.W., Brafford, S.M., Perry, R.B., 2004a. A New Probe of the Planet-forming Region in T Tauri Disks. *ApJL* 614, L133–L136. doi:doi:10.1086/425865, arXiv:arXiv:astro-ph/0409308.
- Bergin, E.A., Alves, J., Huard, T., Lada, C.J., 2002. N_2H^+ and $C^{18}O$ Depletion in a Cold Dark Cloud. *ApJL* 570, L101–L104. doi:doi:10.1086/340950, arXiv:astro-ph/0204016.
- Bergin, E.A., Blake, G.A., Ciesla, F., Hirschmann, M.M., Li, J., 2015. Tracing the ingredients for a habitable earth from interstellar space through planet formation. *Proceedings of the National Academy of Science* 112, 8965–8970. doi:doi:10.1073/pnas.1500954112, arXiv:1507.04756.

- Bergin, E.A., Ciardi, D.R., Lada, C.J., Alves, J., Lada, E.A., 2001. Molecular Excitation and Differential Gas-Phase Depletions in the IC 5146 Dark Cloud. *ApJ* 557, 209–225. doi:doi:10.1086/321625, [arXiv:astro-ph/0103521](#).
- Bergin, E.A., Cleaves, L.I., Crockett, N., Blake, G.A., 2014. Exploring the Origins of Carbon in Terrestrial Worlds. *Faraday Discussions* 168, 61–79. doi:doi:10.1039/C4FD00003J, [arXiv:1405.7394](#).
- Bergin, E.A., Cleaves, L.I., Gorti, U., Zhang, K., Blake, G.A., Green, J.D., Andrews, S.M., Evans, II, N.J., Henning, T., Öberg, K., Pontoppidan, K., Qi, C., Salyk, C., van Dishoeck, E.F., 2013. An old disk still capable of forming a planetary system. *Nature* 493, 644–646. doi:doi:10.1038/nature11805.
- Bergin, E.A., Du, F., Cleaves, L.I., Blake, G.A., Schwarz, K., Visser, R., Zhang, K., 2016. Hydrocarbon Emission Rings in Protoplanetary Disks Induced by Dust Evolution. *ApJ* 831, 101. doi:doi:10.3847/0004-637X/831/1/101, [arXiv:1609.06337](#).
- Bergin, E.A., Hartmann, L.W., Raymond, J.C., Ballesteros-Paredes, J., 2004b. Molecular Cloud Formation behind Shock Waves. *ApJ* 612, 921–939. doi:doi:10.1086/422578, [arXiv:astro-ph/0405329](#).
- Bergin, E.A., Hogerheijde, M.R., Brinch, C., Fogel, J., Yıldız, U.A., Kristensen, L.E., van Dishoeck, E.F., Bell, T.A., Blake, G.A., Cernicharo, J., Dominik, C., Lis, D., Melnick, G., Neufeld, D., Panić, O., Pearson, J.C., Bachiller, R., Baudry, A., Benedettini, M., Benz, A.O., Bjerkeli, P., Bontemps, S., Braine, J., Bruderer, S., Caselli, P., Codella, C., Daniel, F., di Giorgio, A.M., Doty, S.D., Encrenaz, P., Fich, M., Fuente, A., Giannini, T., Goicoechea, J.R., de Graauw, T., Helmich, F., Herczeg, G.J., Herpin, F., Jacq, T., Johnstone, D., Jørgensen, J.K., Larsson, B., Liseau, R., Marseille, M., McCoey, C., Nisini, B., Olberg, M., Parise, B., Plume, R., Risacher, C., Santiago-García, J., Saraceno, P., Shipman, R., Tafalla, M., van Kempen, T.A., Visser, R., Wampfler, S.F., Wyrowski, F., van der Tak, F., Jellema, W., Tielens, A.G.G.M., Hartogh, P., Stützki, J., Szczerba, R., 2010. Sensitive limits on the abundance of cold water vapor in the DM Tauri protoplanetary disk. *A&A* 521, L33+. doi:doi:10.1051/0004-6361/201015104, [arXiv:1007.2129](#).
- Bergin, E.A., Langer, W.D., Goldsmith, P.F., 1995. Gas-phase chemistry in dense interstellar clouds including grain surface molecular depletion and desorption. *ApJ* 441, 222–243. doi:doi:10.1086/175351.
- Bergin, E.A., Melnick, G.J., Stauffer, J.R., Ashby, M.L.N., Chin, G., Erickson, N.R., Goldsmith, P.F., Harwit, M., Howe, J.E., Kleiner, S.C., Koch, D.G., Neufeld, D.A., Patten, B.M., Plume, R., Schieder, R., Snell, R.L., Tolls, V., Wang, Z., Winnewisser, G., Zhang, Y.F., 2000. Implications of Submillimeter Wave Astronomy Satellite Observations for Interstellar Chemistry and Star Formation. *ApJ* 539, L129–L132. doi:doi:10.1086/312843.
- Bergin, E.A., Tafalla, M., 2007. Cold Dark Clouds: The Initial Conditions for Star Formation. *ARA&A* 45, 339–396. doi:doi:10.1146/annurev.astro.45.071206.100404, [arXiv:0705.3765](#).
- Bergin, E.A., Williams, J.P., 2017. The Determination of Protoplanetary Disk Masses. volume 445 of *Astrophysics and Space Science Library*. p. 1. doi:doi:10.1007/978-3-319-60609-5“1.
- Bergner, J.B., Öberg, K.I., Bergin, E.A., Andrews, S.M., Blake, G.A., Carpenter, J.M., Cleaves, L.I., Guzmán, V.V., Huang, J., Jørgensen, J.K., Qi, C., Schwarz, K.R., Williams, J.P., Wilner, D.J., 2020. An Evolutionary Study of Volatile Chemistry in Protoplanetary Disks. *ApJ* 898, 97. doi:doi:10.3847/1538-4357/ab9e71, [arXiv:2006.12584](#).
- Bergner, J.B., Öberg, K.I., Bergin, E.A., Loomis, R.A., Pegues, J., Qi, C., 2019a. A Survey of C₂H, HCN, and C¹⁸O in Protoplanetary Disks. *ApJ* 876, 25. doi:doi:10.3847/1538-4357/ab141e, [arXiv:1904.09315](#).
- Bergner, J.B., Öberg, K.I., Rajappan, M., 2019b. Oxygen Atom Reactions with C₂H₆, C₂H₄, and C₂H₂ in Ices. *ApJ* 874, 115. doi:doi:10.3847/1538-4357/ab07b2, [arXiv:1903.10981](#).
- Bergner, J.B., Öberg, K.I., Walker, S., Guzmán, V.V., Rice, T.S., Bergin, E.A., 2019c. Detection of Phosphorus-bearing Molecules toward a Solar-type Protostar. *ApJ* 884, L36. doi:doi:10.3847/2041-8213/ab48f9, [arXiv:1910.04539](#).
- Bergner, J.B., Öberg, K.I., Walker, S., Guzmán, V.V., Rice, T.S., Bergin, E.A., 2019d. Detection of Phosphorus-bearing Molecules toward a Solar-type Protostar. *ApJ* 884, L36. doi:doi:10.3847/2041-8213/ab48f9, [arXiv:1910.04539](#).
- Bertin, M., Fayolle, E.C., Romanzin, C., Poderoso, H.A.M., Michaut, X., Philippe, L., Jeseck, P., Öberg, K.I., Linnartz, H., Fillion, J.H., 2013. Indirect Ultraviolet Photodesorption from CO:N₂ Binary Ices - an Efficient Grain-gas Process. *ApJ* 779, 120. doi:doi:10.1088/0004-637X/779/2/120, [arXiv:1312.4571](#).
- Bethell, T.J., Bergin, E.A., 2011. The Propagation of Ly α in Evolving Protoplanetary Disks. *ApJ* 739, 78. doi:doi:10.1088/0004-637X/739/2/78, [arXiv:1107.3514](#).
- Bianchi, S., Gonçalves, J., Albrecht, M., Caselli, P., Chini, R., Galli, D., Walmsley, M., 2003. Dust emissivity in the submm/mm. SCUBA and SIMBA observations of Barnard 68. *A&A* 399, L43–L46. doi:doi:10.1051/0004-6361:20030078, [arXiv:astro-ph/0301386](#).
- Birnstiel, T., Dullemond, C.P., Brauer, F., 2010. Gas- and dust evolution in protoplanetary disks. *A&A* 513, A79. doi:doi:10.1051/0004-6361/200913731, [arXiv:1002.0335](#).
- Bisschop, S.E., Fraser, H.J., Öberg, K.I., van Dishoeck, E.F., Schlemmer, S., 2006. Desorption rates and sticking coefficients for CO and N₂ interstellar ices. *A&A* 449, 1297–1309. doi:doi:10.1051/0004-6361:20054051, [arXiv:astro-ph/0601082](#).
- Bizzocchi, L., Caselli, P., Spezzano, S., Leonardo, E., 2014. Deuterated methanol in the pre-stellar core L1544. *A&A* 569, A27. doi:doi:10.1051/0004-6361/201423858, [arXiv:1408.2491](#).
- Bizzocchi, L., Tamassia, F., Laas, J., Giuliano, B.M., Degli Esposti, C., Dore, L., Melosso, M., Canè, E., Pietropoli, Charmet, A., Müller, H.S.P., Spahn, H., Belloche, A., Caselli, P., Menten, K.M., Garrod, R.T., 2017. Rotational and High-resolution Infrared Spectrum of HC₃N: Global Ro-vibrational Analysis and Improved Line Catalog for Astrophysical Observations. *ApJS* 233, 11. doi:doi:10.3847/1538-4365/aa9571, [arXiv:1711.08592](#).
- Blevins, S.M., Pontoppidan, K.M., Banzatti, A., Zhang, K., Najita, J.R., Carr, J.S., Salyk, C., Blake, G.A., 2016. Measurements of Water Surface Snow Lines in Classical Protoplanetary Disks. *ApJ* 818, 22. doi:doi:10.3847/0004-637X/818/1/22, [arXiv:1512.07197](#).
- Blum, J., Wurm, G., 2008. The growth mechanisms of macroscopic bodies in protoplanetary disks. *ARA&A* 46, 21–56. doi:doi:10.1146/annurev.astro.46.060407.145152.
- Boesgaard, A.M., Steigman, G., 1985. Big Bang nucleosynthesis: theories and observations. *ARA&A* 23, 319–378. doi:doi:10.1146/annurev.aa.23.090185.001535.
- Boogert, A.C.A., Gerakines, P.A., Whittet, D.C.B., 2015. Observations of the icy universe. *ARA&A* 53, 541–581. doi:doi:10.1146/annurev-astro-082214-122348, [arXiv:1501.05317](#).
- Boogert, A.C.A., Pontoppidan, K.M., Knez, C., Lahuis, F., Kessler-Silacci, J., van Dishoeck, E.F., Blake, G.A., Augereau, J.C., Bisschop, S.E., Bottinelli, S., Brooke, T.Y., Brown, J., Crapsi, A., Evans, II, N.J., Fraser, H.J., Geers, V., Huard, T.L., Jørgensen, J.K., Öberg, K.I., Allen, L.E., Harvey, P.M., Koerner, D.W., Mundy, L.G., Padgett, D.L., Sargent, A.I., Stapelfeldt, K.R., 2008. The c2d Spitzer Spectroscopic Survey of Ices around Low-Mass Young Stellar Objects. I. H₂O and the 5–8 μ m Bands. *ApJ* 678, 985–1004. doi:doi:10.1086/533425, [arXiv:0801.1167](#).
- Bosman, A.D., Cridland, A.J., Miguel, Y., 2019a. Jupiter formed as a pebble pile around the N₂ ice line. *A&A* 632, L11. doi:doi:10.1051/0004-6361/201936827, [arXiv:1911.11154](#).
- Bosman, A.D., Cridland, A.J., Miguel, Y., 2019b. Jupiter formed as a pebble pile around the N₂ ice line. *A&A* 632, L11. doi:doi:10.1051/0004-6361/201936827, [arXiv:1911.11154](#).
- Bosman, A.D., Tielens, A.G.G.M., van Dishoeck, E.F., 2017. Efficiency of radial transport of ices in protoplanetary disks probed with infrared observations: the case of CO₂. *ArXiv e-prints* [arXiv:1712.03989](#).
- Bosman, A.D., Walsh, C., van Dishoeck, E.F., 2018. CO destruction in protoplanetary disk midplanes: Inside versus outside the CO snow surface. *A&A* 618, A182. doi:doi:10.1051/0004-6361/201833497, [arXiv:1808.02220](#).

- Bottinelli, S., Ceccarelli, C., Lefloch, B., Williams, J.P., Castets, A., Caux, E., Cazaux, S., Maret, S., Parise, B., Tielens, A.G.G.M., 2004. Complex Molecules in the Hot Core of the Low-Mass Protostar NGC 1333 IRAS 4A. *ApJ* 615, 354–358. doi:doi:10.1086/423952, arXiv:arXiv:astro-ph/0407154.
- Brinch, C., Hogerheijde, M.R., 2010. LIME - a flexible, non-LTE line excitation and radiation transfer method for millimeter and far-infrared wavelengths. *A&A* 523, A25. doi:doi:10.1051/0004-6361/201015333, arXiv:1008.1492.
- Bruderer, S., van Dishoeck, E.F., Doty, S.D., Herczeg, G.J., 2012. The warm gas atmosphere of the HD 100546 disk seen by Herschel. Evidence of a gas-rich, carbon-poor atmosphere? *A&A* 541, A91. doi:doi:10.1051/0004-6361/201118218, arXiv:1201.4860.
- Burke, J.R., Hollenbach, D.J., 1983. The gas-grain interaction in the interstellar medium - Thermal accommodation and trapping. *ApJ* 265, 223–234. doi:doi:10.1086/160667.
- Calmonte, U., Altwegg, K., Balsiger, H., Berthelier, J.J., Bieler, A., Cessateur, G., Dhooche, F., van Dishoeck, E.F., Fiethe, B., Fuselier, S.A., Gasc, S., Gombosi, T.I., Hässig, M., Le Roy, L., Rubin, M., Sémon, T., Tzou, C.Y., Wampfler, S.F., 2016. Sulphur-bearing species in the coma of comet 67P/Churyumov-Gerasimenko. *MNRAS* 462, S253–S273. doi:doi:10.1093/mnras/stw2601.
- Carr, J.S., Najita, J.R., 2008. Organic Molecules and Water in the Planet Formation Region of Young Circumstellar Disks. *Science* 319, 1504. doi:doi:10.1126/science.1153807.
- Carr, J.S., Najita, J.R., Salyk, C., 2018. Measuring the Water Snow Line in a Protoplanetary Disk. *Research Notes of the American Astronomical Society* 2, 169. doi:doi:10.3847/2515-5172/aadfe7.
- Caselli, P., Ceccarelli, C., 2012. Our astrochemical heritage. *A&A Rev.* 20, 56. doi:doi:10.1007/s00159-012-0056-x, arXiv:1210.6368.
- Caselli, P., Walmsley, C.M., Tafalla, M., Dore, L., Myers, P.C., 1999. CO Depletion in the Starless Cloud Core L1544. *ApJL* 523, L165–L169. doi:doi:10.1086/312280.
- Caselli, P., Walmsley, C.M., Zucconi, A., Tafalla, M., Dore, L., Myers, P.C., 2002. Molecular Ions in L1544. II. The Ionization Degree. *ApJ* 565, 344–358. doi:doi:10.1086/324302, arXiv:astro-ph/0109023.
- Caux, E., Kahane, C., Castets, A., Coutens, A., Ceccarelli, C., Bacmann, A., Bisschop, S., Bottinelli, S., Comito, C., Helmich, F.P., Lefloch, B., Parise, B., Schilke, P., Tielens, A.G.G.M., van Dishoeck, E., Vastel, C., Wakelam, V., Walters, A., 2011. TIMASSS: the IRAS 16293-2422 millimeter and submillimeter spectral survey. I. Observations, calibration, and analysis of the line kinematics. *A&A* 532, A23. doi:doi:10.1051/0004-6361/201015399, arXiv:1103.5347.
- Cavalié, T., Venot, O., Miguel, Y., Fletcher, L.N., Wurz, P., Mousis, O., Bounaceur, R., Hue, V., Leconte, J., Dobrijevic, M., 2020. The Deep Composition of Uranus and Neptune from In Situ Exploration and Thermochemical Modeling. *Space Sci. Rev.* 216, 58. doi:doi:10.1007/s11214-020-00677-8, arXiv:2004.13987.
- Cazaux, S., Caselli, P., Spaans, M., 2011. Interstellar Ices as Witnesses of Star Formation: Selective Deuteration of Water and Organic Molecules Unveiled. *ApJL* 741, L34. doi:doi:10.1088/2041-8205/741/2/L34, arXiv:1107.1984.
- Ceccarelli, C., Caselli, P., Bockelée-Morvan, D., Mousis, O., Pizzarello, S., Robert, F., Semenov, D., 2014. Deuterium Fractionation: The Ariadne's Thread from the Precollapse Phase to Meteorites and Comets Today, in: Beuther, H., Klessen, R.S., Dullemond, C.P., Henning, T. (Eds.), *Protostars and Planets VI*, p. 859. doi:doi:10.2458/azu“uapress“9780816531240-ch037, arXiv:1403.7143.
- Ceccarelli, C., Caselli, P., Fontani, F., Neri, R., López-Sepulcre, A., Codella, C., Feng, S., Jiménez-Serra, I., Lefloch, B., Pineda, J.E., Vastel, C., Alves, F., Bachiller, R., Balucani, N., Bianchi, E., Bizzocchi, L., Bottinelli, S., Caux, E., Chacón-Tanarro, A., Choudhury, R., Coutens, A., Dulieu, F., Favre, C., Hily-Blant, P., Holdship, J., Kahane, C., Jaber Al-Edhari, A., Laas, J., Ospina, J., Oya, Y., Podio, L., Pon, A., Punanova, A., Quenard, D., Rimola, A., Sakai, N., Sims, I.R., Spezzano, S., Taquet, V., Testi, L., Theulé, P., Ugliengo, P., Vasyunin, A.I., Viti, S., Wiesenfeld, L., Yamamoto, S., 2017. Seeds Of Life In Space (SOLIS): The Organic Composition Diversity at 300-1000 au Scale in Solar-type Star-forming Regions. *ApJ* 850, 176. doi:doi:10.3847/1538-4357/aa961d, arXiv:1710.10437.
- Cernicharo, J., Marcelino, N., Roueff, E., Gerin, M., Jiménez-Escobar, A., Muñoz Caro, G.M., 2012. Discovery of the Methoxy Radical, CH₃O, toward B1: Dust Grain and Gas-phase Chemistry in Cold Dark Clouds. *ApJ* 759, L43. doi:doi:10.1088/2041-8205/759/2/L43.
- Chapillon, E., Dutrey, A., Guilloteau, S., Piétu, V., Wakelam, V., Hersant, F., Gueth, F., Henning, T., Launhardt, R., Schreyer, K., Semenov, D., 2012. Chemistry in Disks. VII. First Detection of HC₃N in Protoplanetary Disks. *ApJ* 756, 58. doi:doi:10.1088/0004-637X/756/1/58, arXiv:1207.2682.
- Chapillon, E., Guilloteau, S., Dutrey, A., Piétu, V., 2008. Disks around CQ Tauri and MWC 758: dense PDR or gas dispersal? *A&A* 488, 565–578. doi:doi:10.1051/0004-6361:200809523, arXiv:0805.3473.
- Charnley, S.B., 1997. Sulfuretted Molecules in Hot Cores. *ApJ* 481, 396. doi:doi:10.1086/304011.
- Charnley, S.B., 1998. Stochastic Astrochemical Kinetics. *ApJL* 509, L121–L124. doi:doi:10.1086/311764.
- Charnley, S.B., Tielens, A.G.G.M., Millar, T.J., 1992. On the molecular complexity of the hot cores in Orion A - Grain surface chemistry as 'The last refuge of the scoundrel'. *ApJL* 399, L71–L74. doi:doi:10.1086/186609.
- Charnley, S.B., Tielens, A.G.G.M., Rodgers, S.D., 1997. Deuterated Methanol in the Orion Compact Ridge. *ApJ* 482, L203–L206. doi:doi:10.1086/310697.
- Chiar, J.E., Tielens, A.G.G.M., Adamson, A.J., Ricca, A., 2013. The Structure, Origin, and Evolution of Interstellar Hydrocarbon Grains. *ApJ* 770, 78. doi:doi:10.1088/0004-637X/770/1/78.
- Chuang, K.J., Fedoseev, G., Ioppolo, S., van Dishoeck, E.F., Linnartz, H., 2016. H-atom addition and abstraction reactions in mixed CO, H₂CO and CH₃OH ices - an extended view on complex organic molecule formation. *MNRAS* 455, 1702–1712. doi:doi:10.1093/mnras/stv2288, arXiv:1606.01049.
- Chuang, K.J., Fedoseev, G., Qasim, D., Ioppolo, S., van Dishoeck, E.F., Linnartz, H., 2017. Production of complex organic molecules: H-atom addition versus UV irradiation. *MNRAS* 467, 2552–2565. doi:doi:10.1093/mnras/stx222, arXiv:1705.07680.
- Ciesla, F.J., 2010. The distributions and ages of refractory objects in the solar nebula. *Icarus* 208, 455–467. doi:doi:10.1016/j.icarus.2010.02.010.
- Ciesla, F.J., Cuzzi, J.N., 2006. The evolution of the water distribution in a viscous protoplanetary disk. *Icarus* 181, 178–204. doi:doi:10.1016/j.icarus.2005.11.009, arXiv:astro-ph/0511372.
- Cieza, L.A., Casassus, S., Tobin, J., Bos, S.P., Williams, J.P., Perez, S., Zhu, Z., Caceres, C., Canovas, H., Dunham, M.M., Hales, A., Prieto, J.L., Principe, D.A., Schreiber, M.R., Ruiz-Rodríguez, D., Zurlo, A., 2016. Imaging the water snow-line during a protostellar outburst. *Nature* 535, 258–261. doi:doi:10.1038/nature18612, arXiv:1607.03757.
- Clark, P.C., Glover, S.C.O., Klessen, R.S., Bonnell, I.A., 2012. How long does it take to form a molecular cloud? *MNRAS* 424, 2599–2613. doi:doi:10.1111/j.1365-2966.2012.21259.x, arXiv:1204.5570.
- Clayton, R.N., 1993. Oxygen Isotopes in Meteorites. *Annual Review of Earth and Planetary Sciences* 21, 115–149. doi:doi:10.1146/annurev.earth.21.050193.000555.
- Cleeves, L.I., Adams, F.C., Bergin, E.A., Visser, R., 2013. Radionuclide Ionization in Protoplanetary Disks: Calculations of Decay Product Radiative Transfer. *ApJ* 777, 28. doi:doi:10.1088/0004-637X/777/1/28, arXiv:1309.0018.

- Cleeves, L.I., Bergin, E.A., Alexander, C.M.O., Du, F., Graninger, D., Öberg, K.I., Harries, T.J., 2014. The ancient heritage of water ice in the solar system. *Science* 345, 1590–1593. doi:doi:10.1126/science.1258055, arXiv:1409.7398.
- Cleeves, L.I., Bergin, E.A., O'D. Alexander, C.M., Du, F., Graninger, D., Öberg, K.I., Harries, T.J., 2016. Exploring the Origins of Deuterium Enrichments in Solar Nebular Organics. *ApJ* 819, 13. doi:doi:10.3847/0004-637X/819/1/13, arXiv:1601.07465.
- Cleeves, L.I., Öberg, K.I., Wilner, D.J., Huang, J., Loomis, R.A., Andrews, S.M., Guzman, V.V., 2018. Constraining Gas-phase Carbon, Oxygen, and Nitrogen in the IM Lup Protoplanetary Disk. *ApJ* 865, 155. doi:doi:10.3847/1538-4357/aae96, arXiv:1808.10682.
- Codella, C., Bianchi, E., Tabone, B., Lee, C.F., Cabrit, S., Ceccarelli, C., Podio, L., Bacciotti, F., Bachiller, R., Chapillon, E., 2018. Water and interstellar complex organics associated with the HH 212 protostellar disc. On disc atmospheres, disc winds, and accretion shocks. *A&A* 617, A10. doi:doi:10.1051/0004-6361/201832765, arXiv:1806.07967.
- Collings, M.P., Anderson, M.A., Chen, R., Dever, J.W., Viti, S., Williams, D.A., McCoustra, M.R.S., 2004. A laboratory survey of the thermal desorption of astrophysically relevant molecules. *MNRAS* 354, 1133–1140. doi:doi:10.1111/j.1365-2966.2004.08272.x.
- Collings, M.P., Dever, J.W., Fraser, H.J., McCoustra, M.R.S., 2003. Laboratory studies of the interaction of carbon monoxide with water ice. *APSS* 285, 633–659. doi:doi:10.1023/A:1026144806831.
- Coutens, A., Vastel, C., Caux, E., Ceccarelli, C., Bottinelli, S., Wiesenfeld, L., Faure, A., Scribano, Y., Kahane, C., 2012. A study of deuterated water in the low-mass protostar IRAS 16293-2422. *A&A* 539, A132. doi:doi:10.1051/0004-6361/201117627, arXiv:1201.1785.
- Crapsi, A., Caselli, P., Walmsley, M.C., Tafalla, M., 2007. Observing the gas temperature drop in the high-density nucleus of L 1544. *A&A* 470, 221–230. doi:doi:10.1051/0004-6361:20077613, arXiv:0705.0471.
- Crockett, N.R., Bergin, E.A., Neill, J.L., Favre, C., Schilke, P., Lis, D.C., Bell, T.A., Blake, G., Cernicharo, J., Emprechtinger, M., Esplugues, G.B., Gupta, H., Kleshcheva, M., Lord, S., Marcelino, N., McGuire, B.A., Pearson, J., Phillips, T.G., Plume, R., van der Tak, F., Tercero, B., Yu, S., 2014. Herschel Observations of Extraordinary Sources: Analysis of the HIFI 1.2 THz Wide Spectral Survey toward Orion KL. I. Methods. *ApJ* 787, 112. doi:doi:10.1088/0004-637X/787/2/112, arXiv:1405.2351.
- Cuppen, H.M., Karssemeijer, L.J., Lamberts, T., 2013. The Kinetic Monte Carlo Method as a Way To Solve the Master Equation for Interstellar Grain Chemistry. *Chemical Reviews* 113, 8840–8871. doi:doi:10.1021/cr400234a.
- Cuppen, H.M., van Dishoeck, E.F., Herbst, E., Tielens, A.G.G.M., 2009. Microscopic simulation of methanol and formaldehyde ice formation in cold dense cores. *A&A* 508, 275–287. doi:doi:10.1051/0004-6361/200913119, arXiv:0911.0283.
- Cuppen, H.M., Walsh, C., Lamberts, T., Semenov, D., Garrod, R.T., Pentead, E.M., Ioppolo, S., 2017. Grain Surface Models and Data for Astrochemistry. *Space Sci. Rev.* 212, 1–58. doi:doi:10.1007/s11214-016-0319-3.
- Cuzzi, J.N., Dobrovolskis, A.R., Champney, J.M., 1993. Particle-Gas Dynamics in the Midplane of a Protoplanetary Nebula. *Icarus* 106, 102–134. doi:doi:10.1006/icar.1993.1161.
- Cuzzi, J.N., Zahnle, K.J., 2004. Material Enhancement in Protoplanetary Nebulae by Particle Drift through Evaporation Fronts. *ApJ* 614, 490–496. doi:doi:10.1086/423611, arXiv:astro-ph/0409276.
- D'Alessio, P., Calvet, N., Hartmann, L., 2001. Accretion Disks around Young Objects. III. Grain Growth. *ApJ* 553, 321–334. doi:doi:10.1086/320655, arXiv:astro-ph/0101443.
- Dalgarno, A., McCray, R.A., 1972. Heating and Ionization of HI Regions. *ARA&A* 10, 375. doi:doi:10.1146/annurev.aa.10.090172.002111.
- D'Angelo, M., Cazaux, S., Kamp, I., Thi, W.F., Voitke, P., 2019. Water delivery in the inner solar nebula. Monte Carlo simulations of forsterite hydration. *A&A* 622, A208. doi:doi:10.1051/0004-6361/201833715, arXiv:1808.06183.
- Daranlot, J., Hincelin, U., Bergeat, A., Costes, M., Loison, J.C., Wakelam, V., Hickson, K.M., 2012. Elemental nitrogen partitioning in dense interstellar clouds. *Proceedings of the National Academy of Science* 109, 10233–10238. doi:doi:10.1073/pnas.1200017109, arXiv:1206.4905.
- Dasgupta, R., Chi, H., Shimizu, N., Buono, A.S., Walker, D., 2013. Carbon solution and partitioning between metallic and silicate melts in a shallow magma ocean: Implications for the origin and distribution of terrestrial carbon. *Geochim. Cosmochim. Acta* 102, 191–212. doi:doi:10.1016/j.gca.2012.10.011.
- Davis, A.M., 2006. Volatile Evolution and Loss. p. 295.
- Dawson, R.I., Johnson, J.A., 2018. Origins of hot jupiters. *Annual Review of Astronomy and Astrophysics* 56, 175–221. URL: <https://doi.org/10.1146/annurev-astro-081817-051853>, doi:doi:10.1146/annurev-astro-081817-051853, arXiv:https://doi.org/10.1146/annurev-astro-081817-051853.
- Debes, J.H., Jang-Condell, H., Weinberger, A.J., Roberge, A., Schneider, G., 2013. The 0.5-2.22 μm Scattered Light Spectrum of the Disk around TW Hya: Detection of a Partially Filled Disk Gap at 80 AU. *ApJ* 771, 45. doi:doi:10.1088/0004-637X/771/1/45, arXiv:1306.2969.
- Dodson-Robinson, S.E., Willacy, K., Bodenheimer, P., Turner, N.J., Beichman, C.A., 2009. Ice lines, planetesimal composition and solid surface density in the solar nebula. *Icarus* 200, 672–693. doi:doi:10.1016/j.icarus.2008.11.023, arXiv:0806.3788.
- Dominik, C., Tielens, A.G.G.M., 1997. The Physics of Dust Coagulation and the Structure of Dust Aggregates in Space. *ApJ* 480, 647–673. doi:doi:10.1086/303996.
- Draine, B.T., 1995. Grain Destruction in Interstellar Shock Waves. *Ap&SS* 233, 111–123. doi:doi:10.1007/BF00627339, arXiv:astro-ph/9508066.
- Draine, B.T., 2003. Interstellar Dust Grains. *ARA&A* 41, 241–289. doi:doi:10.1146/annurev.astro.41.011802.094840, arXiv:astro-ph/0304489.
- Draine, B.T., Salpeter, E.E., 1979. Destruction mechanisms for interstellar dust. *ApJ* 231, 438–455. doi:doi:10.1086/157206.
- Drazkowska, J., Alibert, Y., 2017. Planetesimal formation starts at the snow line. *A&A* 608, A92. doi:doi:10.1051/0004-6361/201731491, arXiv:1710.00009.
- Drouart, A., Dubrulle, B., Gautier, D., Robert, F., 1999. Structure and Transport in the Solar Nebula from Constraints on Deuterium Enrichment and Giant Planets Formation. *Icarus* 140, 129–155. doi:doi:10.1006/icar.1999.6137.
- Drozdovskaya, M.N., van Dishoeck, E.F., Rubin, M., Jørgensen, J.K., Altwegg, K., 2019. Ingredients for Solar-like Systems: protostar IRAS 16293-2422 B versus comet 67P/Churyumov-Gerasimenko. arXiv e-prints, arXiv:1908.11290 arXiv:1908.11290.
- Drozdovskaya, M.N., Walsh, C., van Dishoeck, E.F., Furuya, K., Marboeuf, U., Thiabaud, A., Harsono, D., Visser, R., 2016. Cometary ices in forming protoplanetary disc midplanes. *MNRAS* 462, 977–993. doi:doi:10.1093/mnras/stw1632, arXiv:1607.07861.
- Drozdovskaya, M.N., Walsh, C., Visser, R., Harsono, D., van Dishoeck, E.F., 2014. Methanol along the path from envelope to protoplanetary disc. *MNRAS* 445, 913–929. doi:doi:10.1093/mnras/stu1789, arXiv:1409.2473.
- Du, F., Bergin, E.A., 2014. Water Vapor Distribution in Protoplanetary Disks. *ApJ* 792, 2. doi:doi:10.1088/0004-637X/792/1/2, arXiv:1408.2026.
- Du, F., Bergin, E.A., Hogerheijde, M., van Dishoeck, E.F., Blake, G., Bruderer, S., Cleeves, I., Dominik, C., Fedele, D., Lis, D.C., Melnick, G., Neufeld, D., Pearson, J., Yıldız, U., 2017. Survey of Cold Water Lines in Protoplanetary Disks: Indications of Systematic Volatile Depletion. *ApJ* 842, 98. doi:doi:10.3847/1538-4357/aa70ee, arXiv:1705.00799.

- Dulieu, F., Amiaud, L., Congiu, E., Fillion, J.H., Matar, E., Momeni, A., Pirronello, V., Lemaire, J.L., 2010. Experimental evidence for water formation on interstellar dust grains by hydrogen and oxygen atoms. *A&A* 512, A30. doi:doi:10.1051/0004-6361/200912079, arXiv:0903.3120.
- Dullemond, C.P., Juhasz, A., Pohl, A., Sereshti, F., Shetty, R., Peters, T., Commercon, B., Flock, M., 2012. RADMC-3D: A multi-purpose radiative transfer tool. arXiv:1202.015.
- Dullemond, C.P., Monnier, J.D., 2010. The Inner Regions of Protoplanetary Disks. *ARA&A* 48, 205–239. doi:doi:10.1146/annurev-astro-081309-130932, arXiv:1006.3485.
- Dutrey, A., Guilloteau, S., Guelin, M., 1997. Chemistry of protosolar-like nebulae: The molecular content of the DM Tau and GG Tau disks. *A&A* 317, L55–L58.
- Ehrenfreund, P., Charnley, S.B., 2000. Organic Molecules in the Interstellar Medium, Comets, and Meteorites: A Voyage from Dark Clouds to the Early Earth. *ARA&A* 38, 427–483. doi:doi:10.1146/annurev.astro.38.1.427.
- Ehrenfreund, P., Gerakines, P.A., Schutte, W.A., van Hemert, M.C., van Dishoeck, E.F., 1996. Infrared properties of isolated water ice. *A&A* 312, 263–274.
- Eistrup, C., Walsh, C., van Dishoeck, E.F., 2018. Molecular abundances and C/O ratios in chemically evolving planet-forming disk midplanes. *A&A* 613, A14. doi:doi:10.1051/0004-6361/201731302, arXiv:1709.07863.
- Ercolano, B., Koepferl, C., 2014. The Lifetime of Protoplanetary Disks: Observations and Theory, in: *The Labyrinth of Star Formation*, p. 63. doi:doi:10.1007/978-3-319-03041-8_11.
- Evans, Neal J., I., 1999. Physical Conditions in Regions of Star Formation. *ARA&A* 37, 311–362. doi:doi:10.1146/annurev.astro.37.1.311, arXiv:astro-ph/9905050.
- Evans, II, N.J., Allen, L.E., Blake, G.A., Boogert, A.C.A., Bourke, T., Harvey, P.M., Kessler, J.E., Koerner, D.W., Lee, C.W., Mundy, L.G., Myers, P.C., Padgett, D.L., Pontoppidan, K., Sargent, A.I., Stapelfeldt, K.R., van Dishoeck, E.F., Young, C.H., Young, K.E., 2003. From Molecular Cores to Planet-forming Disks: An SIRTf Legacy Program. *PASP* 115, 965–980. arXiv:arXiv:astro-ph/0305127.
- Favre, C., Cleaves, L.I., Bergin, E.A., Qi, C., Blake, G.A., 2013. A Significantly Low CO Abundance toward the TW Hya Protoplanetary Disk: A Path to Active Carbon Chemistry? *ApJ* 776, L38. doi:doi:10.1088/2041-8205/776/2/L38, arXiv:1309.5370.
- Favre, C., Fedele, D., Semenov, D., Parfenov, S., Codella, C., Ceccarelli, C., Bergin, E.A., Chapillon, E., Testi, L., Hersant, F., Lefloch, B., Fontani, F., Blake, G.A., Cleaves, L.I., Qi, C., Schwarz, K.R., Taquet, V., 2018. First Detection of the Simplest Organic Acid in a Protoplanetary Disk. *ApJ* 862, L2. doi:doi:10.3847/2041-8213/aad046, arXiv:1807.05768.
- Fayolle, E.C., Balfe, J., Loomis, R., Bergner, J., Graninger, D., Rajappan, M., Öberg, K.I., 2016. N₂ and CO Desorption Energies from Water Ice. *ApJ* 816, L28. doi:doi:10.3847/2041-8205/816/2/L28, arXiv:1512.06865.
- Fayolle, E.C., Bertin, M., Romanzin, C., Michaut, X., Öberg, K.I., Linnartz, H., Fillion, J.H., 2011. CO Ice Photodesorption: A Wavelength-dependent Study. *ApJL* 739, L36. doi:doi:10.1088/2041-8205/739/2/L36, arXiv:1109.0281.
- Fayolle, E.C., Öberg, K.I., Garrod, R., Bisschop, S., van Dishoeck, E., 2014. Complex organic molecules in organic-poor massive young stellar objects. submitted to *A&A*.
- Fedoseev, G., Ioppolo, S., Zhao, D., Lamberts, T., Linnartz, H., 2015. Low-temperature surface formation of NH₃ and HNC: hydrogenation of nitrogen atoms in CO-rich interstellar ice analogues. *MNRAS* 446, 439–448. doi:doi:10.1093/mnras/stu2028, arXiv:1705.09184.
- Ferland, G.J., 2003. Quantitative Spectroscopy of Photoionized Clouds. *ARA&A* 41, 517–554. doi:doi:10.1146/annurev.astro.41.011802.094836.
- Finocchi, F., Gail, H.P., Duschl, W.J., 1997. Chemical reactions in protoplanetary accretion disks. II. Carbon dust oxidation. *A&A* 325, 1264–1279.
- Flower, D., 2012. Molecular Collisions in the Interstellar Medium. Flower, D.R., Pineau des Forets, G., Hartquist, T.W., 1985. Theoretical studies of interstellar molecular shocks. I - General formulation and effects of the ion-molecule chemistry. *MNRAS* 216, 775–794. doi:doi:10.1093/mnras/216.4.775.
- Flower, D.R., Pineau Des Forêts, G., Walmsley, C.M., 2006. The importance of the ortho:para H₂ ratio for the deuteration of molecules during pre-protostellar collapse. *A&A* 449, 621–629. doi:doi:10.1051/0004-6361:20054246, arXiv:astro-ph/0601429.
- Fraser, H.J., Collings, M.P., McCoustra, M.R.S., Williams, D.A., 2001. Thermal desorption of water ice in the interstellar medium. *MNRAS* 327, 1165–1172. doi:doi:10.1046/j.1365-8711.2001.04835.x, arXiv:arXiv:astro-ph/0107487.
- Furuya, K., Aikawa, Y., Hincelin, U., Hassel, G.E., Bergin, E.A., Vasyunin, A.I., Herbst, E., 2015. Water deuteration and ortho-to-para nuclear spin ratio of H₂ in molecular clouds formed via the accumulation of H I gas. *A&A* 584, A124. doi:doi:10.1051/0004-6361/201527050, arXiv:1510.05135.
- Furuya, K., Aikawa, Y., Nomura, H., Hersant, F., Wakelam, V., 2013. Water in Protoplanetary Disks: Deuteration and Turbulent Mixing. *ApJ* 779, 11. doi:doi:10.1088/0004-637X/779/1/11, arXiv:1310.3342.
- Furuya, K., van Dishoeck, E.F., Aikawa, Y., 2016. Reconstructing the history of water ice formation from HDO/H₂O and D₂O/HDO ratios in protostellar cores. *A&A* 586, A127. doi:doi:10.1051/0004-6361/201527579, arXiv:1512.04291.
- Furuya, K., Watanabe, Y., Sakai, T., Aikawa, Y., Yamamoto, S., 2018. Depletion of ¹⁵N in the center of L1544: Early transition from atomic to molecular nitrogen? *A&A* 615, L16. doi:doi:10.1051/0004-6361/201833607, arXiv:1807.05480.
- Gail, H.P., 2002. Radial mixing in protoplanetary accretion disks. III. Carbon dust oxidation and abundance of hydrocarbons in comets. *A&A* 390, 253–265. doi:doi:10.1051/0004-6361:20020614.
- Gail, H.P., Trieloff, M., 2017. Spatial distribution of carbon dust in the early solar nebula and the carbon content of planetesimals. *A&A* 606, A16. doi:doi:10.1051/0004-6361/201730480, arXiv:1707.07611.
- Galli, D., Palla, F., 2013. The Dawn of Chemistry. *ARA&A* 51, 163–206. doi:doi:10.1146/annurev-astro-082812-141029, arXiv:1211.3319.
- Garaud, P., Lin, D.N.C., 2007. The Effect of Internal Dissipation and Surface Irradiation on the Structure of Disks and the Location of the Snow Line around Sun-like Stars. *ApJ* 654, 606–624. doi:doi:10.1086/509041, arXiv:astro-ph/0605110.
- Garrod, R.T., 2008. A new modified-rate approach for gas-grain chemical simulations. *A&A* 491, 239–251. doi:doi:10.1051/0004-6361:200810518, arXiv:0809.2934.
- Garrod, R.T., 2013. A Three-phase Chemical Model of Hot Cores: The Formation of Glycine. *ApJ* 765, 60. doi:doi:10.1088/0004-637X/765/1/60.
- Garrod, R.T., Herbst, E., 2006. Formation of methyl formate and other organic species in the warm-up phase of hot molecular cores. *A&A* 457, 927–936. doi:doi:10.1051/0004-6361:20065560, arXiv:arXiv:astro-ph/0607560.
- Garrod, R.T., Pauly, T., 2011. On the Formation of CO₂ and Other Interstellar Ices. *ApJ* 735, 15. doi:doi:10.1088/0004-637X/735/1/15, arXiv:1106.0540.
- Garrod, R.T., Wakelam, V., Herbst, E., 2007. Non-thermal desorption from interstellar dust grains via exothermic surface reactions. *A&A* 467, 1103–1115. doi:doi:10.1051/0004-6361:20066704, arXiv:arXiv:astro-ph/0703188.
- Garrod, R.T., Weaver, S.L.W., Herbst, E., 2008. Complex Chemistry in Star-forming Regions: An Expanded Gas-Grain Warm-up Chemical Model. *ApJ* 682, 283–302. doi:doi:10.1086/588035, arXiv:0803.1214.
- Garrod, R.T., Widicus Weaver, S.L., 2013. Simulations of Hot-Core Chemistry. *Chemical Reviews* 113, 8939–8960.
- Geiss, J., Reeves, H., 1972. Cosmic and Solar System Abundances of Deuterium and Helium-3. *A&A* 18, 126.
- Gerakines, P.A., Schutte, W.A., Greenberg, J.M., van Dishoeck, E.F., 1995. The infrared band strengths of H₂O, CO and CO₂ in laboratory simulations of astrophysical ice mixtures. *A&A* 296, 810. arXiv:arXiv:astro-ph/9409076.

- Gerin, M., Goicoechea, J.R., Pety, J., Hily-Blant, P., 2009. HCO mapping of the Horsehead: tracing the illuminated dense molecular cloud surfaces. *A&A* 494, 977–985. doi:doi:10.1051/0004-6361/200810933, arXiv:0811.1470.
- Gerin, M., Viala, Y., Pauzat, F., Ellinger, Y., 1992. The abundance of nitric oxide in molecular clouds. *A&A* 266, 463–478.
- Gibb, E.L., Whittet, D.C.B., Boogert, A.C.A., Tielens, A.G.G.M., 2004. Interstellar Ice: The Infrared Space Observatory Legacy. *ApJs* 151, 35–73. doi:doi:10.1086/381182.
- Glover, S.C.O., Mac Low, M.M., 2007. Simulating the Formation of Molecular Clouds. II. Rapid Formation from Turbulent Initial Conditions. *ApJ* 659, 1317–1337. doi:doi:10.1086/512227, arXiv:astro-ph/0605121.
- Goldsmith, P.F., Langer, W.D., 1978. Molecular cooling and thermal balance of dense interstellar clouds. *ApJ* 222, 881–895. doi:doi:10.1086/156206.
- Goldsmith, P.F., Langer, W.D., 1999. Population Diagram Analysis of Molecular Line Emission. *ApJ* 517, 209–225. doi:doi:10.1086/307195.
- Goldsmith, P.F., Melnick, G.J., Bergin, E.A., Howe, J.E., Snell, R.L., Neufeld, D.A., Harwit, M., Ashby, M.L.N., Patten, B.M., Kleiner, S.C., Plume, R., Stauffer, J.R., Tolls, V., Wang, Z., Zhang, Y.F., Erickson, N.R., Koch, D.G., Schieder, R., Winnewisser, G., Chin, G., 2000. O₂ in Interstellar Molecular Clouds. *ApJ* 539, L123–L127. doi:doi:10.1086/312854.
- Gordy, W., Cook, R.L., 1970. *Microwave molecular spectra*. John Wiley; New York.
- Gorti, U., Hollenbach, D., 2004. Models of Chemistry, Thermal Balance, and Infrared Spectra from Intermediate-Aged Disks around G and K Stars. *ApJ* 613, 424–447. doi:doi:10.1086/422406, arXiv:astro-ph/0405244.
- Gould, R.J., Salpeter, E.E., 1963. The Interstellar Abundance of the Hydrogen Molecule. I. Basic Processes. *ApJ* 138, 393. doi:doi:10.1086/147654.
- Graedel, T.E., Langer, W.D., Frerking, M.A., 1982. The kinetic chemistry of dense interstellar clouds. *ApJS* 48, 321–368. doi:doi:10.1086/190780.
- Green, S., Chapman, S., 1978. Collisional excitation of interstellar molecules: linear molecules CO, CS, OCS, and HC₃N. *ApJS* 37, 169–194. doi:doi:10.1086/190523.
- Greenberg, J.M., 1983. Chemical evolution in space - A source of prebiotic molecules. *Advances in Space Research* 3, 19–33. doi:doi:10.1016/0273-1177(83)90037-6.
- Grewal, D.S., Dasgupta, R., Sun, C., Tsuno, K., Costin, G., 2019. Delivery of carbon, nitrogen, and sulfur to the silicate Earth by a giant impact. *Science Advances* 5, eaau3669. doi:doi:10.1126/sciadv.aau3669.
- Grossman, L., 1972. Condensation in the primitive solar nebula. *Geochim. Cosmochim. Acta* 36, 597–619. doi:doi:10.1016/0016-7037(72)90078-6.
- Gundlach, B., Blum, J., 2015. The Stickiness of Micrometer-sized Water-ice Particles. *ApJ* 798, 34. doi:doi:10.1088/0004-637X/798/1/34, arXiv:1410.7199.
- Güttler, C., Blum, J., Zsom, A., Ormel, C.W., Dullemond, C.P., 2010. The outcome of protoplanetary dust growth: pebbles, boulders, or planetesimals?. I. Mapping the zoo of laboratory collision experiments. *A&A* 513, A56. doi:doi:10.1051/0004-6361/200912852, arXiv:0910.4251.
- Guzmán, V.V., Pety, J., Goicoechea, J.R., Gerin, M., Roueff, E., Gratier, P., Öberg, K.I., 2015a. Spatially Resolved L-C₃H⁺ Emission in the Horsehead Photodissociation Region: Further Evidence for a Top-Down Hydrocarbon Chemistry. *ApJ* 800, L33. doi:doi:10.1088/2041-8205/800/2/L33, arXiv:1502.02325.
- Guzmán, V.V., Pety, J., Goicoechea, J.R., Gerin, M., Roueff, E., Gratier, P., Öberg, K.I., 2015b. Spatially Resolved L-C₃H₂⁺/SUB₃/SUB₂H₂SUP₂+₁/SUP₂ Emission in the Horsehead Photodissociation Region: Further Evidence for a Top-Down Hydrocarbon Chemistry. *ApJ* 800, L33. doi:doi:10.1088/2041-8205/800/2/L33.
- Hagen, W., Tielens, A.G.G.M., Greenberg, J.M., 1983. A laboratory study of the infrared spectra of interstellar ices. *A&As* 51, 389–416.
- Hama, T., Ueta, H., Kouchi, A., Watanabe, N., 2015. Quantum tunneling observed without its characteristic large kinetic isotope effects. *Proceedings of the National Academy of Science* 112, 7438–7443. doi:doi:10.1073/pnas.1501328112.
- Harsono, D., Bjerkeli, P., van der Wiel, M.H.D., Ramsey, J.P., Maud, L.T., Kristensen, L.E., Jørgensen, J.K., 2018. Evidence for the start of planet formation in a young circumstellar disk. *ArXiv e-prints*, arXiv:1806.09649 arXiv:1806.09649.
- Harsono, D., Persson, M., Ramos, A., Murillo, N., Maud, L., Hogerheijde, M., Bosman, A., Kristensen, L., Jørgensen, J., Bergin, T., Visser, R., Mottram, J., van Dishoeck, E., 2020. Missing water in Class I protostellar disks. *arXiv e-prints*, in press. arXiv:2002.11897.
- Hartmann, L., Herczeg, G., Calvet, N., 2016. Accretion onto Pre-Main-Sequence Stars. *ARA&A* 54, 135–180. doi:doi:10.1146/annurev-astro-081915-023347.
- Hasegawa, T.I., Herbst, E., 1993. Three-Phase Chemical Models of Dense Interstellar Clouds - Gas Dust Particle Mantles and Dust Particle Surfaces. *MNRAS* 263, 589.
- Hasegawa, T.I., Herbst, E., Leung, C.M., 1992. Models of gas-grain chemistry in dense interstellar clouds with complex organic molecules. *ApJs* 82, 167–195. doi:doi:10.1086/191713.
- Hashizume, K., Sugiura, N., 1998. Transportation of gaseous elements and isotopes in a thermally evolving chondritic planetesimal. *Meteoritics and Planetary Science* 33, 1181–1195. doi:doi:10.1111/j.1945-5100.1998.tb01722.x.
- Hayashi, C., 1981. Structure of the Solar Nebula, Growth and Decay of Magnetic Fields and Effects of Magnetic and Turbulent Viscosities on the Nebula. *Progress of Theoretical Physics Supplement* 70, 35–53. doi:doi:10.1143/PTPS.70.35.
- Heays, A.N., Bosman, A.D., van Dishoeck, E.F., 2017. Photodissociation and photoionisation of atoms and molecules of astrophysical interest. *A&A* 602, A105. doi:doi:10.1051/0004-6361/201628742, arXiv:1701.04459.
- Heays, A.N., Visser, R., Gredel, R., Ubachs, W., Lewis, B.R., Gibson, S.T., van Dishoeck, E.F., 2014. Isotope selective photodissociation of N₂ by the interstellar radiation field and cosmic rays. *A&A* 562, A61. doi:doi:10.1051/0004-6361/201322832, arXiv:1401.1630.
- Helled, R., Guillot, T., 2018. Internal Structure of Giant and Icy Planets: Importance of Heavy Elements and Mixing. p. 44. doi:doi:10.1007/978-3-319-55333-7-44.
- Heller, E.J., 1978. Quantum corrections to classical photodissociation models. *J. Chem. Phys.* 68, 2066–2075. doi:doi:10.1063/1.436029.
- Henning, T., Semenov, D., 2013. Chemistry in Protoplanetary Disks. *Chemical Reviews* 113, 9016–9042. doi:doi:10.1021/cr400128p, arXiv:1310.3151.
- Henning, T., Semenov, D., Guilloteau, S., Dutrey, A., Hersant, F., Wakelam, V., Chapillon, E., Launhardt, R., Pietu, V., Schreyer, K., 2010. Chemistry in Disks. III. - Photochemistry and X-ray driven chemistry probed by the ethynyl radical (CCH) in DM Tau, LkCa 15, and MWC 480. *ArXiv e-prints* arXiv:1003.5793.
- Herbst, E., 1995. Chemistry in the Interstellar Medium. *Annual Review of Physical Chemistry* 46, 27–54. doi:doi:10.1146/annurev.pc.46.100195.000331.
- Herbst, E., Klemperer, W., 1973. The Formation and Depletion of Molecules in Dense Interstellar Clouds. *ApJ* 185, 505–534. doi:doi:10.1086/152436.
- Herbst, E., Leung, C.M., 1989. Gas Phase Production of Complex Hydrocarbons, Cyanopolynes, and Related Compounds in Dense Interstellar Clouds. *ApJS* 69, 271. doi:doi:10.1086/191314.
- Herbst, E., van Dishoeck, E.F., 2009. Complex Organic Interstellar Molecules. *ARA&A* 47, 427–480. doi:doi:10.1146/annurev-astro-082708-101654.
- Herzberg, G., 1950. *Molecular spectra and molecular structure. Vol.1: Spectra of diatomic molecules*. New York: Van Nostrand Reinhold, 1950, 2nd ed.
- Heyer, M., Dame, T.M., 2015. Molecular Clouds in the Milky Way. *ARA&A* 53, 583–629. doi:doi:10.1146/annurev-astro-082214-122324.
- Hily-Blant, P., Magalhaes de Souza, V., Kastner, J., Forveille, T., 2019. Multiple nitrogen reservoirs in a protoplanetary disk at the epoch of comet and giant planet formation. *A&A* 632, L12. doi:doi:10.1051/0004-6361/201936750, arXiv:1911.06676.

- Hiraoka, K., Miyagoshi, T., Takayama, T., Yamamoto, K., Kihara, Y., 1998. Gas-Grain Processes for the Formation of CH₄ and H₂O: Reactions of H Atoms with C, O, and CO in the Solid Phase at 12 K. *ApJ* 498, 710. doi:doi:10.1086/305572.
- Hiraoka, K., Sato, T., Sato, S., Sogoshi, N., Yokoyama, T., Takashima, H., Kitagawa, S., 2002. Formation of Formaldehyde by the Tunneling Reaction of H with Solid CO at 10 K Revisited. *ApJ* 577, 265–270. doi:doi:10.1086/342132.
- Hogerheijde, M.R., Bergin, E.A., Brinch, C., Cleaves, L.I., Fogel, J.K.J., Blake, G.A., Dominik, C., Lis, D.C., Melnick, G., Neufeld, D., Panić, O., Pearson, J.C., Kristensen, L., Yıldız, U.A., van Dishoeck, E.F., 2011. Detection of the Water Reservoir in a Forming Planetary System. *Science* 334, 338–. doi:doi:10.1126/science.1208931, arXiv:1110.4600.
- Hogerheijde, M.R., van der Tak, F.F.S., 2000. An accelerated Monte Carlo method to solve two-dimensional radiative transfer and molecular excitation. With applications to axisymmetric models of star formation. *A&A* 362, 697–710. arXiv:astro-ph/0008169.
- Hollenbach, D., Kaufman, M.J., Bergin, E.A., Melnick, G.J., 2009. Water, O₂, and Ice in Molecular Clouds. *ApJ* 690, 1497–1521. doi:doi:10.1088/0004-637X/690/2/1497, arXiv:0809.1642.
- Hollenbach, D., McKee, C.F., 1979. Molecule formation and infrared emission in fast interstellar shocks. I. Physical processes. *ApJS* 41, 555–592. doi:doi:10.1086/190631.
- Hollenbach, D., McKee, C.F., 1989. Molecule Formation and Infrared Emission in Fast Interstellar Shocks. III. Results for J Shocks in Molecular Clouds. *ApJ* 342, 306. doi:doi:10.1086/167595.
- Hollenbach, D., Salpeter, E.E., 1971. Surface Recombination of Hydrogen Molecules. *ApJ* 163, 155. doi:doi:10.1086/150754.
- Hollenbach, D.J., Tielens, A.G.G.M., 1999. Photodissociation regions in the interstellar medium of galaxies. *Reviews of Modern Physics* 71, 173–230. doi:doi:10.1103/RevModPhys.71.173.
- Honda, M., Kudo, T., Takatsuki, S., Inoue, A.K., Nakamoto, T., Fukagawa, M., Tamura, M., Terada, H., Takato, N., 2016. Water Ice at the Surface of the HD 100546 Disk. *ApJ* 821, 2. doi:doi:10.3847/0004-637X/821/1/2, arXiv:1603.09512.
- Howard, K.T., Bailey, M.J., Berhanu, D., Bland, P.A., Cressey, G., Howard, L.E., Jaynes, C., Matthewman, R., Martins, Z., Sephton, M.A., Stolojan, V., Verchovsky, S., 2013. Biomass preservation in impact melt ejecta. *Nature Geoscience* 6, 1018–1022. doi:doi:10.1038/ngeo1996.
- Huang, J., Andrews, S.M., Dullemond, C.P., Isella, A., Pérez, L.M., Guzmán, V.V., Öberg, K.I., Zhu, Z., Zhang, S., Bai, X.N., Benisty, M., Birnstiel, T., Carpenter, J.M., Hughes, A.M., Ricci, L., Weaver, E., Wilner, D.J., 2018. The Disk Substructures at High Angular Resolution Project (DSHARP). II. Characteristics of Annular Substructures. *ApJ* 869, L42. doi:doi:10.3847/2041-8213/aa740, arXiv:1812.04041.
- Huang, J., Öberg, K.I., Qi, C., Aikawa, Y., Andrews, S.M., Furuya, K., Guzmán, V.V., Loomis, R.A., van Dishoeck, E.F., Wilner, D.J., 2017. An ALMA Survey of DCN/H¹³CN and DCO⁺/H¹³CO⁺ in Protoplanetary Disks. *ApJ* 835, 231. doi:doi:10.3847/1538-4357/835/2/231, arXiv:1701.01735.
- Hugo, E., Asvany, O., Schlemmer, S., 2009. H₃⁺+H₂ isotopic system at low temperatures: Microcanonical model and experimental study. *Journal of Chemical Physics* 130, 164302–164302. doi:doi:10.1063/1.3089422.
- Ida, S., Yamamura, T., Okuzumi, S., 2019. Water delivery by pebble accretion to rocky planets in habitable zones in evolving disks. *A&A* 624, A28. doi:doi:10.1051/0004-6361/201834556, arXiv:1901.04611.
- Ioppolo, S., Cuppen, H.M., Romanzin, C., van Dishoeck, E.F., Linnartz, H., 2008. Laboratory Evidence for Efficient Water Formation in Interstellar Ices. *ApJ* 686, 1474–1479. doi:doi:10.1086/591506, arXiv:0807.0129.
- Ioppolo, S., Cuppen, H.M., van Dishoeck, E.F., Linnartz, H., 2011a. Surface formation of HCOOH at low temperature. *MNRAS* 410, 1089–1095. doi:doi:10.1111/j.1365-2966.2010.17515.x.
- Ioppolo, S., van Boheemen, Y., Cuppen, H.M., van Dishoeck, E.F., Linnartz, H., 2011b. Surface formation of CO₂ ice at low temperatures. *MNRAS* 413, 2281–2287. doi:doi:10.1111/j.1365-2966.2011.18306.x.
- Jacq, T., Henkel, C., Walmsley, C.M., Jewell, P.R., Baudry, A., 1988. H₂(0-18) in hot dense molecular cloud cores. *A&A* 199, L5–L8.
- Jiménez-Serra, I., Vasyunin, A.I., Caselli, P., Marcelino, N., Billot, N., Viti, S., Testi, L., Vastel, C., Lefloch, B., Bachiller, R., 2016. The Spatial Distribution of Complex Organic Molecules in the L1544 Pre-stellar Core. *ApJ* 830, L6. doi:doi:10.3847/2041-8205/830/1/L6, arXiv:1609.05045.
- Jiménez-Serra, I., Viti, S., Quénard, D., Holdship, J., 2018. The Chemistry of Phosphorus-bearing Molecules under Energetic Phenomena. *ApJ* 862, 128. doi:doi:10.3847/1538-4357/aacdf2, arXiv:1806.07281.
- Johansen, A., Lambrechts, M., 2017. Forming Planets via Pebble Accretion. *Annual Review of Earth and Planetary Sciences* 45, 359–387. doi:doi:10.1146/annurev-earth-063016-020226.
- Jones, A.P., Fanciullo, L., Köhler, M., Verstraete, L., Guillet, V., Bocchio, M., Ysard, N., 2013. The evolution of amorphous hydrocarbons in the ISM: dust modelling from a new vantage point. *A&A* 558, A62. doi:doi:10.1051/0004-6361/201321686, arXiv:1411.6293.
- Jones, A.P., Ysard, N., 2019. The essential elements of dust evolution. A viable solution to the interstellar oxygen depletion problem? *A&A* 627, A38. doi:doi:10.1051/0004-6361/201935532, arXiv:1906.01382.
- Jonkheid, B., Faas, F.G.A., van Zadelhoff, G., van Dishoeck, E.F., 2004. The gas temperature in flaring disks around pre-main sequence stars. *A&A* 428, 511–521. doi:doi:10.1051/0004-6361:20048013, arXiv:arXiv:astro-ph/0408503.
- Jørgensen, J.K., Schöier, F.L., van Dishoeck, E.F., 2002. Physical structure and CO abundance of low-mass protostellar envelopes. *A&A* 389, 908–930. doi:doi:10.1051/0004-6361:20020681, arXiv:arXiv:astro-ph/0205068.
- Jørgensen, J.K., van der Wiel, M.H.D., Coutens, A., Lykke, J.M., Müller, H.S.P., van Dishoeck, E.F., Calcutt, H., Bjerkekl, P., Bourke, T.L., Drozdovskaya, M.N., Favre, C., Fayolle, E.C., Garrod, R.T., Jacobsen, S.K., Öberg, K.I., Persson, M.V., Wampfler, S.F., 2016. The ALMA Protostellar Interferometric Line Survey (PILS). First results from an unbiased submillimeter wavelength line survey of the Class 0 protostellar binary IRAS 16293-2422 with ALMA. *A&A* 595, A117. doi:doi:10.1051/0004-6361/201628648, arXiv:1607.08733.
- Jura, M., Dufour, P., Xu, S., Zuckerman, B., Klein, B., Young, E.D., Melis, C., 2015. Evidence for an Anhydrous Carbonaceous Extrasolar Minor Planet. *ApJ* 799, 109. doi:doi:10.1088/0004-637X/799/1/109, arXiv:1411.5036.
- Kama, M., Bruderer, S., van Dishoeck, E.F., Hogerheijde, M., Folsom, C.P., Miotello, A., Fedele, D., Belloche, A., Güsten, R., Wyrowski, F., 2016. Volatile-carbon locking and release in protoplanetary disks. A study of TW Hya and HD 100546. *A&A* 592, A83. doi:doi:10.1051/0004-6361/201526991, arXiv:1605.05093.
- Kama, M., Shorttle, O., Jermyn, A.S., Folsom, C.P., Furuya, K., Bergin, E.A., Walsh, C., Keller, L., 2019. Abundant refractory sulfur in protoplanetary disks. *Astrophysical Journal*, in press arXiv:1908.05169.
- Kamp, I., Scheepstra, A., Min, M., Klarmann, L., Riviere-Marichalar, P., 2018. Diagnostic value of far-IR water ice features in T Tauri disks. *A&A* 617, A1. doi:doi:10.1051/0004-6361/201732368, arXiv:1804.05324.
- Kamp, I., Tilling, I., Woitke, P., Thi, W.F., Hogerheijde, M., 2010. Radiation thermo-chemical models of protoplanetary disks. II. Line diagnostics. *A&A* 510, A18. doi:doi:10.1051/0004-6361/200913076, arXiv:0911.1949.
- Katz, N., Furman, I., Biham, O., Pirronello, V., Vidali, G., 1999. Molecular Hydrogen Formation on Astrophysically Relevant Surfaces. *ApJ* 522, 305–312. doi:doi:10.1086/307642, arXiv:astro-ph/9906071.
- Kaufman, M.J., Neufeld, D.A., 1996. Far-Infrared Water Emission from Magnetohydrodynamic Shock Waves. *ApJ* 456, 611. doi:doi:10.1086/176683.
- Kaufman, M.J., Wolfire, M.G., Hollenbach, D.J., Luhman, M.L., 1999. Far-Infrared and Submillimeter Emission from Galactic and Extragalactic Photodissociation Regions. *ApJ* 527, 795–813. doi:doi:10.1086/308102, arXiv:astro-ph/9907255.

- King, H.E., Stimpfl, M., Deymier, P., Drake, M.J., Catlow, C.R.A., Putnis, A., de Leeuw, N.H., 2010. Computer simulations of water interactions with low-coordinated forsterite surface sites: Implications for the origin of water in the inner solar system. *Earth and Planetary Science Letters* 300, 11–18. doi:doi:10.1016/j.epsl.2010.10.019.
- Klarmann, L., Ormel, C.W., Dominik, C., 2018. Radial and vertical dust transport inhibit refractory carbon depletion in protoplanetary disks. *A&A* 618, L1. doi:doi:10.1051/0004-6361/201833719, arXiv:1809.01648.
- Krijt, S., Ciesla, F.J., Bergin, E.A., 2016. Tracing Water Vapor and Ice During Dust Growth. *ApJ* 833, 285. doi:doi:10.3847/1538-4357/833/2/285, arXiv:1610.06463.
- Krijt, S., Schwarz, K.R., Bergin, E.A., Ciesla, F.J., 2018. Transport of CO in Protoplanetary Disks: Consequences of Pebble Formation, Settling, and Radial Drift. *ApJ* 864, 78. doi:doi:10.3847/1538-4357/aad69b, arXiv:1808.01840.
- Laas, J.C., Caselli, P., 2019. Modeling sulfur depletion in interstellar clouds. *A&A* 624, A108. doi:doi:10.1051/0004-6361/201834446, arXiv:1903.01232.
- Lambrechts, M., Johansen, A., 2014. Forming the cores of giant planets from the radial pebble flux in protoplanetary discs. *A&A* 572, A107. doi:doi:10.1051/0004-6361/201424343, arXiv:1408.6094.
- Langer, W.D., Graedel, T.E., 1989. Ion-Molecule Chemistry of Dense Interstellar Clouds: Nitrogen-, Oxygen-, and Carbon-bearing Molecule Abundances and Isotopic Ratios. *ApJS* 69, 241. doi:doi:10.1086/191313.
- Langer, W.D., Graedel, T.E., Frerking, M.A., Armentrout, P.B., 1984. Carbon and oxygen isotope fractionation in dense interstellar clouds. *ApJ* 277, 581–604. doi:doi:10.1086/161730.
- Langer, W.D., Penzias, A.A., 1990. $^{12}\text{C}/^{13}\text{C}$ Isotope Ratio across the Galaxy from Observations of ^{13}C ^{18}O in Molecular Clouds. *ApJ* 357, 477. doi:doi:10.1086/168935.
- Law, C.J., Öberg, K.I., Bergner, J.B., Graninger, D., 2018. Carbon Chain Molecules toward Embedded Low-mass Protostars. *ApJ* 863, 88. doi:doi:10.3847/1538-4357/aacf9d, arXiv:1807.05231.
- Le Gal, R., Brady, M.T., Öberg, K.I., Roueff, E., Le Petit, F., 2019a. The Role of C/O in Nitrile Astrochemistry in PDRs and Planet-forming Disks. *ApJ* 886, 86. doi:doi:10.3847/1538-4357/ab4ad9, arXiv:1910.01554.
- Le Gal, R., Herbst, E., Dufour, G., Gratier, P., Ruaud, M., Vidal, T.H.G., Wakelam, V., 2017. A new study of the chemical structure of the Horsehead nebula: the influence of grain-surface chemistry. *A&A* 605, A88. doi:doi:10.1051/0004-6361/201730980, arXiv:1706.00454.
- Le Gal, R., Öberg, K.I., Loomis, R.A., Pegues, J., Bergner, J.B., 2019b. Sulfur Chemistry in Protoplanetary Disks: CS and H_2CS . *ApJ* 876, 72. doi:doi:10.3847/1538-4357/ab1416, arXiv:1903.11105.
- Le Petit, F., Nehmé, C., Le Bourlot, J., Roueff, E., 2006. A Model for Atomic and Molecular Interstellar Gas: The Meudon PDR Code. *ApJS* 164, 506–529. doi:doi:10.1086/503252, arXiv:astro-ph/0602150.
- Lee, C.F., Codella, C., Li, Z.Y., Liu, S.Y., 2019. First Abundance Measurement of Organic Molecules in the Atmosphere of HH 212 Protostellar Disk. *ApJ* 876, 63. doi:doi:10.3847/1538-4357/ab15db, arXiv:1904.10572.
- Lee, C.F., Li, Z.Y., Ho, P.T.P., Hirano, N., Zhang, Q., Shang, H., 2017. Formation and Atmosphere of Complex Organic Molecules of the HH 212 Protostellar Disk. *ApJ* 843, 27. doi:doi:10.3847/1538-4357/aa7757, arXiv:1706.06041.
- Lee, H.H., Herbst, E., Pineau des Forets, G., Roueff, E., Le Bourlot, J., 1996. Photodissociation of H_2 and CO and time dependent chemistry in inhomogeneous interstellar clouds. *A&A* 311, 690–707.
- Lee, J.E., Bergin, E.A., 2015. The D/H Ratio of Water Ice at Low Temperatures. *ApJ* 799, 104. doi:doi:10.1088/0004-637X/799/1/104, arXiv:1411.4231.
- Lee, J.E., Bergin, E.A., Lyons, J.R., 2008. Oxygen isotope anomalies of the Sun and the original environment of the solar system. *Meteoritics and Planetary Science* 43, 1351–1362. doi:doi:10.1111/j.1945-5100.2008.tb00702.x, arXiv:0803.0692.
- Lee, J.E., Bergin, E.A., Nomura, H., 2010. The Solar Nebula on Fire: A Solution to the Carbon Deficit in the Inner Solar System. *ApJ* 710, L21–L25. doi:doi:10.1088/2041-8205/710/1/L21, arXiv:1001.0818.
- Lefloch, B., Ceccarelli, C., Codella, C., Favre, C., Podio, L., Vastel, C., Viti, S., Bachiller, R., 2017. L1157-B1, a factory of complex organic molecules in a solar-type star-forming region. *MNRAS* 469, L73–L77. doi:doi:10.1093/mnras/slx050, arXiv:1704.04646.
- Lefloch, B., Vastel, C., Viti, S., Jimenez-Serra, I., Codella, C., Podio, L., Ceccarelli, C., Mendoza, E., Lepine, J.R.D., Bachiller, R., 2016. Phosphorus-bearing molecules in solar-type star-forming regions: first PO detection. *MNRAS* 462, 3937–3944. doi:doi:10.1093/mnras/stw1918, arXiv:1608.00048.
- Léger, A., Jura, M., Omont, A., 1985. Desorption from interstellar grains. *A&A* 144, 147–160.
- Lepp, S., Dalgarno, A., Sternberg, A., 1987. The abundance of H_3^+ ions in dense interstellar clouds. *ApJ* 321, 383–385. doi:doi:10.1086/165636.
- Levine, R.D., 2009. Molecular reaction dynamics. Cambridge University Press.
- Li, C., Ingersoll, A., Bolton, S., Levin, S., Janssen, M., Atreya, S., Lunine, J., Steffes, P., Brown, S., Guillot, T., Allison, M., Arballo, J., Bellotti, A., Adumitroaie, V., Gulkis, S., Hodges, A., Li, L., Misra, S., Orton, G., Oyafuso, F., Santos-Costa, D., Waite, H., Zhang, Z., 2020. The water abundance in Jupiter's equatorial zone. *Nature Astronomy* doi:doi:10.1038/s41550-020-1009-3.
- Lichtenberg, T., Golabek, G.J., Burn, R., Meyer, M.R., Alibert, Y., Gerya, T.V., Mordasini, C., 2019. A water budget dichotomy of rocky protoplanets from ^{26}Al -heating. *Nature Astronomy* 3, 307–313. doi:doi:10.1038/s41550-018-0688-5, arXiv:1902.04026.
- Lis, D.C., Bockelée-Morvan, D., Güsten, R., Biver, N., Stutzki, J., Delorme, Y., Durán, C., Wiesemeyer, H., Okada, Y., 2019. Terrestrial deuterium-to-hydrogen ratio in water in hyperactive comets. *A&A* 625, L5. doi:doi:10.1051/0004-6361/201935554, arXiv:1904.09175.
- Liseau, R., Goldsmith, P.F., Larsson, B., Pagani, L., Bergman, P., Le Bourlot, J., Bell, T.A., Benz, A.O., Bergin, E.A., Bjerkelí, P., Black, J.H., Bruderer, S., Caselli, P., Caux, E., Chen, J.H., de Luca, M., Encrenaz, P., Falgarone, E., Gerin, M., Goicoechea, J.R., Hjalmarson, A., Hollenbach, D.J., Justanont, K., Kaufman, M.J., Le Petit, F., Li, D., Lis, D.C., Melnick, G.J., Nagy, Z., Olofsson, A.O.H., Olofsson, G., Roueff, E., Sandqvist, A., Snell, R.L., van der Tak, F.F.S., van Dishoeck, E.F., Vastel, C., Viti, S., Yıldız, U.A., 2012. Multi-line detection of O_2 toward ρ Ophiuchi A. *A&A* 541, A73. doi:doi:10.1051/0004-6361/201118575, arXiv:1202.5637.
- Lissauer, J.J., 1993. Planet formation. *Annual Review of Astronomy and Astrophysics* 31, 129–172. URL: <https://doi.org/10.1146/annurev.aa.31.090193.001021>, doi:doi:10.1146/annurev.aa.31.090193.001021, arXiv:https://doi.org/10.1146/annurev.aa.31.090193.001021.
- Lodders, K., 2003. Solar System Abundances and Condensation Temperatures of the Elements. *ApJ* 591, 1220–1247. doi:doi:10.1086/375492.
- Lodders, K., 2010. Solar System Abundances of the Elements. *Astrophysics and Space Science Proceedings* 16, 379. doi:doi:10.1007/978-3-642-10352-0“8, arXiv:1010.2746.
- Loison, J.C., Wakelam, V., Gratier, P., Hickson, K.M., Bacmann, A., Agúndez, M., Marcelino, N., Cernicharo, J., Guzman, V., Gerin, M., Goicoechea, J.R., Roueff, E., Petit, F.L., Pety, J., Fuente, A., Riviere-Marichalar, P., 2019. Oxygen fractionation in dense molecular clouds. *MNRAS* 485, 5777–5789. doi:doi:10.1093/mnras/stz560, arXiv:1902.08840.
- Long, F., Pinilla, P., Herczeg, G.J., Harsono, D., Dipierro, G., Pascucci, I., Hendlér, N., Tazzari, M., Ragusa, E., Salyk, C., Edwards, S., Lodato, G., van de Plas, G., Johnstone, D., Liu, Y., Boehler, Y., Cabrit, S., Manara, C.F., Menard, F., Mulders, G.D., Nisini, B., Fischer, W.J., Rigliaco, E., Banzatti, A., Avenhaus, H., Gully-Santiago, M., 2018. Gaps and Rings in an ALMA Survey of Disks in the Taurus Star-forming Region. *ApJ* 869, 17. doi:doi:10.3847/1538-4357/aae8e1, arXiv:1810.06044.

- Loomis, R.A., Cleaves, L.I., Öberg, K.I., Aikawa, Y., Bergner, J., Furuya, K., Guzman, V.V., Walsh, C., 2018. The Distribution and Excitation of CH₃CN in a Solar Nebula Analog. *ApJ* 859, 131. doi:doi:10.3847/1538-4357/aac169, arXiv:1805.01458.
- Louvet, F., Dougados, C., Cabrit, S., Mardones, D., Ménard, F., Tabone, B., Pinte, C., Dent, W.R.F., 2018. The HH30 edge-on T Tauri star. A rotating and precessing monopolar outflow scrutinized by ALMA. *A&A* 618, A120. doi:doi:10.1051/0004-6361/201731733, arXiv:1808.03285.
- Luhman, K.L., 2012. The Formation and Early Evolution of Low-Mass Stars and Brown Dwarfs. *Annual Review of Astronomy and Astrophysics* 50, 65–106. doi:doi:10.1146/annurev-astro-081811-125528, arXiv:1208.5800.
- Lunine, J.I., Engel, S., Rizk, B., Horanyi, M., 1991. Sublimation and reformation of icy grains in the primitive solar nebula. *Icarus* 94, 333–344. doi:doi:10.1016/0019-1035(91)90232-I.
- Lynden-Bell, D., Pringle, J.E., 1974. The evolution of viscous discs and the origin of the nebular variables. *MNRAS* 168, 603–637.
- Lyons, J.R., Young, E.D., 2005. CO self-shielding as the origin of oxygen isotope anomalies in the early solar nebula. *Nature* 435, 317–320. doi:doi:10.1038/nature03557.
- Madhusudhan, N., 2019. Exoplanetary atmospheres: Key insights, challenges, and prospects. *Annual Review of Astronomy and Astrophysics* 57, 617–663. URL: <https://doi.org/10.1146/annurev-astro-081817-051846>, doi:doi:10.1146/annurev-astro-081817-051846, arXiv:https://doi.org/10.1146/annurev-astro-081817-051846.
- Malfait, K., Waelkens, C., Waters, L.B.F.M., Vand enbusche, B., Huygen, E., de Graauw, M.S., 1998. The spectrum of the young star HD 100546 observed with the Infrared Space Observatory. *A&A* 332, L25–L28.
- Mamajek, E.E., 2009. Initial Conditions of Planet Formation: Lifetimes of Primordial Disks, in: Usuda, T., Tamura, M., Ishii, M. (Eds.), *American Institute of Physics Conference Series*, pp. 3–10. doi:doi:10.1063/1.3215910, arXiv:0906.5011.
- Mangum, J.G., Shirley, Y.L., 2015. How to Calculate Molecular Column Density. *PASP* 127, 266. doi:doi:10.1086/680323, arXiv:1501.01703.
- Maret, S., Bergin, E.A., 2007. The Ionization Fraction of Barnard 68: Implications for Star and Planet Formation. *ApJ* 664, 956–963. doi:doi:10.1086/519152, arXiv:0704.3188.
- Maret, S., Bergin, E.A., Lada, C.J., 2006. A low fraction of nitrogen in molecular form in a dark cloud. *Nature* 442, 425–427. doi:doi:10.1038/nature04919.
- Martín-Doménech, R., Bergner, J.B., Öberg, K.I., Jørgensen, J.K., 2019. A New, Rotating Hot Corino in Serpens. *ApJ* 880, 130. doi:doi:10.3847/1538-4357/ab2a08, arXiv:1906.08848.
- Martinez, Oscar, J., Betts, N.B., Villano, S.M., Eyet, N., Snow, T.P., Bierbaum, V.M., 2008. Gas Phase Study of C⁺ Reactions of Interstellar Relevance. *ApJ* 686, 1486–1492. doi:doi:10.1086/591548.
- Marty, B., 2012. The origins and concentrations of water, carbon, nitrogen and noble gases on Earth. *Earth and Planetary Science Letters* 313, 56–66. doi:doi:10.1016/j.epsl.2011.10.040, arXiv:1405.6336.
- Marty, B., Chaussidon, M., Wiens, R.C., Jurewicz, A.J.G., Burnett, D.S., 2011. A ¹⁵N-Poor Isotopic Composition for the Solar System As Shown by Genesis Solar Wind Samples. *Science* 332, 1533. doi:doi:10.1126/science.1204656.
- Mathis, J.S., Rumpl, W., Nordsieck, K.H., 1977. The size distribution of interstellar grains. *ApJ* 217, 425–433. doi:doi:10.1086/155591.
- McCarthy, M.C., Gottlieb, C.A., Gupta, H., Thaddeus, P., 2006. Laboratory and Astronomical Identification of the Negative Molecular Ion C₆H⁻. *ApJ* 652, L141–L144. doi:doi:10.1086/510238.
- McClure, M.K., Espaillat, C., Calvet, N., Bergin, E., D’Alessio, P., Watson, D.M., Manoj, P., Sargent, B., Cleaves, L.I., 2015. Detections of Trans-Neptunian Ice in Protoplanetary Disks. *ApJ* 799, 162. doi:doi:10.1088/0004-637X/799/2/162, arXiv:1411.7618.
- McDonough, W.F., Sun, S.s., 1995. The composition of the Earth. *Chemical Geology* 120, 223–253. doi:doi:10.1016/0009-2541(94)00140-4.
- McElroy, D., Walsh, C., Markwick, A.J., Cordiner, M.A., Smith, K., Millar, T.J., 2013. The UMIST database for astrochemistry 2012. *A&A* 550, A36. doi:doi:10.1051/0004-6361/201220465, arXiv:1212.6362.
- McGuire, B.A., 2018. 2018 Census of Interstellar, Circumstellar, Extragalactic, Protoplanetary Disk, and Exoplanetary Molecules. *ApJS* 239, 17. doi:doi:10.3847/1538-4365/aae5d2, arXiv:1809.09132.
- McGuire, B.A., Burkhardt, A.M., Kalenskii, S., Shingledecker, C.N., Remijan, A.J., Herbst, E., McCarthy, M.C., 2018. Detection of the aromatic molecule benzonitrile (c-C₆H₅CN) in the interstellar medium. *Science* 359, 202–205. doi:doi:10.1126/science.aao4890, arXiv:1801.04228.
- McKee, C.F., Ostriker, E.C., 2007. Theory of star formation. *Annual Review of Astronomy and Astrophysics* 45, 565–687. URL: <https://doi.org/10.1146/annurev.astro.45.051806.110602>, doi:doi:10.1146/annurev.astro.45.051806.110602, arXiv:https://doi.org/10.1146/annurev.astro.45.051806.110602.
- Meijerink, R., Pontoppidan, K.M., Blake, G.A., Poelman, D.R., Dullemond, C.P., 2009. Radiative Transfer Models of Mid-Infrared H₂O Lines in the Planet-Forming Region of Circumstellar Disks. *ApJ* 704, 1471–1481. doi:doi:10.1088/0004-637X/704/2/1471, arXiv:0909.0975.
- Mennella, V., Palumbo, M.E., Baratta, G.A., 2004. Formation of CO and CO₂ Molecules by Ion Irradiation of Water Ice-covered Hydrogenated Carbon Grains. *ApJ* 615, 1073–1080. doi:doi:10.1086/424685.
- Milam, S.N., Savage, C., Brewster, M.A., Ziurys, L.M., Wyckoff, S., 2005. The ¹²C/¹³C Isotope Gradient Derived from Millimeter Transitions of CN: The Case for Galactic Chemical Evolution. *ApJ* 634, 1126–1132. doi:doi:10.1086/497123.
- Millar, T.J., Bennett, A., Herbst, E., 1989. Deuterium Fractionation in Dense Interstellar Clouds. *ApJ* 340, 906. doi:doi:10.1086/167444.
- Millar, T.J., Bennett, A., Rawlings, J.M.C., Brown, P.D., Charnley, S.B., 1991. Gas phase reactions and rate coefficients for use in astrochemistry - The UMIST ratefile. *A&AS* 87, 585–619.
- Millar, T.J., Walsh, C., Cordiner, M.A., Ní Chuimín, R., Herbst, E., 2007. Hydrocarbon Anions in Interstellar Clouds and Circumstellar Envelopes. *ApJ* 662, L87–L90. doi:doi:10.1086/519376, arXiv:0705.0639.
- Min, M., Bouwman, J., Dominik, C., Waters, L.B.F.M., Pontoppidan, K.M., Hony, S., Mulders, G.D., Henning, T., van Dishoeck, E.F., Woitke, P., Evans, Neal J., I., Digit Team, 2016. The abundance and thermal history of water ice in the disk surrounding HD 142527 from the DIGIT Herschel Key Program. *A&A* 593, A11. doi:doi:10.1051/0004-6361/201425432, arXiv:1606.07266.
- Minissale, M., Moudens, A., Baouche, S., Chaabouni, H., Dulieu, F., 2016. Hydrogenation of CO-bearing species on grains: unexpected chemical desorption of CO. *MNRAS* 458, 2953–2961. doi:doi:10.1093/mnras/stw373.
- Miotello, A., van Dishoeck, E.F., Kama, M., Bruderer, S., 2016. Determining protoplanetary disk gas masses from CO isotopologues line observations. *A&A* 594, A85. doi:doi:10.1051/0004-6361/201628159, arXiv:1605.07780.
- Mishra, A., Li, A., 2015. Probing the Role of Carbon in the Interstellar Ultraviolet Extinction. *ApJ* 809, 120. doi:doi:10.1088/0004-637X/809/2/120, arXiv:1507.06599.
- Miura, H., Yamamoto, T., Nomura, H., Nakamoto, T., Tanaka, K.K., Tanaka, H., Nagasawa, M., 2017. Comprehensive Study of Thermal Desorption of Grain-surface Species by Accretion Shocks around Protostars. *ApJ* 839, 47. doi:doi:10.3847/1538-4357/aa67df.
- Miyachi, N., Hidaka, H., Chigai, T., Nagaoka, A., Watanabe, N., Kouchi, A., 2008. Formation of hydrogen peroxide and water from the reaction of cold hydrogen atoms with solid oxygen at 10 K. *Chem. Phys. Lett.* 456, 27–30. doi:doi:10.1016/j.cplett.2008.02.095, arXiv:0805.0055.
- Mokrane, H., Chaabouni, H., Accolla, M., Congiu, E., Dulieu, F., Chehrouri, M., Lemaire, J.L., 2009. Experimental Evidence for Water Formation Via Ozone Hydrogenation on Dust Grains at 10 K. *ApJ* 705, L195–L198. doi:doi:10.1088/0004-637X/705/2/L195, arXiv:0907.5173.

- Morbidelli, A., Bitsch, B., Crida, A., Gounelle, M., Guillot, T., Jacobson, S., Johansen, A., Lambrechts, M., Lega, E., 2016. Fossilized condensation lines in the Solar System protoplanetary disk. *Icarus* 267, 368–376. doi:doi:10.1016/j.icarus.2015.11.027, arXiv:1511.06556.
- Morbidelli, A., Lambrechts, M., Jacobson, S., Bitsch, B., 2015. The great dichotomy of the Solar System: Small terrestrial embryos and massive giant planet cores. *Icarus* 258, 418–429. doi:doi:10.1016/j.icarus.2015.06.003, arXiv:1506.01666.
- Müller, H.S.P., Schlöder, F., Stutzki, J., Winnewisser, G., 2005. The Cologne Database for Molecular Spectroscopy, CDMS: a useful tool for astronomers and spectroscopists. *Journal of Molecular Structure* 742, 215–227. doi:doi:10.1016/j.molstruc.2005.01.027.
- Mumma, M.J., Charnley, S.B., 2011. The Chemical Composition of Comets: Emerging Taxonomies and Natal Heritage. *ARA&A* 49, 471–524. doi:doi:10.1146/annurev-astro-081309-130811.
- Muralidharan, K., Deymier, P., Stimpfl, M., de Leeuw, N.H., Drake, M.J., 2008. Origin of water in the inner Solar System: A kinetic Monte Carlo study of water adsorption on forsterite. *Icarus* 198, 400–407. doi:doi:10.1016/j.icarus.2008.07.017.
- Musioli, G., Teiser, J., Jankowski, T., Wurm, G., 2016. Ice Grain Collisions in Comparison: CO₂, H₂O, and Their Mixtures. *ApJ* 827, 63. doi:doi:10.3847/0004-637X/827/1/63, arXiv:1608.05017.
- Najita, J.R., Carr, J.S., Pontoppidan, K.M., Salyk, C., van Dishoeck, E.F., Blake, G.A., 2013. The HCN-Water Ratio in the Planet Formation Region of Disks. *ApJ* 766, 134. doi:doi:10.1088/0004-637X/766/2/134, arXiv:1303.2692.
- Najita, J.R., Carr, J.S., Strom, S.E., Watson, D.M., Pascucci, I., Hollenbach, D., Gorti, U., Keller, L., 2010. Spitzer Spectroscopy of the Transition Object TW Hya. *ApJ* 712, 274–286. doi:doi:10.1088/0004-637X/712/1/274, arXiv:1002.4623.
- Narayanan, G., Heyer, M.H., Brunt, C., Goldsmith, P.F., Snell, R., Li, D., 2008. The Five College Radio Astronomy Observatory CO Mapping Survey of the Taurus Molecular Cloud. *ApJS* 177, 341–361. doi:doi:10.1086/587786, arXiv:0802.2556.
- Neill, J.L., Wang, S., Bergin, E.A., Crockett, N.R., Favre, C., Plume, R., Melnick, G.J., 2013. The Abundance of H₂O and HDO in Orion K1 from Herschel/HIFI. *ApJ* 770, 142. doi:doi:10.1088/0004-637X/770/2/142, arXiv:1305.2247.
- Neufeld, D.A., Dalgarno, A., 1989. Fast Molecular Shocks. I. Re-formation of Molecules behind a Dissociative Shock. *ApJ* 340, 869. doi:doi:10.1086/167441.
- Neufeld, D.A., Hollenbach, D.J., 1994. Dense molecular shocks and accretion onto protostellar disks. *ApJ* 428, 170–185. doi:doi:10.1086/174230.
- Nguyen, T., Baouche, S., Congiu, E., Diana, S., Pagani, L., Dulieu, F., 2018. Segregation effect and N₂ binding energy reduction in CO-N₂ systems adsorbed on water ice substrates. *A&A* 619, A111. doi:doi:10.1051/0004-6361/201832774.
- Nisini, B., Benedettini, M., Codella, C., Giannini, T., Liseau, R., Neufeld, D., Tafalla, M., van Dishoeck, E.F., Bachiller, R., Baudry, A., 2010. Water cooling of shocks in protostellar outflows. Herschel-PACS map of L1157. *A&A* 518, L120. doi:doi:10.1051/0004-6361/201014603, arXiv:1005.4517.
- Nomura, H., Aikawa, Y., Tsujimoto, M., Nakagawa, Y., Millar, T.J., 2007. Molecular Hydrogen Emission from Protoplanetary Disks. II. Effects of X-Ray Irradiation and Dust Evolution. *ApJ* 661, 334–353. doi:doi:10.1086/513419, arXiv:astro-ph/0702030.
- Nomura, H., Millar, T.J., 2005. Molecular hydrogen emission from protoplanetary disks. *A&A* 438, 923–938. doi:doi:10.1051/0004-6361:20052809, arXiv:astro-ph/0505126.
- Nomura, H., Nakagawa, Y., 2006. Dust Size Growth and Settling in a Protoplanetary Disk. *ApJ* 640, 1099–1109. doi:doi:10.1086/500251, arXiv:astro-ph/0601013.
- Notsu, S., Akiyama, E., Booth, A., Nomura, H., Walsh, C., Hirota, T., Honda, M., Tsukagoshi, T., Millar, T.J., 2019. Dust Continuum Emission and the Upper Limit Fluxes of Submillimeter Water Lines of the Protoplanetary Disk around HD 163296 Observed by ALMA. *ApJ* 875, 96. doi:doi:10.3847/1538-4357/ab0ae9, arXiv:1902.09932.
- Notsu, S., Nomura, H., Ishimoto, D., Walsh, C., Honda, M., Hirota, T., Millar, T.J., 2016. Candidate Water Vapor Lines to Locate the H₂O Snowline through High-dispersion Spectroscopic Observations. I. The Case of a T Tauri Star. *ApJ* 827, 113. doi:doi:10.3847/0004-637X/827/2/113, arXiv:1606.05828.
- Öberg, K.I., 2016. Photochemistry and astrochemistry: Photochemical pathways to interstellar complex organic molecules. *Chemical Reviews* 116, 9631–9663. URL: <https://doi.org/10.1021/acs.chemrev.5b00694>, doi:doi:10.1021/acs.chemrev.5b00694, arXiv:https://doi.org/10.1021/acs.chemrev.5b00694. PMID: 27099922.
- Öberg, K.I., Boogert, A.C.A., Pontoppidan, K.M., van den Broek, S., van Dishoeck, E.F., Bottinelli, S., Blake, G.A., Evans, II, N.J., 2011a. The Spitzer Ice Legacy: Ice Evolution from Cores to Protostars. *ApJ* 740, 109. doi:doi:10.1088/0004-637X/740/2/109, arXiv:1107.5825.
- Öberg, K.I., Bottinelli, S., Jørgensen, J.K., van Dishoeck, E.F., 2010. A Cold Complex Chemistry Toward the Low-mass Protostar B1-b: Evidence for Complex Molecule Production in Ices. *ApJ* 716, 825–834. doi:doi:10.1088/0004-637X/716/1/825, arXiv:1005.0637.
- Öberg, K.I., Bottinelli, S., van Dishoeck, E.F., 2009a. Cold gas as an ice diagnostic toward low mass protostars. *A&A* 494, L13–L16. doi:doi:10.1051/0004-6361:200811228.
- Öberg, K.I., Fuchs, G.W., Awad, Z., Fraser, H.J., Schlemmer, S., van Dishoeck, E.F., Linnartz, H., 2007. Photodesorption of CO Ice. *ApJL* 662, L23–L26. doi:doi:10.1086/519281.
- Öberg, K.I., Garrod, R.T., van Dishoeck, E.F., Linnartz, H., 2009b. Formation rates of complex organics in UV irradiated CH₃OH-rich ices. I. Experiments. *A&A* 504, 891–913. doi:doi:10.1051/0004-6361/200912559, arXiv:0908.1169.
- Öberg, K.I., Guzmán, V.V., Furuya, K., Qi, C., Aikawa, Y., Andrews, S.M., Loomis, R., Wilner, D.J., 2015. The comet-like composition of a protoplanetary disk as revealed by complex cyanides. *Nature* 520, 198–201. doi:doi:10.1038/nature14276, arXiv:1505.06347.
- Öberg, K.I., Guzmán, V.V., Merchantz, C.J., Qi, C., Andrews, S.M., Cleeves, L.I., Huang, J., Loomis, R.A., Wilner, D.J., Brinch, C., Hogerheijde, M., 2017. H₂CO Distribution and Formation in the TW HYA Disk. *ApJ* 839, 43. doi:doi:10.3847/1538-4357/aa689a, arXiv:1704.05133.
- Öberg, K.I., Murray-Clay, R., Bergin, E.A., 2011b. The Effects of Snowlines on C/O in Planetary Atmospheres. *ApJL* 743, L16. doi:doi:10.1088/2041-8205/743/1/L16, arXiv:1110.5567.
- Öberg, K.I., Qi, C., Wilner, D.J., Andrews, S.M., 2011c. The Ionization Fraction in the DM Tau Protoplanetary Disk. *ApJ* 743, 152. doi:doi:10.1088/0004-637X/743/2/152, arXiv:1109.2578.
- Öberg, K.I., van Broekhuizen, F., Fraser, H.J., Bisschop, S.E., van Dishoeck, E.F., Schlemmer, S., 2005. Competition between CO and N₂ Desorption from Interstellar Ices. *ApJL* 621, L33–L36. doi:doi:10.1086/428901.
- Öberg, K.I., van Dishoeck, E.F., Linnartz, H., 2009c. Photodesorption of ices I: CO, N₂, and CO₂. *A&A* 496, 281–293. doi:doi:10.1051/0004-6361/200810207.
- Öberg, K.I., Wordsworth, R., 2019. Jupiter’s Composition Suggests its Core Assembled Exterior to the N₂ Snowline. *AJ* 158, 194. doi:doi:10.3847/1538-3881/ab46a8, arXiv:1909.11246.
- O’Brien, D.P., Izidoro, A., Jacobson, S.A., Raymond, S.N., Rubie, D.C., 2018. The Delivery of Water During Terrestrial Planet Formation. *Space Sci. Rev.* 214, 47. doi:doi:10.1007/s11214-018-0475-8, arXiv:1801.05456.
- Oka, A., Nakamoto, T., Ida, S., 2011. Evolution of Snow Line in Optically Thick Protoplanetary Disks: Effects of Water Ice Opacity and Dust Grain Size. *ApJ* 738, 141. doi:doi:10.1088/0004-637X/738/2/141, arXiv:1106.2682.
- Pagani, L., Bacmann, A., Cabrit, S., Vastel, C., 2007. Depletion and low gas temperature in the L183 (=L134N) prestellar core: the N₂H⁺-N₂D⁺ tool. *A&A* 467, 179–186. doi:doi:10.1051/0004-6361:20066670, arXiv:astro-ph/0701823.

- Pagani, L., Lesaffre, P., Jorfi, M., Honvault, P., González-Lezana, T., Faure, A., 2013. Ortho-H₂ and the age of prestellar cores. *A&A* 551, A38. doi:doi:10.1051/0004-6361/201117161.
- Pagani, L., Olofsson, A.O.H., Bergman, P., Bernath, P., Black, J.H., Booth, R.S., Buat, V., Crovisier, J., Curry, C.L., Encrenaz, P.J., Falgarone, E., Feldman, P.A., Fich, M., Floren, H.G., Frisk, U., Gerin, M., Gregersen, E.M., Harju, J., Hasegawa, T., Hjalmarsen, Å., Johansson, L.E.B., Kwok, S., Larsson, B., Lecacheux, A., Liljeström, T., Lindqvist, M., Liseau, R., Mattila, K., Mitchell, G.F., Nordh, L.H., Olberg, M., Olofsson, G., Ristorcelli, I., Sandqvist, A., von Scheele, F., Serra, G., Tothill, N.F., Volk, K., Wiklind, T., Wilson, C.D., 2003. Low upper limits on the O₂ abundance from the Odin satellite. *A&A* 402, L77–L81. doi:doi:10.1051/0004-6361:20030344.
- Pagani, L., Salez, M., Wannier, P.G., 1992. The chemistry of H₂D⁺ in cold clouds. *A&A* 258, 479–488.
- Parise, B., Ceccarelli, C., Tielens, A.G.G.M., Herbst, E., Lefloch, B., Caux, E., Castets, A., Mukhopadhyay, I., Pagani, L., Loinard, L., 2002. Detection of doubly-deuterated methanol in the solar-type protostar IRAS 16293-2422. *A&A* 393, L49–L53. doi:doi:10.1051/0004-6361:20021131, arXiv:astro-ph/0207577.
- Pascucci, I., Apai, D., Luhman, K., Henning, T., Bouwman, J., Meyer, M.R., Lahuis, F., Natta, A., 2009. The Different Evolution of Gas and Dust in Disks around Sun-Like and Cool Stars. *ApJ* 696, 143–159. doi:doi:10.1088/0004-637X/696/1/143, arXiv:0810.2552.
- Pascucci, I., Tachibana, S., 2010. The Clearing of Protoplanetary Disks and of the Protosolar Nebula. pp. 263–298.
- Pearce, B.K.D., Pudritz, R.E., Semenov, D.A., Henning, T.K., 2017. Origin of the RNA world: The fate of nucleobases in warm little ponds. *Proceedings of the National Academy of Science* 114, 11327–11332. doi:doi:10.1073/pnas.1710339114, arXiv:1710.00434.
- Pegues, J., Öberg, K.I., Bergner, J.B., Loomis, R.A., Qi, C., Gal, R.L., Cleaves, L.I., Guzmán, V.V., Huang, J., Jørgensen, J.K., Andrews, S.M., Blake, G.A., Carpenter, J.M., Schwarz, K.R., Williams, J.P., Wilner, D.J., 2020. An ALMA Survey of H₂CO in Protoplanetary Disks. *ApJ* 890, 142. doi:doi:10.3847/1538-4357/ab64d9.
- Persson, M.V., Harsono, D., Tobin, J.J., van Dishoeck, E.F., Jørgensen, J.K., Murillo, N., Lai, S.P., 2016. Constraining the physical structure of the inner few 100 AU scales of deeply embedded low-mass protostars. *A&A* 590, A33. doi:doi:10.1051/0004-6361/201527666, arXiv:1603.01061.
- Persson, M.V., Jørgensen, J.K., van Dishoeck, E.F., 2013. Warm water deuterium fractionation in IRAS 16293-2422. The high-resolution ALMA and SMA view. *A&A* 549, L3. doi:doi:10.1051/0004-6361/201220638, arXiv:1211.6605.
- Persson, M.V., Jørgensen, J.K., van Dishoeck, E.F., Harsono, D., 2014. The deuterium fractionation of water on solar-system scales in deeply-embedded low-mass protostars. *A&A* 563, A74. doi:doi:10.1051/0004-6361/201322845, arXiv:1402.1398.
- Pety, J., Goicoechea, J.R., Hily-Blant, P., Gerin, M., Teyssier, D., 2007. Deuterium fractionation in the Horsehead edge. *A&A* 464, L41–L44. doi:doi:10.1051/0004-6361:20067009, arXiv:astro-ph/0701700.
- Pety, J., Guzmán, V.V., Orkisz, J.H., Liszt, H.S., Gerin, M., Bron, E., Bardeau, S., Goicoechea, J.R., Gratier, P., Le Petit, F., Levrier, F., Öberg, K.I., Roueff, E., Sievers, A., 2017. The anatomy of the Orion B giant molecular cloud: A local template for studies of nearby galaxies. *A&A* 599, A98. doi:doi:10.1051/0004-6361/201629862.
- Pety, J., Teyssier, D., Fossé, D., Gerin, M., Roueff, E., Abergel, A., Habart, E., Cernicharo, J., 2005. Are PAHs precursors of small hydrocarbons in photo-dissociation regions? The Horsehead case. *A&A* 435, 885–899. doi:doi:10.1051/0004-6361:20041170, arXiv:astro-ph/0501339.
- Pineau des Forets, G., Flower, D.R., McCarroll, R., 1991. The para-H₂:ortho-H₂ ratio and the deuteration of interstellar molecules. *MNRAS* 248, 173–175. doi:doi:10.1093/mnras/248.1.173.
- Pineau des Forets, G., Roueff, E., Flower, D.R., 1990. The formation of nitrogen-bearing species in dark interstellar clouds. *MNRAS* 244, 668–674.
- Pinilla, P., Pohl, A., Stammer, S.M., Birnstiel, T., 2017. Dust Density Distribution and Imaging Analysis of Different Ice Lines in Protoplanetary Disks. *ApJ* 845, 68. doi:doi:10.3847/1538-4357/aa7edb, arXiv:1707.02321.
- Piso, A.M.A., Öberg, K.I., Birnstiel, T., Murray-Clay, R.A., 2015. C/O and Snowline Locations in Protoplanetary Disks: The Effect of Radial Drift and Viscous Gas Accretion. *ApJ* 815, 109. doi:doi:10.1088/0004-637X/815/2/109, arXiv:1511.05563.
- Piso, A.M.A., Pegues, J., Öberg, K.I., 2016. The Role of Ice Compositions for Snowlines and the C/N/O Ratios in Active Disks. *ApJ* 833, 203. doi:doi:10.3847/1538-4357/833/2/203, arXiv:1611.00741.
- Pontoppidan, K.M., 2006. Spatial mapping of ices in the Ophiuchus-F core. A direct measurement of CO depletion and the formation of CO₂. *A&A* 453, L47–L50. doi:doi:10.1051/0004-6361:20065569, arXiv:astro-ph/0605576.
- Pontoppidan, K.M., Blake, G.A., van Dishoeck, E.F., Smette, A., Ireland, M.J., Brown, J., 2008a. Spectroastrometric Imaging of Molecular Gas within Protoplanetary Disk Gaps. *ApJ* 684, 1323–1329. doi:doi:10.1086/590400, arXiv:0805.3314.
- Pontoppidan, K.M., Boogert, A.C.A., Fraser, H.J., van Dishoeck, E.F., Blake, G.A., Lahuis, F., Öberg, K.I., Evans, II, N.J., Salyk, C., 2008b. The c2d Spitzer Spectroscopic Survey of Ices around Low-Mass Young Stellar Objects. II. CO₂. *ApJ* 678, 1005–1031. doi:doi:10.1086/533431, arXiv:0711.4616.
- Pontoppidan, K.M., Salyk, C., Bergin, E.A., Brittain, S., Marty, B., Mousis, O., Öberg, K.I., 2014. Volatiles in Protoplanetary Disks, in: Beuther, H., Klessen, R.S., Dullemond, C.P., Henning, T. (Eds.), *Protostars and Planets VI*, p. 363. doi:doi:10.2458/azu“uapress“9780816531240-ch016, arXiv:1401.2423.
- Pontoppidan, K.M., Salyk, C., Blake, G.A., Meijerink, R., Carr, J.S., Najita, J., 2010. A Spitzer Survey of Mid-infrared Molecular Emission from Protoplanetary Disks. I. Detection Rates. *ApJ* 720, 887–903. doi:doi:10.1088/0004-637X/720/1/887.
- Pontoppidan, K.M., van Dishoeck, E.F., Dartois, E., 2004. Mapping ices in protostellar environments on 1000 AU scales. Methanol-rich ice in the envelope of Serpens SMM 4. *A&A* 426, 925–940. doi:doi:10.1051/0004-6361:20041276, arXiv:astro-ph/0407316.
- Poteet, C.A., Whittet, D.C.B., Draine, B.T., 2015. The Composition of Interstellar Grains toward ζ Ophiuchi: Constraining the Elemental Budget near the Diffuse-dense Cloud Transition. *ApJ* 801, 110. doi:doi:10.1088/0004-637X/801/2/110, arXiv:1501.02810.
- Prasad, S.S., Tarafdar, S.P., 1983. UV radiation field inside dense clouds - Its possible existence and chemical implications. *ApJ* 267, 603–609. doi:doi:10.1086/160896.
- Qi, C., Öberg, K.I., Espaillat, C.C., Robinson, C.E., Andrews, S.M., Wilner, D.J., Blake, G.A., Bergin, E.A., Cleaves, L.I., 2019. Probing CO and N₂ Snow Surfaces in Protoplanetary Disks with N₂H⁺ Emission. *ApJ* 882, 160. doi:doi:10.3847/1538-4357/ab35d3, arXiv:1907.10647.
- Qi, C., Öberg, K.I., Wilner, D.J., D’Alessio, P., Bergin, E., Andrews, S.M., Blake, G.A., Hogerheijde, M.R., van Dishoeck, E.F., 2013. Imaging of the CO Snow Line in a Solar Nebula Analog. *Science* 341, 630–632. doi:doi:10.1126/science.1239560, arXiv:1307.7439.
- Rauls, E., Hornekaer, L., 2008. Catalyzed Routes to Molecular Hydrogen Formation and Hydrogen Addition Reactions on Neutral Polycyclic Aromatic Hydrocarbons under Interstellar Conditions. *ApJ* 679, 531–536. doi:doi:10.1086/587614.
- Raymond, S.N., Morbidelli, A., 2020. Planet formation: key mechanisms and global models. arXiv e-prints, arXiv:2002.05756arXiv:2002.05756.
- Reboussin, L., Wakelam, V., Guilloteau, S., Hersant, F., Dutrey, A., 2015. Chemistry in protoplanetary disks: the gas-phase CO/H₂ ratio and the carbon reservoir. *A&A* 579, A82. doi:doi:10.1051/0004-6361/201525885, arXiv:1505.01309.
- Rice, T.S., Bergin, E.A., Jørgensen, J.K., Wampfler, S.F., 2018. Exploring the Origins of Earth’s Nitrogen: Astronomical Observations of Nitrogen-bearing Organics in Protostellar Environments. *ApJ* 866, 156. doi:doi:10.3847/1538-4357/aadfdb, arXiv:1809.07514.

- Rivilla, V.M., Drozdovskaya, M.N., Altwegg, K., Caselli, P., Beltrán, M.T., Fontani, F., van der Tak, F.F.S., Cesaroni, R., Vasyunin, A., Rubin, M., Lique, F., Marinakis, S., Testi, L., Rosina Team, Balsiger, H., Berthelier, J.J., de Keyser, J., Fiethe, B., Fuselier, S.A., Gasc, S., Gombosi, T.I., Sémon, T., Tzou, C.Y., 2020. ALMA and ROSINA detections of phosphorus-bearing molecules: the interstellar thread between star-forming regions and comets. *MNRAS* 492, 1180–1198. doi:doi:10.1093/mnras/stz3336, [arXiv:1911.11647](https://arxiv.org/abs/1911.11647).
- Rivilla, V.M., Fontani, F., Beltrán, M.T., Vasyunin, A., Caselli, P., Martín-Pintado, J., Cesaroni, R., 2016. The First Detections of the Key Prebiotic Molecule PO in Star-forming Regions. *ApJ* 826, 161. doi:doi:10.3847/0004-637X/826/2/161, [arXiv:1605.06109](https://arxiv.org/abs/1605.06109).
- Rodgers, S.D., Millar, T.J., 1996. The chemistry of deuterium in hot molecular cores. *MNRAS* 280, 1046–1054. doi:doi:10.1093/mnras/280.4.1046.
- Röllig, M., Ossenkopf, V., 2013. Carbon fractionation in photo-dissociation regions. *A&A* 550, A56. doi:doi:10.1051/0004-6361/201220130, [arXiv:1211.3562](https://arxiv.org/abs/1211.3562).
- Ros, K., Johansen, A., 2013. Ice condensation as a planet formation mechanism. *A&A* 552, A137. doi:doi:10.1051/0004-6361/201220536, [arXiv:1302.3755](https://arxiv.org/abs/1302.3755).
- Ros, K., Johansen, A., Riipinen, I., Schlesinger, D., 2019. Effect of nucleation on icy pebble growth in protoplanetary discs. *A&A* 629, A65. doi:doi:10.1051/0004-6361/201834331, [arXiv:1907.08471](https://arxiv.org/abs/1907.08471).
- Roueff, E., Loison, J.C., Hickson, K.M., 2015. Isotopic fractionation of carbon, deuterium, and nitrogen: a full chemical study. *A&A* 576, A99. doi:doi:10.1051/0004-6361/201425113, [arXiv:1501.01141](https://arxiv.org/abs/1501.01141).
- Rubin, M., Altwegg, K., Balsiger, H., Berthelier, J.J., Combi, M.R., De Keyser, J., Drozdovskaya, M., Fiethe, B., Fuselier, S.A., Gasc, S., Gombosi, T.I., Hänni, N., Hansen, K.C., Mall, U., Rème, H., Schroeder, I.R.H.G., Schuhmann, M., Sémon, T., Waite, J.H., Wampfler, S.F., Wurz, P., 2019. Elemental and molecular abundances in comet 67P/Churyumov-Gerasimenko. *arXiv e-prints*, [arXiv:1907.11044](https://arxiv.org/abs/1907.11044).
- Sakai, N., Oya, Y., Sakai, T., Watanabe, Y., Hirota, T., Ceccarelli, C., Kahane, C., Lopez-Sepulcre, A., Lefloch, B., Vastel, C., Bottinelli, S., Caux, E., Coutens, A., Aikawa, Y., Takakuwa, S., Ohashi, N., Yen, H.W., Yamamoto, S., 2014a. A Chemical View of Protostellar-disk Formation in L1527. *ApJ* 791, L38. doi:doi:10.1088/2041-8205/791/2/L38.
- Sakai, N., Sakai, T., Hirota, T., Watanabe, Y., Ceccarelli, C., Kahane, C., Bottinelli, S., Caux, E., Demyk, K., Vastel, C., Coutens, A., Taquet, V., Ohashi, N., Takakuwa, S., Yen, H.W., Aikawa, Y., Yamamoto, S., 2014b. Change in the chemical composition of infalling gas forming a disk around a protostar. *Nature* 507, 78–80. doi:doi:10.1038/nature13000.
- Sakai, N., Sakai, T., Yamamoto, S., 2008. Complex organic molecules in an early stage of protostellar evolution. *APSS* 313, 153–157. doi:doi:10.1007/s10509-007-9625-2.
- Sakai, N., Yamamoto, S., 2013. Warm Carbon-Chain Chemistry. *Chemical Reviews* 113, 8981–9015. doi:doi:10.1021/cr4001308.
- Salyk, C., Lacy, J., Richter, M., Zhang, K., Pontoppidan, K., Carr, J.S., Najita, J.R., Blake, G.A., 2019. A High-resolution Mid-infrared Survey of Water Emission from Protoplanetary Disks. *ApJ* 874, 24. doi:doi:10.3847/1538-4357/ab05c3, [arXiv:1902.02708](https://arxiv.org/abs/1902.02708).
- Salyk, C., Pontoppidan, K.M., Blake, G.A., Lahuis, F., van Dishoeck, E.F., Evans, II, N.J., 2008. H₂O and OH Gas in the Terrestrial Planet-forming Zones of Protoplanetary Disks. *ApJL* 676, L49–L52. doi:doi:10.1086/586894, [arXiv:0802.0037](https://arxiv.org/abs/0802.0037).
- Salyk, C., Pontoppidan, K.M., Blake, G.A., Najita, J.R., Carr, J.S., 2011. A Spitzer Survey of Mid-infrared Molecular Emission from Protoplanetary Disks. II. Correlations and Local Thermal Equilibrium Models. *ApJ* 731, 130. doi:doi:10.1088/0004-637X/731/2/130, [arXiv:1104.0948](https://arxiv.org/abs/1104.0948).
- Sato, T., Okuzumi, S., Ida, S., 2016. On the water delivery to terrestrial embryos by ice pebble accretion. *A&A* 589, A15. doi:doi:10.1051/0004-6361/201527069, [arXiv:1512.02414](https://arxiv.org/abs/1512.02414).
- Schlichting, H.E., Sari, R., Yalinewich, A., 2015. Atmospheric mass loss during planet formation: The importance of planetesimal impacts. *Icarus* 247, 81–94. doi:doi:10.1016/j.icarus.2014.09.053, [arXiv:1406.6435](https://arxiv.org/abs/1406.6435).
- Schöier, F.L., van der Tak, F.F.S., van Dishoeck, E.F., Black, J.H., 2005. An atomic and molecular database for analysis of submillimetre line observations. *A&A* 432, 369–379. doi:doi:10.1051/0004-6361:20041729, [arXiv:astro-ph/0411110](https://arxiv.org/abs/astro-ph/0411110).
- Schoonenberg, D., Ormel, C.W., 2017. Planetesimal formation near the snowline: in or out? *A&A* 602, A21. doi:doi:10.1051/0004-6361/201630013, [arXiv:1702.02151](https://arxiv.org/abs/1702.02151).
- Schwarz, K.R., Bergin, E.A., Cleaves, L.I., Blake, G.A., Zhang, K., Öberg, K.I., van Dishoeck, E.F., Qi, C., 2016. The Radial Distribution of H₂ and CO in TW Hya as Revealed by Resolved ALMA Observations of CO Isotopologues. *ApJ* 823, 91. doi:doi:10.3847/0004-637X/823/2/91, [arXiv:1603.08520](https://arxiv.org/abs/1603.08520).
- Schwarz, K.R., Bergin, E.A., Cleaves, L.I., Zhang, K., Öberg, K.I., Blake, G.A., Anderson, D., 2018. Unlocking CO Depletion in Protoplanetary Disks I. The Warm Molecular Layer. *ArXiv e-prints* [arXiv:1802.02590](https://arxiv.org/abs/1802.02590).
- Schwarz, K.R., Bergin, E.A., Cleaves, L.I., Zhang, K., Öberg, K.I., Blake, G.A., Anderson, D.E., 2019. Unlocking CO Depletion in Protoplanetary Disks. II. Primordial C/H Predictions inside the CO Snowline. *ApJ* 877, 131. doi:doi:10.3847/1538-4357/ab1c5e, [arXiv:1904.10422](https://arxiv.org/abs/1904.10422).
- Scibelli, S., Shirley, Y., 2020. Prevalence of Complex Organic Molecules in Starless and Prestellar Cores within the Taurus Molecular Cloud. *ApJ* 891, 73. doi:doi:10.3847/1538-4357/ab7375, [arXiv:2002.02469](https://arxiv.org/abs/2002.02469).
- Seifried, D., Walch, S., Girichidis, P., Naab, T., Wunsch, R., Klessen, R.S., Glover, S.C.O., Peters, T., Clark, P., 2017. SILCC-Zoom: the dynamic and chemical evolution of molecular clouds. *MNRAS* 472, 4797–4818. doi:doi:10.1093/mnras/stx2343, [arXiv:1704.06487](https://arxiv.org/abs/1704.06487).
- Semenov, D., Wiebe, D., 2011. Chemical Evolution of Turbulent Protoplanetary Disks and the Solar Nebula. *ApJs* 196, 25. doi:doi:10.1088/0067-0049/196/2/25, [arXiv:1104.4358](https://arxiv.org/abs/1104.4358).
- Shannon, R.J., Blitz, M.A., Goddard, A., Heard, D.E., 2013. Accelerated chemistry in the reaction between the hydroxyl radical and methanol at interstellar temperatures facilitated by tunnelling. *Nature Chemistry* 5, 745–749. doi:doi:10.1038/nchem.1692.
- Shingledecker, C.N., Tennis, J., Le Gal, R., Herbst, E., 2018. On Cosmic-Ray-driven Grain Chemistry in Cold Core Models. *ApJ* 861, 20. doi:doi:10.3847/1538-4357/aac5ee, [arXiv:1805.05764](https://arxiv.org/abs/1805.05764).
- Shirley, Y.L., 2015. The Critical Density and the Effective Excitation Density of Commonly Observed Molecular Dense Gas Tracers. *PASP* 127, 299. doi:doi:10.1086/680342, [arXiv:1501.01629](https://arxiv.org/abs/1501.01629).
- Shu, F.H., 1977. Self-similar collapse of isothermal spheres and star formation. *ApJ* 214, 488–497. doi:doi:10.1086/155274.
- Shu, F.H., Adams, F.C., Lizano, S., 1987. Star formation in molecular clouds: Observation and theory. *Ann. Rev. Astr. Astroph.* 25, 23–81. URL: <https://doi.org/10.1146/annurev.aa.25.090187.000323>, doi:doi:10.1146/annurev.aa.25.090187.000323, [arXiv:https://doi.org/10.1146/annurev.aa.25.090187.000323](https://arxiv.org/abs/https://doi.org/10.1146/annurev.aa.25.090187.000323).
- Sims, I.R., Queffelec, J.L., Travers, D., Rowe, B.R., Herbert, L.B., Karthäuser, J., Smith, I.W.M., 1993. Rate constants for the reactions of CN with hydrocarbons at low and ultra-low temperatures. *Chemical Physics Letters* 211, 461–468. doi:doi:10.1016/0009-2614(93)87091-G.
- Sipilä, O., Caselli, P., Harju, J., 2015. Benchmarking spin-state chemistry in starless core models. *A&A* 578, A55. doi:doi:10.1051/0004-6361/201424364, [arXiv:1501.04825](https://arxiv.org/abs/1501.04825).
- Smith, I.W.M., 2011. Laboratory Astrochemistry: Gas-Phase Processes. *ARA&A* 49, 29–66. doi:doi:10.1146/annurev-astro-081710-102533.
- Snell, R.L., Howe, J.E., Ashby, M.L.N., Bergin, E.A., Chin, G., Erickson, N.R., Goldsmith, P.F., Harwit, M., Kleiner, S.C., Koch, D.G., Neufeld, D.A., Patten, B.M., Plume, R., Schieder, R., Stauffer, J.R., Tolls, V., Wang, Z., Winniewisser, G., Zhang, Y.F., Melnick, G.J., 2000. Water Abundance in Molecular Cloud Cores. *ApJ* 539, L101–L105. doi:doi:10.1086/312848, [arXiv:astro-ph/0010393](https://arxiv.org/abs/astro-ph/0010393).
- Sternberg, A., Dalgarno, A., 1995. Chemistry in Dense Photon-dominated Regions. *ApJS* 99, 565. doi:doi:10.1086/192198.

- Stevenson, D.J., Lunine, J.I., 1988. Rapid formation of Jupiter by diffuse redistribution of water vapor in the solar nebula. *Icarus* 75, 146–155. doi:doi:10.1016/0019-1035(88)90133-9.
- Stimpff, M., Walker, A.M., Drake, M.J., de Leeuw, N.H., Deymier, P., 2006. An ångström-sized window on the origin of water in the inner solar system: Atomistic simulation of adsorption of water on olivine. *Journal of Crystal Growth* 294, 83–95. doi:doi:10.1016/j.jcrysgro.2006.05.057.
- Taquet, V., Bianchi, E., Codella, C., Persson, M.V., Ceccarelli, C., Cabrit, S., Jørgensen, J.K., Kahane, C., López-Sepulcre, A., Neri, R., 2019. Interferometric observations of warm deuterated methanol in the inner regions of low-mass protostars. *A&A* 632, A19. doi:doi:10.1051/0004-6361/201936044, arXiv:1909.08515.
- Taquet, V., Peters, P.S., Kahane, C., Ceccarelli, C., López-Sepulcre, A., Toubin, C., Duflot, D., Wiesenfeld, L., 2013. Water ice deuteration: a tracer of the chemical history of protostars. *A&A* 550, A127. doi:doi:10.1051/0004-6361/201220084, arXiv:1211.0514.
- Teague, R., Bae, J., Bergin, E.A., 2019. Meridional flows in the disk around a young star. *Nature* 574, 378–381. doi:doi:10.1038/s41586-019-1642-0, arXiv:1910.06980.
- Terebey, S., Shu, F.H., Cassen, P., 1984. The collapse of the cores of slowly rotating isothermal clouds. *ApJ* 286, 529–551. doi:doi:10.1086/162628.
- Terziva, R., Herbst, E., 2000. The possibility of nitrogen isotopic fractionation in interstellar clouds. *MNRAS* 317, 563–568. doi:doi:10.1046/j.1365-8711.2000.03618.x.
- Thi, W., van Zadelhoff, G., van Dishoeck, E.F., 2004. Organic molecules in protoplanetary disks around T Tauri and Herbig Ae stars. *A&A* 425, 955–972. doi:doi:10.1051/0004-6361:200400026, arXiv:arXiv:astro-ph/0406577.
- Thi, W.F., Woitke, P., Kamp, I., 2010. Warm non-equilibrium gas phase chemistry as a possible origin of high HDO/H₂O ratios in hot and dense gases: application to inner protoplanetary discs. *MNRAS* 407, 232–246. doi:doi:10.1111/j.1365-2966.2009.16162.x, arXiv:0912.0701.
- Tielens, A.G.G.M., 1983. Surface chemistry of deuterated molecules. *A&A* 119, 177–184.
- Tielens, A.G.G.M., Hagen, W., 1982. Model calculations of the molecular composition of interstellar grain mantles. *A&A* 114, 245–260.
- Tielens, A.G.G.M., Hollenbach, D., 1985. Photodissociation regions. I - Basic model. II - A model for the Orion photodissociation region. *ApJ* 291, 722–754. doi:doi:10.1086/163111.
- Tobin, J.J., Hartmann, L., Chiang, H.F., Wilner, D.J., Looney, L.W., Loinard, L., Calvet, N., D'Alessio, P., 2012. A ~0.2-solar-mass protostar with a Keplerian disk in the very young L1527 IRS system. *Nature* 492, 83–85. doi:doi:10.1038/nature11610, arXiv:1212.0861.
- Townes, C.H., Schawlow, A.L., 1955. *Microwave Spectroscopy*. Microwave Spectroscopy, New York: McGraw-Hill, 1955.
- Turner, B.E., 2001. Deuterated Molecules in Translucent and Dark Clouds. *ApJS* 136, 579–629. doi:doi:10.1086/322536.
- van Boekel, R., Min, M., Leinert, C., Waters, L.B.F.M., Richichi, A., Chesneau, O., Dominik, C., Jaffe, W., Dutrey, A., Graser, U., Henning, T., de Jong, J., Köhler, R., de Koter, A., Lopez, B., Malbet, F., Morel, S., Paresce, F., Perrin, G., Preibisch, T., Przygodda, F., Schöller, M., Wittkowski, M., 2004. The building blocks of planets within the 'terrestrial' region of protoplanetary disks. *Nature* 432, 479–482. doi:doi:10.1038/nature03088.
- van der Tak, F., 2011. Radiative Transfer and Molecular Data for Astrochemistry, in: Cernicharo, J., Bachiller, R. (Eds.), *The Molecular Universe*, pp. 449–460. doi:doi:10.1017/S1743921311025191, arXiv:1107.3368.
- van Dishoeck, E.F., 2006. Inaugural Article by a Recently Elected Academy Member: Proceedings of the National Academy of Science 103, 12249–12256. doi:doi:10.1073/pnas.0602207103.
- van Dishoeck, E.F., Bergin, E.A., Lis, D.C., Lunine, J.I., 2014. Water: From Clouds to Planets, in: Beuther, H., Klessen, R.S., Dullemond, C.P., Henning, T. (Eds.), *Protostars and Planets VI*, p. 835. doi:doi:10.2458/azu“uapress“9780816531240-ch036, arXiv:1401.8103.
- van Dishoeck, E.F., Black, J.H., 1988. The Photodissociation and Chemistry of Interstellar CO. *ApJ* 334, 771. doi:doi:10.1086/166877.
- van Dishoeck, E.F., Blake, G.A., 1998. Chemical Evolution of Star-Forming Regions. *ARA&A* 36, 317–368. doi:doi:10.1146/annurev.astro.36.1.317.
- van Dishoeck, E.F., Blake, G.A., Draine, B.T., Lunine, J.I., 1993. The Chemical Evolution of Protostellar and Protoplanetary Matter, in: Levy, E.H., Lunine, J.I. (Eds.), *Protostars and Planets III*, p. 163.
- van Dishoeck, E.F., Blake, G.A., Jansen, D.J., Groesbeck, T.D., 1995. Molecular Abundances and Low-Mass Star Formation. II. Organic and Deuterated Species toward IRAS 16293-2422. *ApJ* 447, 760. doi:doi:10.1086/175915.
- van Dishoeck, E.F., Kristensen, L.E., Benz, A.O., Bergin, E.A., Caselli, P., Cernicharo, J., Herpin, F., Hogerheijde, M.R., Johnstone, D., Liseau, R., Nisini, B., Shipman, R., Tafalla, M., van der Tak, F., Wyrowski, F., Aikawa, Y., Bachiller, R., Baudry, A., Benedettini, M., Bjerkerli, P., Blake, G.A., Bontemps, S., Braine, J., Brinch, C., Bruderer, S., Chavarría, L., Codella, C., Daniel, F., de Graauw, T., Deul, E., di Giorgio, A.M., Dominik, C., Doty, S.D., Dubernet, M.L., Encernaz, P., Feuchtgruber, H., Fich, M., Frieswijk, W., Fuente, A., Giannini, T., Goicoechea, J.R., Helmich, F.P., Herczeg, G.J., Jacq, T., Jørgensen, J.K., Karska, A., Kaufman, M.J., Keto, E., Larsson, B., Lefloch, B., Lis, D., Marseille, M., McCoy, C., Melnick, G., Neufeld, D., Olberg, M., Pagani, L., Panić, O., Parise, B., Pearson, J.C., Plume, R., Risacher, C., Salter, D., Santiago-García, J., Saraceno, P., Stäuber, P., van Kempen, T.A., Visser, R., Viti, S., Walmsley, M., Wampfler, S.F., Yıldız, U.A., 2011. Water in Star-forming Regions with the Herschel Space Observatory (WISH). I. Overview of Key Program and First Results. *PASP* 123, 138. doi:doi:10.1086/658676, arXiv:1012.4570.
- van 't Hoff, M.L.R., Tobin, J.J., Trapman, L., Harsono, D., Sheehan, P.D., Fischer, W.J., Megeath, S.T., van Dishoeck, E.F., 2018. Methanol and its Relation to the Water Snowline in the Disk around the Young Outbursting Star V883 Ori. *ApJ* 864, L23. doi:doi:10.3847/2041-8213/aad8a, arXiv:1808.08258.
- van 't Hoff, M.L.R., Walsh, C., Kama, M., Facchini, S., van Dishoeck, E.F., 2017. Robustness of N₂H⁺ as tracer of the CO snowline. *A&A* 599, A101. doi:doi:10.1051/0004-6361/201629452, arXiv:1610.06788.
- van Zadelhoff, G., van Dishoeck, E.F., Thi, W., Blake, G.A., 2001. Submillimeter lines from circumstellar disks around pre-main sequence stars. *A&A* 377, 566–580. doi:doi:10.1051/0004-6361:20011137, arXiv:arXiv:astro-ph/0108375.
- van't Hoff, M.L.R., van Dishoeck, E.F., Jørgensen, J.K., Calcutt, H., 2020. Temperature profiles of young disk-like structures. The case of IRAS 16293A. *A&A* 633, A7. doi:doi:10.1051/0004-6361/201936839, arXiv:1911.03495.
- Vastel, C., Ceccarelli, C., Lefloch, B., Bachiller, R., 2014. The Origin of Complex Organic Molecules in Prestellar Cores. *ApJ* 795, L2. doi:doi:10.1088/2041-8205/795/1/L2, arXiv:1409.6565.
- Vastel, C., Quénard, D., Le Gal, R., Wakelam, V., Andrianasolo, A., Caselli, P., Vidal, T., Ceccarelli, C., Lefloch, B., Bachiller, R., 2018. Sulphur chemistry in the L1544 pre-stellar core. *MNRAS* 478, 5514–5532. doi:doi:10.1093/mnras/sty1336, arXiv:1806.01102.
- Vasyunin, A.I., Caselli, P., Dulieu, F., Jiménez-Serra, I., 2017. Formation of Complex Molecules in Prestellar Cores: A Multilayer Approach. *ApJ* 842, 33. doi:doi:10.3847/1538-4357/aa72ec, arXiv:1705.04747.
- Vasyunin, A.I., Herbst, E., 2013. A Unified Monte Carlo Treatment of Gas-Grain Chemistry for Large Reaction Networks. II. A Multiphase Gas-surface-layered Bulk Model. *ApJ* 762, 86. doi:doi:10.1088/0004-637X/762/2/86, arXiv:1211.3025.
- Vasyunin, A.I., Semenov, D.A., Wiebe, D.S., Henning, T., 2009. A Unified Monte Carlo Treatment of Gas-Grain Chemistry for Large Reaction Networks. I. Testing Validity of Rate Equations in Molecular Clouds. *ApJ* 691, 1459–1469. doi:doi:10.1088/0004-637X/691/2/1459, arXiv:0810.1591.

- Vidal, T.H.G., Loison, J.C., Jaziri, A.Y., Ruaud, M., Gratier, P., Wakelam, V., 2017. On the reservoir of sulphur in dark clouds: chemistry and elemental abundance reconciled. *MNRAS* 469, 435–447. doi:doi:10.1093/mnras/stx828, arXiv:1704.01404.
- Visser, R., Bruderer, S., Cazzoletti, P., Facchini, S., Heays, A.N., van Dishoeck, E.F., 2018. Nitrogen isotope fractionation in protoplanetary disks. *A&A* 615, A75. doi:doi:10.1051/0004-6361/201731898, arXiv:1802.02841.
- Visser, R., Dullemond, C.P., 2010. Sub-Keplerian accretion onto circumstellar disks. *A&A* 519, A28. doi:doi:10.1051/0004-6361/200913604, arXiv:1005.1261.
- Visser, R., van Dishoeck, E.F., Doty, S.D., Dullemond, C.P., 2009. The chemical history of molecules in circumstellar disks. I. Ices. *A&A* 495, 881–897. doi:doi:10.1051/0004-6361/200810846, arXiv:0901.1313.
- Wada, K., Tanaka, H., Okuzumi, S., Kobayashi, H., Suyama, T., Kimura, H., Yamamoto, T., 2013. Growth efficiency of dust aggregates through collisions with high mass ratios. *A&A* 559, A62. doi:doi:10.1051/0004-6361/201322259.
- Waelkens, C., Waters, L.B.F.M., de Graauw, M.S., Huygen, E., Malfait, K., Plets, H., Vandenbussche, B., Beintema, D.A., Boxhoorn, D.R., Habing, H.J., Heras, A.M., Kester, D.J.M., Lahuis, F., Morris, P.W., Roelfsema, P.R., Salama, A., Siebenmorgen, R., Trams, N.R., van der Blik, N.R., Valentijn, E.A., Wesseliuss, P.R., 1996. SWS observations of young main-sequence stars with dusty circumstellar disks. *A&A* 315, L245–L248.
- Wänke, H., Dreibus, G., 1988. Chemical Composition and Accretion History of Terrestrial Planets. *Philosophical Transactions of the Royal Society of London Series A* 325, 545–557. doi:doi:10.1098/rsta.1988.0067.
- Wagner, A.F., Graff, M.M., 1987. Oxygen Chemistry of Shocked Interstellar Clouds. I. Rate Constants for Thermal and Nonthermal Internal Energy Distributions. *ApJ* 317, 423. doi:doi:10.1086/165287.
- Wakelam, V., Bron, E., Cazaux, S., Dulieu, F., Gry, C., Guillard, P., Habart, E., Hornekar, L., Morisset, S., Nyman, G., Pirronello, V., Price, S.D., Valdivia, V., Vidali, G., Watanabe, N., 2017. H₂ formation on interstellar dust grains: The viewpoints of theory, experiments, models and observations. *Molecular Astrophysics* 9, 1–36. doi:doi:10.1016/j.molap.2017.11.001, arXiv:1711.10568.
- Wakelam, V., Loison, J.C., Herbst, E., Pavone, B., Bergeat, A., Béroff, K., Chabot, M., Faure, A., Galli, D., Geppert, W.D., Gerlich, D., Gratier, P., Harada, N., Hickson, K.M., Honvault, P., Klippenstein, S.J., Le Picard, S.D., Nyman, G., Ruaud, M., Schlemmer, S., Sims, I.R., Talbi, D., Tennyson, J., Wester, R., 2015. The 2014 KIDA Network for Interstellar Chemistry. *ApJS* 217, 20. doi:doi:10.1088/0067-0049/217/2/20, arXiv:1503.01594.
- Wakelam, V., Ruaud, M., Hersant, F., Dutrey, A., Semenov, D., Majumdar, L., Guilloteau, S., 2016. Importance of the H₂ abundance in protoplanetary disk ices for the molecular layer chemical composition. *A&A* 594, A35. doi:doi:10.1051/0004-6361/201628748, arXiv:1609.01471.
- Wakelam, V., Smith, I.W.M., Herbst, E., Troe, J., Geppert, W., Linnartz, H., Öberg, K., Roueff, E., Agúndez, M., Pernot, P., Cuppen, H.M., Loison, J.C., Talbi, D., 2010. Reaction Networks for Interstellar Chemical Modelling: Improvements and Challenges. *Space Sci. Rev.* 156, 13–72. doi:doi:10.1007/s11214-010-9712-5, arXiv:1011.1184.
- Walsh, C., Loomis, R.A., Öberg, K.L., Kama, M., van 't Hoff, M.L.R., Millar, T.J., Aikawa, Y., Herbst, E., Widicus Weaver, S.L., Nomura, H., 2016. First Detection of Gas-phase Methanol in a Protoplanetary Disk. *ApJ* 823, L10. doi:doi:10.3847/2041-8205/823/1/L10, arXiv:1606.06492.
- Walsh, C., Millar, T.J., Nomura, H., 2010. Chemical Processes in Protoplanetary Disks. *ApJ* 722, 1607–1623. doi:doi:10.1088/0004-637X/722/2/1607, arXiv:1008.4305.
- Walsh, C., Nomura, H., van Dishoeck, E., 2015. The molecular composition of the planet-forming regions of protoplanetary disks across the luminosity regime. *A&A* 582, A88. doi:doi:10.1051/0004-6361/201526751, arXiv:1507.08544.
- Wang, H.S., Lineweaver, C.H., Ireland, T.R., 2018. The elemental abundances (with uncertainties) of the most Earth-like planet. *Icarus* 299, 460–474. doi:doi:10.1016/j.icarus.2017.08.024, arXiv:1708.08718.
- Wang, H.S., Lineweaver, C.H., Ireland, T.R., 2019. The volatility trend of protosolar and terrestrial elemental abundances. *Icarus* 328, 287–305. doi:doi:10.1016/j.icarus.2019.03.018, arXiv:1810.12741.
- Watanabe, N., Kouchi, A., 2002. Measurements of Conversion Rates of CO to CO₂ in Ultraviolet-induced Reaction of D₂O(H₂O)/CO Amorphous Ice. *ApJ* 567, 651–655. doi:doi:10.1086/338491.
- Watson, D.M., Leisenring, J.M., Furlan, E., Bohac, C.J., Sargent, B., Forrest, W.J., Calvet, N., Hartmann, L., Nordhaus, J.T., Green, J.D., Kim, K.H., Sloan, G.C., Chen, C.H., Keller, L.D., d'Alessio, P., Najita, J., Uchida, K.I., Houck, J.R., 2009. Crystalline Silicates and Dust Processing in the Protoplanetary Disks of the Taurus Young Cluster. *ApJS* 180, 84–101. doi:doi:10.1088/0067-0049/180/1/84, arXiv:0704.1518.
- Weidenschilling, S.J., 1977. Aerodynamics of solid bodies in the solar nebula. *MNRAS* 180, 57–70. doi:doi:10.1093/mnras/180.1.57.
- Weisberg, M.K., McCoy, T.J., Krot, A.N., 2006. Systematics and Evaluation of Meteorite Classification. p. 19.
- Westley, M.S., Baragiola, R.A., Johnson, R.E., Baratta, G.A., 1995. Photodesorption from Low-Temperature Water Ice in Interstellar and Circumsolar Grains. *Nature* 373, 405. doi:doi:10.1038/373405a0.
- Whipple, F.L., 1972. On certain aerodynamic processes for asteroids and comets, in: Elvius, A. (Ed.), *From Plasma to Planet*, p. 211.
- Whittet, D.C.B., 2010. Oxygen Depletion in the Interstellar Medium: Implications for Grain Models and the Distribution of Elemental Oxygen. *ApJ* 710, 1009–1016. doi:doi:10.1088/0004-637X/710/2/1009, arXiv:0912.3298.
- Widicus Weaver, S.L., 2019. Millimeterwave and Submillimeterwave Laboratory Spectroscopy in Support of Observational Astronomy. *ARA&A* 57, 79–112. doi:doi:10.1146/annurev-astro-091918-104438.
- Willacy, K., Langer, W., Allen, M., Bryden, G., 2006. Turbulence-driven Diffusion in Protoplanetary Disks: Chemical Effects in the Outer Regions. *ApJ* 644, 1202–1213. doi:doi:10.1086/503702, arXiv:astro-ph/0603103.
- Williams, J.P., Cieza, L.A., 2011. Protoplanetary Disks and Their Evolution. *ARA&A* 49, 67–117. doi:doi:10.1146/annurev-astro-081710-102548, arXiv:1103.0556.
- Wilson, R.W., Jefferts, K.B., Penzias, A.A., 1970. Carbon Monoxide in the Orion Nebula. *ApJ* 161, L43. doi:doi:10.1086/180567.
- Winn, J.N., Fabrycky, D.C., 2015. The occurrence and architecture of exoplanetary systems. *Annual Review of Astronomy and Astrophysics* 53, 409–447. URL: <https://doi.org/10.1146/annurev-astro-082214-122246>, doi:doi:10.1146/annurev-astro-082214-122246, arXiv:https://doi.org/10.1146/annurev-astro-082214-122246.
- Wirström, E.S., Charnley, S.B., 2018. Revised models of interstellar nitrogen isotopic fractionation. *MNRAS* 474, 3720–3726. doi:doi:10.1093/mnras/stx3030, arXiv:1711.08254.
- Wirström, E.S., Charnley, S.B., Cordiner, M.A., Ceccarelli, C., 2016. A Search for O₂ in CO-depleted Molecular Cloud Cores with Herschel. *ApJ* 830, 102. doi:doi:10.3847/0004-637X/830/2/102, arXiv:1608.02714.
- Wittenmyer, R.A., Wang, S., Horner, J., Butler, R.P., Tinney, C.G., Carter, B.D., Wright, D.J., Jones, H.R.A., Bailey, J., O'Toole, S.J., Johns, D., 2020. Cool Jupiters greatly outnumber their toasty siblings: occurrence rates from the Anglo-Australian Planet Search. *MNRAS* 492, 377–383. doi:doi:10.1093/mnras/stz3436, arXiv:1912.01821.
- Woitke, P., Kamp, I., Thi, W.F., 2009. Radiation thermo-chemical models of protoplanetary disks. I. Hydrostatic disk structure and inner rim. *A&A* 501, 383–406. doi:doi:10.1051/0004-6361/200911821, arXiv:0904.0334.
- Wolfire, M.G., Hollenbach, D., McKee, C.F., Tielens, A.G.G.M., Bakes, E.L.O., 1995. The Neutral Atomic Phases of the Interstellar Medium. *ApJ* 443, 152. doi:doi:10.1086/175510.

- Wong, M.H., Mahaffy, P.R., Atreya, S.K., Niemann, H.B., Owen, T.C., 2004. Updated Galileo probe mass spectrometer measurements of carbon, oxygen, nitrogen, and sulfur on Jupiter. *Icarus* 171, 153–170. doi:doi:10.1016/j.icarus.2004.04.010.
- Wood, B.J., Smythe, D.J., Harrison, T., 2019. The condensation temperatures of the elements: A reappraisal. *American Mineralogist* 104, 844–856. doi:doi:10.2138/am-2019-6852CCBY.
- Xu, S., Dufour, P., Klein, B., Melis, C., Monson, N.N., Zuckerman, B., Young, E.D., Jura, M.A., 2019. Compositions of Planetary Debris around Dusty White Dwarfs. *AJ* 158, 242. doi:doi:10.3847/1538-3881/ab4cee, arXiv:1910.07197.
- Yamaguchi, T., Takano, S., Sakai, N., Sakai, T., Liu, S.Y., Su, Y.N., Hirano, N., Takakuwa, S., Aikawa, Y., Nomura, H., Yamamoto, S., 2011. Detection of Phosphorus Nitride in the Lynds 1157 B1 Shocked Region. *PASJ* 63, L37–L41. doi:doi:10.1093/pasj/63.5.L37.
- Yoneda, H., Tsukamoto, Y., Furuya, K., Aikawa, Y., 2016. Chemistry in a Forming Protoplanetary Disk: Main Accretion Phase. *ApJ* 833, 105. doi:doi:10.3847/1538-4357/833/1/105, arXiv:1611.03587.
- Yu, M., Evans, Neal J., I., Dodson-Robinson, S.E., Willacy, K., Turner, N.J., 2017. Disk Masses around Solar-mass Stars are Underestimated by CO Observations. *ApJ* 841, 39. doi:doi:10.3847/1538-4357/aa6e4c, arXiv:1704.05508.
- Yurimoto, H., Kuramoto, K., 2004. Molecular Cloud Origin for the Oxygen Isotope Heterogeneity in the Solar System. *Science* 305, 1763–1766. doi:doi:10.1126/science.1100989.
- Zernickel, A., Schilke, P., Schmiedeke, A., Lis, D.C., Brogan, C.L., Ceccarelli, C., Comito, C., Emprechtinger, M., Hunter, T.R., Möller, T., 2012. Molecular line survey of the high-mass star-forming region NGC 6334I with Herschel/HIFI and the Submillimeter Array. *A&A* 546, A87. doi:doi:10.1051/0004-6361/201219803, arXiv:1208.5516.
- Zhang, K., Bergin, E.A., Blake, G.A., Cleeves, L.I., Schwarz, K.R., 2017. Mass inventory of the giant-planet formation zone in a solar nebula analogue. *Nature Astronomy* 1, 0130. doi:doi:10.1038/s41550-017-0130, arXiv:1705.04746.
- Zhang, K., Bergin, E.A., Schwarz, K., Krijt, S., Ciesla, F., 2019. Systematic Variations of CO Gas Abundance with Radius in Gas-rich Protoplanetary Disks. *ApJ* 883, 98. doi:doi:10.3847/1538-4357/ab38b9, arXiv:1908.03267.
- Zhang, K., Pontoppidan, K.M., Salyk, C., Blake, G.A., 2013. Evidence for a Snow Line beyond the Transitional Radius in the TW Hya Protoplanetary Disk. *ApJ* 766, 82. doi:doi:10.1088/0004-637X/766/2/82, arXiv:1302.3655.
- Zhang, K., Schwarz, K.R., Bergin, E.A., 2020. Rapid Evolution of Volatile CO from the Protostellar Disk Stage to the Protoplanetary Disk Stage. *ApJ* 891, L17. doi:doi:10.3847/2041-8213/ab7823, arXiv:2002.08522.
- Ziurys, L.M., Schmidt, D.R., Bernal, J.J., 2018. New Circumstellar Sources of PO and PN: The Increasing Role of Phosphorus Chemistry in Oxygen-rich Stars. *ApJ* 856, 169. doi:doi:10.3847/1538-4357/aaafc6.